CHAPTER 2:
AFRICA'S FUTURE UNDER A CURRENT POLICY TRAJECTORY

UN environment programme

CLIMATE & CLEAN AIR COALITION
TO REDUCE SHORT-LIVED CLIMATE POLLUTANTS

African Union

ISBN: 978-92-807-3989-3

DISCLAIMERS

COVER PHOTOGRAPHY

Renewables (geothermal plant in picture) is one of the five key areas for air pollution and climate change mitigation action in Africa,Shutterstock

SUGGESTED CITATION

United Nations Environment Programme (2023). Integrated Assessment of Air Pollution and Climate Change for Sustainable Development in Africa, Nairobi.

PRODUCTION

Climate and Clean Air Coalition (CCAC) convened by United Nations Environment Programme (UNEP), African Union Commission, Stockholm Environment Institute (SEI)

ACKNOWLEDGMENTS

The United Nations Environment Programme (UNEP) would like to thank the authors, reviewers and the secretariat for their contribution to the preparation of this assessment report. Authors and reviewers have contributed to the report in their individual capacities. Their affiliations are only mentioned for identification purposes. The preparation of this assessment has been supported by the Swedish International Development Cooperation Agency (Sida) through funding to the Stockholm Environment Institute (SEI) that coordinated the process and publication of the assessment report.

CO-CHAIRS OF THE ASSESSMENT

Alice Akinyi Kaudia (Pristine Sustainable Ecosystems, Kenya), Youba Sokona (Goupe de Réflexion et d'actions novatrices [GRAIN]), Brian Mantlana (Council for Scientific and Industrial Research [CSIR], Pretoria, South Africa)

INTERNATIONAL ADVISORY GROUP

Co-chaired by: Harsen Nyambe Nyambe (AUC) and Charles Sebukeera (UNEP ROA).

Members: Al-Hamndou Dorsouma (AfDB), Olushola Olayide (AUC), Jean Baptiste Havugimana, Ladislaus Kyaruz (EAC), Yao Bernard Koffi (ECOWAS), Martial Bernoux (FAO), Laura Cozzi, Jasmine Samantar (IEA), Philip Landrigan (IHME), Frank Murray (Murdoch University), Markus Amann (IIASA), Sibongile Mavimbela, Shepherd Muchuru (SADC), Mohamed Atani (UNEP), Veronique Yoboue (WASCAL), Shem Oyoo Wandiga (UoN), Cynthia Davis (WHO), Matshidiso Moeti, Adelheid Onyango, Antonis Kolimenakis, Guy Mbayo (WHO AFRO), Alexander Baklanov, Oksana Tarasova (WMO), Sara Terry (USEPA)

NATIONAL FOCAL POINTS

Algeria - Ms Medani Sihem, Director of Cooperation at Ministry of Environment and Ms Saida Laouar, Deputy Director Adaptation to Climate Change;

Botswana - Kgosietsile Modise, Department of Waste Management and Pollution Control;

Central African Republic - David Melchisédéck, Yangbondo, Ministère de l'Environnement et du Développement Durable;

Côte d'Ivoire - Ange-Benjamin Brida, Ministry of Salubrity, Environment and Sustainable Development;

Democratic Republic of Congo - Adelard Mutombo Kazadi, Ministry of Environment and Sustainable Development;

Egypt - Eng. Lydia Elewa, Manager of Climate Change Researchers, Ministry of Environment and Head of Air Quality and Dr. Mohamed Saad Noise Protection Central Department, Ministry of Environment;

Ethiopia - Grima Gemechu, Director General, Environmental Compliance Monitoring and Control Directorate Environment Forest and Climate Change Commission;

Guinea-Bisau - Mr. Per Infali Cassamá;

Kenya - Dr. Pacifica Achieng Ogola, Director, Climate Change, Ministry of Environment and Forestry;

Mali - Sekou N'Faly Sissoko, Directeur par interim des Applications Meteorologiques et Climatologiques de Mali-Meteo;

Mauritius - Mrs. Anita Kawol, Acting Divisional Environment Officer, Department of Climate Change;

Morocco - Mr. Bouzekri Raz, Director of Climate Change, Biodiversity and Green Economy;

Nigeria - Asmau Jibril, National focal point to the Coalition;

Rwanda - Beatrice Cyiza, DG of Environment & Climate Change, Ministry of Environment;

Republic of Guinea - Aboubacar Kaba, Ministère de l'Environnement, des Eaux et Forêts;

Senegal - Mr. Saliou Souare, Direction de l'Environnement et des Etablissements Classés (DEEC) and Ms Aminata Mbow Diokhané, Centre de Gestion de la Qualité de l'Air (CGQA);

South Africa - PA Kungawo Nxesi, Deputy Director-General Climate Change and Air Quality Management;

Sudan - Mona Abdelhafeez, General Dept of Environmental Affairs, National Council for Environment;

Tanzania - Dr. Fredrick Manyika, Principal Forest Officer and UNFCCC Focal Point;

Togo - Bouléwoué Sankoutcha, Direction de l'Environnement;

Uganda - Ms Jenifer Kutesakwe, National Management Authority of Uganda;

Zimbabwe - Mr Alpha Chikurira, Environmental Management Agency and Ms Charity Denhere, Ministry of Environment, Climate, Tourism and Hospitality Industry.

REGIONAL ECONOMIC COMMUNITIES

Arab Maghreb Union - Mr. Habib Hlali

East Africa Community (EAC) - Dr. Jean Baptiste Havugimana, Engineer Leonidas

Economic Community of West African States (ECOWAS) - Mr. Yao Bernard Koffi

Southern African Development Community (SADC) - Ms Sibongile Mavimbela, Shepherd Muchuru

TECHNICAL REVIEWERS

Noureddine Yassaa (Commissariat aux Energies Renouvelables et à l'Efficacité Energétique, Algeria), Langley DeWitt (University of Colorado, USA), Dajuma Alima (University Pelefero Gon Coulibaly, Côte d'Ivoire), Eric Zusman (Institute for Global Environmental Strategies (IGES), Japan), Patrin Watanatada (Clean Air Fund), Philip Landrigan (Boston College, USA), Frank Murray (formerly Murdoch University, Australia), Sara Terry (USEPA), Francis Gorman Ofosu (Ghana Atomic Energy Commission), Aminata Mbow Diokhane (Direction de l'Environnement et des Etablissements Classés (DEEC), Senegal), Peter Gilruth (World Agroforestry Centre, ex-UNEP Science), Nino Kuenzli (Swiss Tropical and Public Health Institute), Michel Grutter (Universidad Nacional Autónoma de México (UNAM)), Kristin Aunan (Center for International Climate Research (CICERO), Norway), Desta Mebratu (Stellenbosch University, South Africa), Amal Saad Hussein (National Research Centre, Egypt), Noah Misati Kerandi (South Eastern Kenya Univeristy), Reda Elwakil (Ain Shams University, Egypt), Ernesto Sanchez-Triana (World Bank), Santiago Enriquez (World Bank), Claudia Serrano (World Bank), Lisa Emberson (University of York, UK)

PROJECT COORDINATION TEAM

Alice Akinyi Kaudia (Co-ordinating Co-Chair of the Assessment, Pristine Sustainable Ecosystems, Kenya), Aderiana Mbandi (UNEP Regional Office for Africa), Caroline Tagwireyi (seconded to the African Union Commission), Philip Osano, Anderson Kebila, Lawrence Malindi Nzuve, Cynthia Sitati and Jacinta Musyoki (SEI Africa, Kenya), Kevin Hicks and Eve Palmer (SEI, University of York, UK), Valentin Foltescu and Emily Kaldjian (CCAC)

EDITING AND COMMUNICATIONS

COPY EDITOR: Bart Ullstein (Banson, UK)

MANAGING AND PRODUCTION EDITOR: Kevin Hicks (SEI, University of York, UK)

COMMUNICATIONS: Lawrence Malindi Nzuve (SEI Africa, Kenya), Emily Kaldjian and Tiy Chung (CCAC, France), Mohamed Atani (UNEP, Kenya), Molalet Tsedeke (Africa Union, Ethiopia), Frances Dixon (SEI York, UK), Andrea Lindblom (SEI, Stockholm, Sweden)

GRAPHIC DESIGN AND LAYOUT: Katharine Mugridge

SPECIAL THANKS

The Climate and Clean Air Coalition and partners appreciate the leadership and support from the H.E. Ambassador Josefa Leonel Correia Sacko, Commissioner for Agriculture, Rural Development, Blue Economy and Sustainable Environment, African Union Commission, and the entire team of officers for supporting and providing policy guidance to the assessment. We express gratitude to Dr. Harsen Nyambe, for Co-Chairing the International Advisory Group, Ms. Olushola Oyalide and Ms. Leah Naess Wanambwa for their policy support to the assessment coordination team. We would also like to express our gratitude to Frank Turyatunga (Regional Director) andCharles Sebukeera, UNEP Regional Office for Africa, and David Ombisi and Julie Kaibe at the African Ministerial Conference on Environment (AMCEN) Secretariat, for their support of the Assessment and especially the policy engagement process. Special thanks also go to Andrea Hinwood, UNEP Chief Scientist, the head of the CCAC Secretariat, Martina Otto, and the Co-Chairs and Science Advisory Panel of the CCAC for advice and comments.

AUTHORS

Coordinating Lead Authors: Rebecca M. Garland (University of Pretoria, South Africa), N'datchoh Evelyne Touré (Université Félix Houphouët Boigny, Cote d'Ivoire)

Lead Authors: Olawale E. Abiye (Obafemi Awolowo University, Nigeria), Benjamin Brida (Government of Cote d'Ivoire), Charles Heaps (SEI, Boston, USA), Sekou Keita (University Peleforo Gon Coulibaly, Cote d'Ivoire), Prashant Kumar (University of Surrey, UK), Chris Malley (SEI, University of York), Drew Shindell (Duke University, USA), Paul Young (University of Lancaster, UK)

Contributing Authors: Aissatou Faye (Department of Environmental Sciences, University of Virginia, USA), Malan Ketcha Armand Kablan (Université Félix Houphouët-Boigny, Côte d'Ivoire), Rajesh Kumar (National Center for Atmospheric Research (NCAR), USA), Robert Karisa Masumbuko (SEI Africa, Kenya), Eleni Michalopoulou (SEI, University of York, UK), Raeesa Moolla (University of the Witwatersrand, South Africa), Emily Nagamoto (Duke University, USA), Luke Parsons (Duke University, USA), Francis Pope (University of Birmingham, UK), Wenfu Tang (NCAR, USA), Sylvia Ulloa (SEI, Boston, USA)

CONTENTS

2.1 INTRODUCTION

MAIN MESSAGES

This chapter reviews current knowledge of present day and possible future climate and air quality across Africa before describing the future of Africa under a baseline scenario. The scenario assumes the current trajectories and policies in the energy, agricultural and waste sectors continue, with no further policy development. It was developed as a storyline over historical (up to and including 2018) and future (2019–2063) periods, in line with the African Union's Agenda 2063 and covers the entire African continent, with national-scale resolution of key variables.

- All scenarios in this Assessment, including the baseline scenario (this chapter) and SLCP and Agenda 2063 scenarios (Chapter 3) use the same population, GDP growth and urbanization projections.
- The Low Emissions Analysis Platform (LEAP) system is the main modelling framework for the Assessment and includes analysis of all key energy consuming and producing sectors, with a particular focus on households, transport and electricity generation, as well as summaries of emissions from the non-energy sectors agriculture and waste management.
- The model quantifies total national emissions of all GHGs – CO_2, CH_4, N_2O and HFCs; SLCPs – BC, CH_4, HFCs; and other air pollutants – NOx, NMVOC, SO_2, NH_3; $PM_{2.5}$ and PM_{10}, made up of OC, BC, mineral dust, etc., and CO – from both the energy and non-energy sectors.
- A global atmospheric circulation model (GISS-E2.1-G) was used to simulate future climate change scenarios and outdoor air pollution levels, i.e., $PM_{2.5}$ and ground-level O_3. The output from these simulations was also used to calculate impacts of outdoor air pollution on human health as well as the impacts of outdoor air pollution and climate change on crop yields.
- Human health impacts were also estimated for changes in household air pollution using approaches compatible with WHO and Global Burden of Disease studies.

2.1.1 MODELLING THE BASELINE SCENARIO

This chapter reviews current knowledge of present day and possible future climate and air quality across Africa before describing the future of Africa under a baseline scenario modelled in this Assessment. As discussed further below, this baseline scenario assumes the current trajectories and policies in the energy, agricultural and waste sectors continue, with no further policy development. It was developed as a storyline over historical (up to and including 2018) and future (2019–2063) periods, and covers the entire African continent, with national-scale resolution of key variables. This chapter describes the development of the projected future population, economic, and urbanization trends (Section 2.3); the trajectories of drivers of the different sectors (Section 2.4); and the emissions of air pollutants and GHGs that result (Section 2.5). The consequences of this scenario for outdoor and household air quality, future temperature and precipitation, and human and crop health are also discussed (Section 2.6). To create the scenario and assess its impacts, the chapter – and the entire Assessment –makes use of state-of-the-art modelling tools, which are summarized below and described more fully in this chapter's annexes.

It is important to note that all scenarios in this Assessment, i.e., the baseline scenario (this chapter) and SLCP and Agenda 2063 scenarios (Chapter 3) use the same population[1], GDP growth[2] and urbanization[3] projections. These projections are described in Section 2.3 but are used in all scenarios. From these projections, the different scenarios are then developed against different levels of emissions reductions through specific technology measures, often related to policies and plans, across sectors (Chapter 3). All scenarios were developed through a consultative process with the broader Assessment team.

BOX 2.1 TECHNICAL TOOLS USED IN THE ASSESSMENT

This box provides a high-level summary of the technical tools used in this Assessment to estimate emissions, outdoor and household pollutant concentrations, impacts and future temperature and precipitation. Further details for each tool are provided in the annexes to this chapter.

LOW EMISSIONS ANALYSIS PLATFORM

The Low Emissions Analysis Platform (LEAP) system is the main modelling framework for this Assessment and is a widely used software tool for integrated planning of energy policy, emissions abatement and climate change mitigation assessments (Heaps 2021). It is a scenario-based planning tool developed by SEI. The LEAP is configured to track energy consumption, conversion and resource extraction in all sectors of the economy (SEI 2017). For this Assessment, SEI developed an Africa-wide version of LEAP with national scale resolution that covers the continent. This LEAP-Africa version includes historical data for the period 2000–2018 and three scenarios with projections for the period 2019–2063. The model includes analysis of all key energy consuming and producing sectors, with a particular focus on households, transport and electricity generation, as well as summaries of emissions from non-energy sectors. The model quantifies total national emissions of all GHGs – CO_2, CH_4, N_2O and HFCs; SLCPs – BC, CH_4, HFCs; and other air pollutants – NOX, NMVOC, SO_2, NH_3; $PM_{2.5}$ and PM_{10}, made up of OC, BC, mineral dust, etc., and CO – from both the energy and non-energy sectors. The model was used to produce annual results for the period 2000–2063, for Africa as a whole, for regions of the continent – Southern Africa, East Africa, North Africa, West Africa and Central Africa –and for individual countries.

GODDARD INSTITUTE FOR SPACE STUDIES MODEL

The Goddard Institute for Space Studies (GISS) model was used to project the impacts of the emissions scenarios on outdoor air quality, temperature and precipitation, and human and crop health. The model, a global atmospheric circulation model, has been used in almost all phases of the Coupled Model Intercomparison Project (CMIP), so it has been continuously updated to maintain and improve its realism – better inclusion of processes and higher skill – in order to

1. Population from UN World Population Prospects 2019 Revision (Medium Variant)
2. Historical GDP from (World Bank WDI): NY.GDP.MKTP.PP.KD (2017 Int. $ PPP). Long-range projections based on growth rates of Shared Socioeconomic Pathway SSP#2 (Middle of the Road). Updated to reflect recent growth rates and expected impacts of COVID-19 (based on IMF World Economic Outlook (IMF WEO, April 2021).
3. Urbanization from the United Nations Department of Economic and Social Affairs (UN DESA) World Urbanization Prospects: 2018 Revision. Household sizes from Global Data Labs Database v 4.0 (Feb 2021). Note: Not projected into the future, so may tend to slightly underestimate future households/ future HH energy demand.

continue its participation in international and national climate-model assessment projects. The current implementation of the GISS series of coupled atmosphere-ocean models is called ModelE. It provides the ability to simulate many different configurations of Earth-system models, including interactive atmospheric chemistry, aerosols, the carbon cycle and other tracers, as well as the standard atmosphere, ocean, sea ice and land surface components.

In this Assessment, the GISS-E2.1-G model (Kelley *et al.* 2020) was used to simulate future climate change scenarios and outdoor air pollution levels, i.e., $PM_{2.5}$ and ground-level O_3. The output from these simulations was also used to calculate impacts of outdoor air pollution on human health as well as the impacts of outdoor air pollution and climate change on crop yields. GISS is a global model and only the emissions in Africa were updated to those in this Assessment. For the rest of the globe, emissions appropriate to the shared socioeconomic pathways SSP3-7.0 climate scenario were used, as was also used in the recent Sixth Assessment Report of the IPCC (IPCC 2021).

HEALTH IMPACT ASSESSMENT

Human health impacts were also estimated for changes in household air pollution. Exposure to this, the annual average $PM_{2.5}$ concentration, was estimated separately for household cooking using different fuels and stove types. Exposure was estimated separately for the primary household cook, other adults and children. The impact of household air pollution on human health was quantified as the number of premature deaths attributable to household air pollution exposure for six diseases: ischaemic heart disease, stroke, lung cancer, chronic obstructive pulmonary disease, Type-2 diabetes, and LRTI in children. The baseline mortality rates for these diseases, disaggregated by gender and age, were extracted from the GBD Study (GBD 2019) and used for years before 2020. To estimate future mortality rates, the change in overall death rate projected by UN World Population Prospects (UN WPP) between 2019 and future years was applied to the GBD disease-specific mortality rates for 2019 to estimate future disease-specific mortality rates (United Nations World Population Prospects 2019).

2.2 CURRENT AND FUTURE EMISSIONS, AIR POLLUTION AND CLIMATE CHANGE IN AFRICA

MAIN MESSAGES

- Although there are recent improvements, air quality monitoring is generally sparse in Africa. The available data indicate elevated levels of outdoor air pollution across the continent that will have negative impacts on health, ecosystems and agriculture.
- An overview on the current emissions, their main sources and trends indicate that air pollution is getting worse. Increases in future emissions of pollutants in many places in Africa is found by several studies. There is, therefore, a high risk of the air pollution worsening in these areas in the future because of these increased emissions.
- There are significant projected impacts of climate change on temperature and precipitation. For temperature, the sub-tropics are projected to see warming that is greater than the global average. Projected changes in precipitation patterns and intensity are variable across the continent.
- The impact of poor air quality and climate change are a significant issue, but the evidence from which to make decisions is limited. This Assessment specifically addresses this gap by delivering emission estimates and scenarios and assessing the likely impacts in Africa. It also highlights the areas of future action and research.

2.2.1 STATE OF AIR QUALITY MONITORING

Air quality data come from ground-based and *in-situ* monitoring, satellites and from a broad range of model-measurement fusion techniques, which combine measurements with process models using various statistical approaches. The general availability of these for Africa, as well as examples of findings per region, is summarized below.

GROUND-BASED AND *IN-SITU* MONITORING

Air quality monitoring across Africa is characterized by few long-term, routine air-quality monitoring networks, supplemented by sporadic field campaigns. Of the few countries that have established permanent monitoring stations, many have not been able to sustain their operation and many such stations have ceased to supply measurement data. In addition, field campaigns are typically short in duration and characterized by the use of a range of measurement systems, making national and regional comparisons difficult. Further to these challenges is poor database management: data are often neither readily available nor freely accessible, limiting scientific study, public awareness and effective policy making.

Regardless of this sparseness of air-quality monitoring in Africa, the available literature indicates elevated levels of outdoor air pollution across the continent (Petkova *et al.* 2013; Amegah 2018; Fayiga *et al.* 2018; Agbo *et al.* 2020). Particulate matter (PM), mainly less than 2.5 µm in diameter ($PM_{2.5}$) and less than 10 µm in diameter (PM_{10}), pollution has been the most widely monitored species from ground-based measurements, with studies showing that most countries exceed their own standards, where applicable, and the WHO Guidelines ($PM_{2.5}$ 24-hr average = 15 µg/m^3, annual average = 5 µg/m^3; (Petkoval *et al.* 2013; Katoto *et al.* 2019; WHO 2021).

The current monitoring structure and field campaign data are summarized on a regional basis in Annex 2.1, while Table 2.1 presents a sample of the results from measurement data on a regional basis.

Table 2.1 Examples of pollutant concentrations measured in different regions from ground-based or in-situ monitoring, including permanent networks and field campaigns

REGION	LOCATION	SPECIES	LEVEL	REFERENCE(S)
WESTERN AFRICA	NIGERIA	$PM_{2.5}$	248 µg/m³ (hourly max)	Abiye et al. 2013; Offor et al. 2016; Owoade et al. 2021
		PM_{10}	930 µg/m³ (hourly max)	
	SOUTHERN WEST AFRICA (DACCIWA FIELD CAMPAIGN OVER BENIN, TOGO, GHANA, CÔTE D'IVOIRE)	CO	176 ppb (boundary layer measurement at 5s resolution averaged over ATR42 daily flight trajectory;)	Brito et al. 2018
NORTHERN AFRICA	ZOUAGHI, ALGERIA	$PM_{2.5}$	57.8 µg/m³ (roadside)	Terrouche et al. 2016
		PM_{10}	105.2 µg/m³ (roadside)	
	CASABLANCA, MOROCCO	PM_{10}	105–106 µg/m³ (roadside)	Tahri et al. 2013
	TUNISIA	Total suspended particles (TSP)[4],sizes up to 25 µm	95–470 µg/m³ (coastal area, daily values of filter-based sampling)	Ellouz et al. 2014
	EGYPT	TSP	466–680 µg/m³ (annual levels in power plant outdoor environment)	Hindy and Abdelmaksod, 2016
CENTRAL AFRICA	LUANDA, ANGOLA (TRAFFIC CORRIDORS)	NO_2	35 - 130 µg/m³ (hourly max)	Campos et al. 2021
		SO_2	584 µg/m³ (hourly max) and 42 - 164 µg/m³ (daily average)	
		$PM_{2.5}$	11 - 46 µg/m³ (daily average)	
	CAMEROUN (INTRA-CITY; BAFOUSSAM, BAMENDA AND YOUNDE)	PM	$PM_{2.5}$ (hourly max): residential 41–109 µg/m³, market area 100–229 µg/m³, bus station 69–229 µg/m³, city outskirts 57–160 µg/m³ PM_{10} (hourly max): residential 4–139 µg/m³, market area 127–327 µg/m³, bus station 95–327 µg/m³, city outskirt 76–255 µg/m³, commercial food preparation 709 µg/m³	Antonel and Chowdhury 2014
SOUTHERN AFRICA	SOUTH AFRICA	PM	PM_{10} and $PM_{2.5}$ levels in low-income settlements exceed National Outdoor Air Quality Standards of PM_{10} 24-hr = 75 µg/m³; PM_{10} annual average = 40 µg/m³ $PM_{2.5}$ 24-hr average = 40 µg/m³; $PM_{2.5}$ annual average = 20 µg/m³	Venter et al. 2012; Hersey et al. 2015; Feig et al. 2019; Govendar and Sivakumar 2019
EASTERN AFRICA	ETHIOPIA, KENYA AND UGANDA	Visibility (reflects pollution)	Decreasing trend, 1974–2018	ASAP-East Africa Synthesis Report 2020
	ETHIOPIA	$PM_{2.5}$	15–40 µg/m³ (hourly average at outdoor environment, pollution level plateauing)	ASAP-East Africa Synthesis Report 2020
	KENYA, UGANDA		25–80 µg/m³ (classrooms and household environments, current levels are unhealthy)	ASAP-East Africa Synthesis Report 2020

4. TSP includes all particle sizes suspended in the atmosphere that could trapped depending on the configuration of the sampler used while PM_{10} and $PM_{2.5}$ are particles with aerodynamic diameter of ≤2.5µm and ≤10µm respectively

SATELLITE MEASUREMENTS

Satellite-derived atmospheric composition measurements are an important supplement to the sparse ground-based and *in-situ* monitoring for Africa, providing increased spatial coverage. Moreover, satellite data can be used in conjunction with *in-situ* observations to better quantify ground-level concentrations of air pollution in data-scarce regions, which can then be applied to applications such as improving information from low-cost sensors (de Souza *et al.* 2020; Malings *et al.* 2020), model evaluation (Ridley *et al.* 2012; Kumar *et al.* 2022a) and assessing health impacts (Heft-Neal *et al.* 2018). Combining surface-based observations with satellite products is, however, challenging in general and there are several studies that have found poor agreement between satellite aerosol optical depth (AOD) and ground-based measurements (Hersey *et al.* 2015; Alvarado *et al.* 2019; Shindell *et al.* 2022). Key limitations include that satellite products often provide vertically integrated information, which may not always represent surface conditions, and that the spatial resolution and temporal frequency of satellite products can introduce representativeness errors (Tang *et al.* 2021; World Bank 2022a). Additionally, satellite products rely on *in-situ* observations for calibration and validation (Velazco *et al.* 2019; Paton-Walsh *et al.* 2022) and the limited *in-situ* observations over Africa mean that there is limited satellite validation for the continent. For example, in countries where ground-level monitoring data are not available, satellite estimates of surface $PM_{2.5}$ concentrations may have uncertainties up to 85 per cent (Alvarado *et al.* 2019). Ground-level monitoring networks and satellite products should be used together to monitor and understand air quality over Africa

For some instruments, the satellite data covers a long enough period over which pollutant trends can be determined. Tropospheric column NO_2 over Johannesburg, South Africa, for instance, and the Mpumalanga Province in South Africa decreased over 2005–2014 using data from the O_3 monitoring instrument (OMI) (Duncan *et al.* 2016). However, tropospheric SO_2 data from the Tropospheric Monitoring Instrument (TROPOMI) increased between December 2018 and September 2019 over coal-fired power stations in Mpumalanga, Gauteng and Limpopo in South Africa (Shikwambana *et al.* 2020). There are no trends in AOD and CO over Central and Southern Africa from the Measurement of Pollution in the Troposphere (MOPITT) and moderate resolution imaging spectroradiometer (MODIS) data over 2002–2018 (Buchholz *et al.* 2021).

Currently there are no existing or planned geostationary Earth orbit (GEO) satellites for air quality over Africa, and the studies above are all based on polar-orbiting satellites. GEO satellites have unique advantages in air-quality monitoring and study due to the possibility of high temporal resolution observations that are needed to resolve air quality-related processes. The air-quality monitoring and study would therefore benefit substantially from a GEO satellite for air quality over Africa in the future (Marais and Chance 2015).

MODEL-MEASUREMENT FUSION: RESULTS FROM THE GLOBAL BURDEN OF DISEASE FRAMEWORK

As well as combining satellite and *in-situ* measurement data, spatiotemporal coverage and information can be improved by the further addition of data from atmospheric chemistry models. Such combinations describe the basic premise of reanalysis products, which use a data assimilation framework to merge physical model output and measurements to provide a spatiotemporally continuous and consistent description of the state of the atmosphere (Inness *et al.* 2019). Other statistical approaches are available that do not require facilities to run complex data assimilation frameworks, such as the approaches of Shaddick *et al.* (2018a) and Shaddick *et al.* (2018b) for outdoor $PM_{2.5}$ and Zhang *et al.* (2019) for outdoor O_3, which both inform the GBD (GBD 2019) and the State of the Global Air reports (Health Effect Institute 2020). In brief, these similar approaches combine the output of global atmospheric chemistry models with ground-based monitoring and satellite observations of $PM_{2.5}$ or ground-based monitoring alone of O_3 in a Bayesian hierarchical framework, producing global estimates of $PM_{2.5}$ or O_3 on a 0.1° × 0.1° horizontal grid, ~10 km near the equator. One benefit of such frameworks over earlier approaches is that they also provide uncertainty information, such as 95 per cent credible intervals, although validation efforts still show biases (Garland *et al.* 2017).

Trends in population-weighted $PM_{2.5}$ and O_3 pollution from these approaches are shown in Figure 2.1 for five African regions from GBD (2019), which closely correlate to this Assessment's regions.

Over the whole 1990–2019 period, Western Africa consistently has the highest annual average population-weighted $PM_{2.5}$ levels, which reach up to 70 μg/m^3. The lowest levels are in Southern Africa, which were below 30 μg/m^3. Nevertheless, levels for all regions are consistently well above the WHO (2021) recommended limit of 5 μg/m^3. In terms of trends, $PM_{2.5}$ levels marginally decrease from 2010 across all regions except for Western Africa. These trends are consistent with two independent multi-year studies that use similar data sources (van Donkelaar *et al.* 2016; Rushingabigwi *et al.* 2020).

O_3 pollution, as $PM_{2.5}$, is also consistently at or above the WHO (2021) recommended limit of 30 ppbv (6-month mean of maximum 8-hour daily average),

with estimated population-weighted levels between 40–55 ppbv, depending on region. Unlike $PM_{2.5}$, O_3 is estimated to have increased since 2010. This decadal increase is strongest Western Africa, around +12.1 ppbv; followed by Central and Eastern Africa, approximately +11.4 ppbv; Southern Africa, about +8.3 ppb; and North Africa and the Middle East, around +2.3 ppbv, although this last region has the highest concentrations.

Figure 2.1 also shows the trends in the proportion of the population using solid fuel for cooking, an important contributor to household air pollution in several parts of Africa (Amegah *et al.* 2014). This information is not the output from a model-measurement fusion process but does form a critical part of the GBD Assessments. Figure 2.1 shows that the proportion of the population in Africa estimated to be dependent on solid fuels for domestic energy consumption has been decreasing, albeit with large variations between regions. This proportion is smallest in Northern Africa and has decreased from 22 per cent to 13 per cent of the population in the past decade. Measured in proportions, the largest decline is in Southern Africa, where solid fuel use has decreased from 58 per cent to 32 per cent of the population. Proportions are highest in Western, Eastern, and Central Africa, ~ 80–90 per cent, and this proportion has only declined marginally in Eastern Africa in the last three decades.

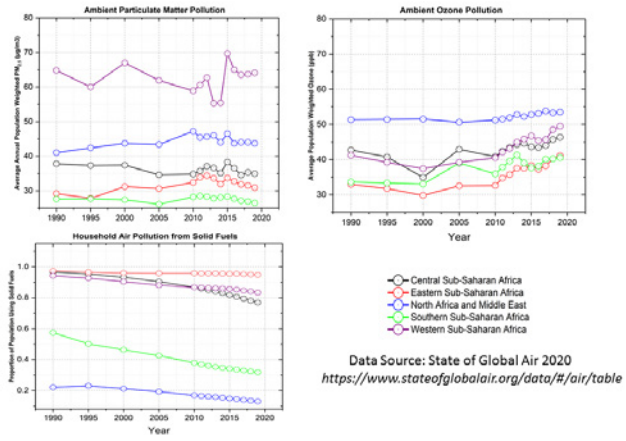

Figure 2.1 Africa, time series of population-weighted levels of (a) annual average outdoor fine particulate matter, microgams per cubic metre; (b) highest 8-hour daily average ozone, parts per billion; and (c) the proportion of population using solid fuels, 1990–2019, per cent Source: data are taken from the State of the Global Atmosphere report (Health Effect Institute 2020) which is based on GBD (2019).

2.2.2 CURRENT STATE OF POLLUTANT EMISSION ESTIMATES

Emissions data are needed as inputs to atmospheric models and to assess the impact of economic growth and mitigation policies. Africa is a global hotspot of dust and emissions from biomass burning (Ginoux *et al.* 2012; van der Werf *et al.* 2017; Kok *et al.* 2021), and these sources have received more attention than anthropogenic emission sources. In general, however, there is a paucity of emissions information and what is there is often highly uncertain. This in turn translates into large uncertainties in the understanding of air quality.

DUST

The Sahara and Sahel represent very significant sources of dust, which can be transported across the Atlantic (D'Almeida 1986; Swap *et al.* 1992; Moulin *et al.* 1998; Laurent *et al.* 2008; Toure *et al.* 2012; Prospero *et al.* 2014), towards Europe (Prospero and Lamb 2003; Borbely -Kiss *et al.* 2004), the Near East and Middle East (Israelevich *et al.* 2003), and possibly as far as Japan (Tanaka *et al.* 2005). Dust emissions may be directly calculated by atmospheric models based on several different physical parametrization schemes, which usually have a strong dependence on wind. Commonly used schemes, such as in the Weather and Research Forecasting (WRF) model, broadly reproduce the observed spatiotemporal distribution of dust., They fail, however, to correctly capture total dust (Zhao *et al.* 2010) and distribution dust maxima (Saidou Chaibou *et al.* 2020), biases which are difficult to resolve for all locations consistently (Flaounas *et al.* 2017), and are sensitive to the model's horizontal (Gueye and Jenkins 2019) and vertical (Teixeira *et al.* 2016) resolution.

BIOMASS BURNING

Burned area and biomass burning emissions in Africa contribute a large portion to the global budget, including an estimated 37 per cent of biomass burning CO_2 emissions and 35 per cent of biomass burning CO emissions (Wiedinmyer *et al.* 2022). Satellite products are critical to estimating biomass burning emissions at global or continental scales. Some inventories use satellite retrievals of the burned area combined with estimates of the fuel load, fuel-dependent emissions factors and combustion completeness, such as the Global Fire Emissions Database (GFED) (van Der Werf *et al.* 2017) and the Fire INventory from NCAR (FINN) (Wiedinmyer *et al.* 2011). Other inventories use satellite retrievals of

active fire detection and calculate emissions based on fire radiative power and emissions coefficients, such as the Global Fire Assimilation System (GFAS) (Kaiser *et al.* 2012), the Quick Fire Emissions Dataset (QFED) (Koster et al. 2015), and the Fire Energetics and Emissions Research (FEER) (Wang *et al.* 2018). Satellite-based inventories have important limitations and sources of uncertainty, including difficulties in detecting fires under clouds, when viewing angles are large, and in the gaps among satellites' consecutive swaths. Approaches to address these issues has resulted in improved atmospheric composition simulations over northern Africa (Wang *et al.* 2018) although it may also be needed to improve estimates of anthropogenic sources (Kuik *et al.* 2015).

Trends apparent in a recently constructed long-term inventory suggest that African biomass burning emissions declined overall between 1950 and 2015, attributed to the conversion of savanna to cropland (van Marle *et al.* 2017). At the same time, other inventories suggest a slight increasing trend over 2012–2019 (Wiedinmyer *et al.* 2022).

ANTHROPOGENIC EMISSIONS

Estimates of anthropogenic emissions depend on knowing the type and distribution of different emission sources as well as their use, so called activity factors, information that is not consistently available nor of consistent quality across Africa. These are important to know since it is expected that Africa's anthropogenic emissions are projected to grow hugely un the 21st century, contributing ~ 50 per cent to the global total anthropogenic of OC emissions by 2030, (Liousse et al. 2014). In an Africa wide study, Keita et al. (2021) reported that emissions of BC, OC, NOX, CO, SO_2 and microbial volatile organic compounds (MVOCs) increased by 95 per cent, 86 per cent, 113 per cent, 112 per cent, 97 per cent and 130 per cent, respectively between 1990 and 2015.

2.2.3 MODELLED PRESENT-DAY AND FUTURE AIR POLLUTION

There is a growing number of Africa-focused air pollution modelling studies, investigating questions related to atmospheric transport, isolating key drivers of air pollution, and assessing human and crop health impact. Over Nigeria, for instance, diffuse and inefficient combustion emissions have been found to have the largest individual contribution of >5 μg/m^3. to annual mean surface $PM_{2.5}$ (Marais and Wiedinmyer 2016), whereas open fires and fuel/industrial emissions make important contributions to surface O_3 (Marias *et al.* 2014). Over the whole of Africa, solid fuel combustion is estimated to lead to 84 000 premature deaths per year due to its impact on outdoor $PM_{2.5}$ levels (Gordon *et al.* 2021). In addition to local emissions, transboundary transport of CO emitted outside Africa, as well as its regional transport across African regions, is also important (Kumar *et al.* 2022a).

Many studies have found that under the current growth and policy trajectories, air pollution in many places in Africa is projected to increase. Annual emissions of SO_2, NOx and primary $PM_{2.5}$ from power plants and vehicles are projected to increase by 2030 relative to 2012. This increase will lead to a rise in outdoor $PM_{2.5}$, which is estimated to lead to ~ 48 000 additional air pollution related premature deaths from $PM_{2.5}$ in Africa, with three-times higher mortality rates from power plants than transport (Marais *et al.* 2019). In 2014, the emissions of trace gases and aerosols associated with charcoal production in Africa are estimated to have increased outdoor concentrations of $PM_{2.5}$ by 0.5–1.4 μg/m^3 and O_3 by 0.4–0.7 ppbv around densely populated cities in East and West Africa (Bockarie *et al.* 2020). Residential emissions are estimated to contribute the most, ~ 38 per cent to present-day air pollution from anthropogenic sources in Africa, with projected changes by 2030 estimated to make emissions related to energy combustion at ~ 45 per cent the most important cause of premature deaths from anthropogenic sources, ~ 79 000 (Lacey *et al.* 2017). Finally, additional NO emissions from enhanced fertilizer application are estimated to currently increase surface NOx and O_3 concentrations during the growing season, in turn leading to crop yield declines of 0.8 per cent in O_3-sensitive crops (Huang *et al.* 2018).

LOOKING FORWARD: AIR-QUALITY FORECASTS AS A USEFUL TOOL

Air quality forecasts for Africa can be accessed from the quasi-operational to operational air-quality forecasting systems run by different centres of the world, including the European Centre for Medium Range Weather Forecasting (ECMWF), the US-based Global Modeling and Assimilation Office (GMAO), the US NCAR, and ensemble dust forecasts generated by the Barcelona Supercomputing Center (BSC). International partnerships led by African researchers must be developed to downscale these global air-quality forecasts at regional and urban scales in

Africa and evaluate the accuracy of such multi-scale forecasts from observations. In addition, the World Meteorological Organization (WMO) has launched a multi-model intercomparison exercise – Air Quality Prediction and Forecasting Improvement for Africa (PREFIA) – to understand the ability of different models to simulate air quality in Africa.

2.2.4 FUTURE PROJECTIONS OF TEMPERATURE AND PRECIPITATION

Future global climate projections are available for a range of future scenarios from coordinated multi-climate model experiments conducted in support of the IPCC reports (IPCC 2021). The most recent of these is the Sixth Coupled Model Intercomparison Project (CMIP6) (Eyring *et al.* 2016) and a comprehensive analysis of the output from those models is available in the most recent IPCC report (IPCC 2021).

Figure 2.2 shows the CMIP6 multi-model mean of the multi-year annual mean current (2015–2024) and projected (2050–2059) near surface temperature and precipitation for Africa, and their difference, under the SSP3-7.0 scenario (van Vuuren *et al.* 2014). This scenario broadly represents a storyline in which there are significant challenges to both climate change mitigation and adaptation, resulting in global mean near-surface temperatures being more than 2 °C warmer than the pre-industrial period (1850–1900) by the middle of the century and being close to 4 °C warmer by the end of the century.

Under this scenario, temperature increases are projected across the continent, with the largest projected increases of more than 1 °C seen in the sub-tropics. The projected changes in precipitation are variable across Africa and the projections differ more strongly between models (IPCC 2021). Much of equatorial Africa is projected to see increases in precipitation, but drying is projected in parts of southern Africa, coastal western Africa, the western part of the northern Africa and northern part of Madagascar.

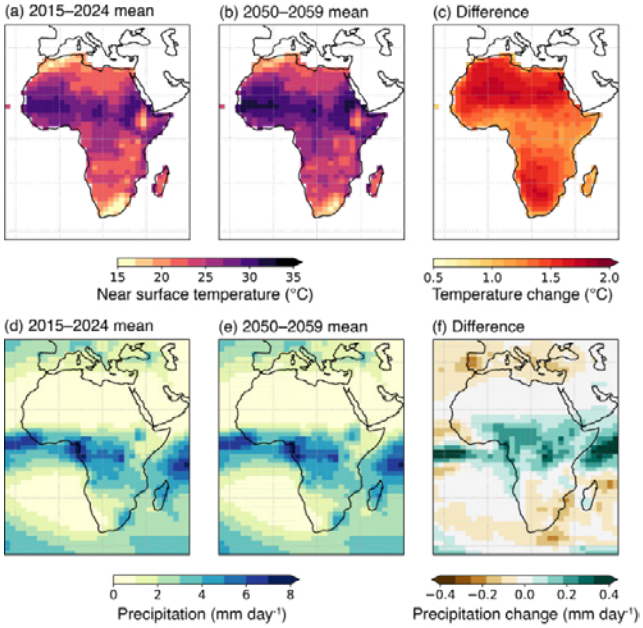

Figure 2.2 Africa, annual mean temperature and precipitation spatial distribution, 2015–2024 and 2050–2059, millimetres per day.

Annual mean, ensemble mean (top) near surface temperature (°C) and (bottom) precipitation (mm/day) over Africa for (a and d) the present day (2015–2024 mean), (b and e) the middle of the century (2050–2059 mean), and (c and f) the change (future minus past) between those two periods, as simulated by the CMIP6 models under the SSP3-7.0 scenario.

2.2.5 SUMMARY

Studies across Africa are sparse. Significant data gaps exist in relation to the current and future state of air quality and its impacts. Whatever available data exists indicates the elevated levels of outdoor air pollution across the continent. Factors such as increasing urbanization, the growth of populations and anthropogenic sources, poor fuel quality and slow technological interventions suggest increased emissions are expected in many areas and may worsen air quality in the future. This highlights the need for a continent-wide analysis of current and future emissions in order to better quantify the current and future impacts on health, climate and agriculture. The comprehensive and coherent approach of this Assessment will provide such an evidence base.

2.3 CURRENT AND FUTURE ECONOMIC, POPULATION AND URBANIZATION TRENDS IN AFRICA

MAIN MESSAGES

- By 2063, it is projected that 30 per cent of the global population will be living in Africa. This translates into Africa's population growing substantially, from 1.3 billion people in 2018 to 3.0 billion in 2063.
- Economic growth is projected to be driven by increases in the services sector and will account for the majority of GDP by 2063. The agricultural and industrial sectors are also projected to increase but will make up a relatively smaller fraction of Africa's economy by 2063.
- Africa's current rapid urbanization will continue its rising trend, leading to a higher proportion of households being in urban areas, about 69 per cent, than in rural areas by 2063.

It has been established that air pollution is a growing concern globally and the foremost environmental challenge in the developing countries of Africa (Assamoi and Liousse 2010; Knippertz *et al.* 2015a) primarily due to increasing population, subsequent rural-urban migration and the attendant rapid rate of urbanization which outpaces the infrastructural planning process, and coupled with industrialization (Liousse *et al.* 2014). With increasing population, urbanization becomes unavoidable, and both promote the drive for industrialization as a means to economic growth. Energy consumption, which is at the core of economic growth, is directly linked to anthropogenic emissions of pollutants. A projection of Africa's emission scenario would therefore require an understanding of the present and future trend of the drivers of population, urbanization and economic growth. This section presents results for the current and future economic, population and urbanization trends in Africa. These, the large-scale drivers that will impact Africa's growth in the future, were used in the LEAP model to develop the projected emission futures for the baseline scenario (this chapter) and mitigation scenarios (Chapter 3).

2.3.1 POPULATION TREND

The population for each country is projected based on the UN Population Division World Population Prospects Medium Variant (Figure 2.3, orange line). It is projected that the total African population will increase from 1.3 billion people in 2018 to 1.7 billion in 2030, and to 3.0 billion people in 2063 (Figure 2.3). In terms of the population growth rate, these increases represent a rate of 2.4 per cent per year between 2018 and 2030 and 1.8 per cent per year between 2030 and 2063. By 2063, there will 10.2 billion people in the world according to UN WPP Medium Variant estimates, meaning that about 30 per cent of the global population are estimated to be living in Africa, up from only 17 per cent in 2018. Currently in the 2020s, the African growth population rate of 2.3 per cent per year is more than twice the global average of 0.9 per cent per year. Also, by 2063, the global population growth rate is projected to fall to 0.33 per cent per year with population in regions such as Asia, Europe and Latin America projected to decline. Similarly, Africa's population growth rate will also decline to 1.37 projected to decline, but which will be around four times the global rate.

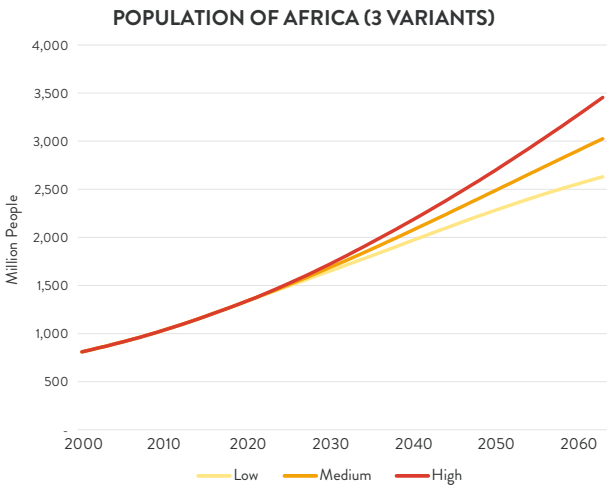

Figure 2.3 Africa, UN population projections, 2000–2063

Note: The medium variant (orange line) is used in this Assessment
Source: UN Population Division World Population Prospects

2.3.2 ECONOMIC TRENDS

The shared socioeconomic pathways (SSPs) provide alternative storylines as to how economies globally will develop. Substantial variations in the projections of economic growth across Africa are seen for 2018–2063 in the different SSPs (Figure 2.4a). In this Assessment the GDP projections from SSP2 (Figure 2.4a, orange line) have been used as the basis for projecting long-term economic growth across Africa. SSP2 provides a middle-of-the-road scenario, and a central estimate of economic growth across Africa compared to the other SSPs. Because the SSP scenarios were quantified before the advent of the COVID-19 pandemic, this Assessment made adjustments in the near term to account for the likely impacts of COVID-19 on medium term growth

prospects for each country in the region. Specifically, medium-term growth forecasts from the International Monetary Fund IMF's International Economic Outlook were applied to historical GDP data for the period up to 2025. Thereafter, GDP projections were based on the long-term growth rates in the SSP2 scenario.

Under the SSP2 scenario, the structure of Africa's economy is projected to change as a result of changes that will occur in the overall GDP from the agricultural, service and industrial sectors (Figure 2.4b). For example, while the services sector is projected to increase most substantially, accounting for the majority in the economy by 2063, the agricultural and industrial sectors are also projected to increase but make up a relatively smaller fraction of Africa's economy by 2063 (Figure 2.4b).

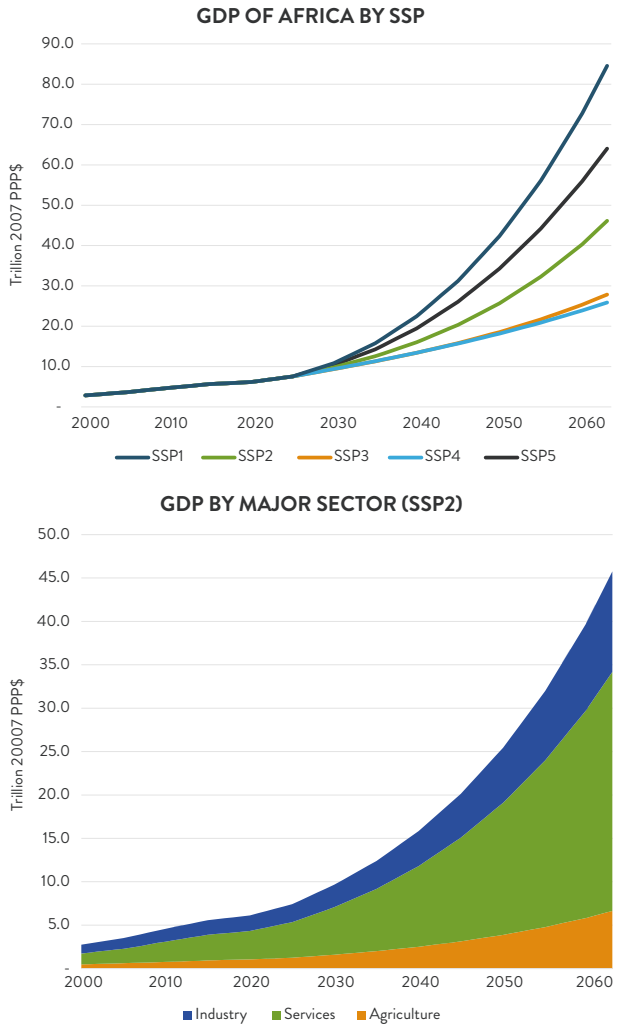

Figure 2.4 Africa's gross domestic product, 2000–2063, trillion[5] 2007 purchasing power parity dollars, (a) different shared socioeconomic pathways, and (b) the Shared Socioeconomic Pathway 2 scenario, disaggregated by the value added from the agricultural, services and industrial sectors. Source: WDI (2021).

5. Throughout this Assessment, trillion = 10^{12}

Total GDP is broken down into its three major components: the value added from the agricultural, services and industrial sectors using historical data from the World Bank's World Development Indicators (WDI 2021). Shares of value added are projected into the future using historical trends in the normalized shares of each sector. These trends indicate a growing share of GDP will come from the services sector, matching the trends seen in other regions of the world as income levels increase. Although the shares of industry and agriculture decrease, both sectors continue to grow significantly in absolute terms over the study period.

2.3.3 URBANIZATION TREND

The urbanization trends in this Assessment are based on the 2018 revision of the World Urbanization Prospects report (UNDESA 2018), with linear extrapolations for the period 2050–2063.

As the African continent is undergoing rapid urbanization (Chirisa 2008), this Assessment has included urbanization as a driver of development and emissions. Results reveal that by 2063 Africa is estimated to have almost 500 million households, more than double of the estimated number of households in 2018, with around six people per household. Also, the about 55 per cent of African households were estimated to be rural in 2018 (UN 2014). It is projected that there will be an increase in urban households and by 2030, there will be more urban households than rural ones in Africa (Figure 2.5). This increasing trend in urban households is projected to continue, reaching 69 per cent by 2063. Moreover, this increasing trend in urban households suggests an increase in urbanization all over the African continent.

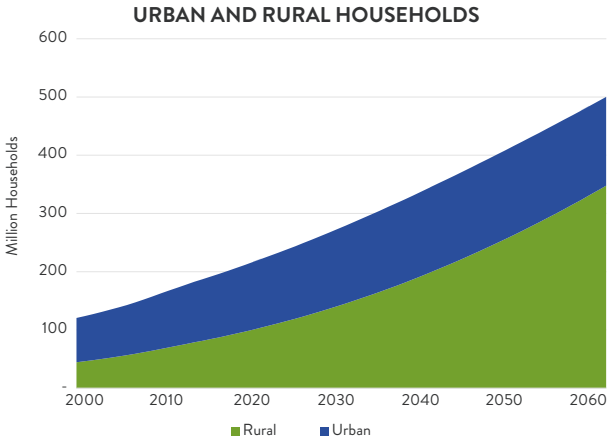

Figure 2.5 African households, 2000–2063, millions. Source: UNDESA (2018)

Into the future, the drivers of population, economy and urbanization in Africa will undergo rapid changes. As the total African population is expected to increase from 1.3 billion people in 2018 to 1.7 billion in 2030, and 3.0 billion people in 2063, the GDP will also increase, with the services sector becoming predominant. The current rapid urbanization of Africa will continue, leading to about 69 per cent of households being in urban areas by 2063.

2.4 DESCRIBING THE SECTOR TRAJECTORIES IN THE BASELINE SCENARIO

MAIN MESSAGES

- Historical and future projections under a baseline scenario of the drivers of the agricultural, energy and waste sectors' emissions are presented. Under the baseline assumptions, the modelling projects large increases in air pollution and GHG emissions for all parts of Africa.
- In the modelling framework applied, the agricultural sector is driven by the demand for food. As a result of the increases in population and income, total food demand in Africa is also projected to increase substantially, by almost 50 per cent between 2018 and 2030, and more than 2.5 times larger by 2063 compared to 2018 levels. The composition of the average diet is also projected to shift in the baseline scenario, with an increase in meat and dairy consumption.
- The baseline scenario shows an increase in energy demand. The residential sector will account for a significant share of this energy demand, though the total energy consumption in this sector will decrease slightly due to the transition to cleaner efficient fuels and stoves as a result of increasing incomes.
- By 2063, transport will be the largest energy consuming sector followed by the industrial sector. The large increase in transport energy demand will overwhelmingly come from road transport, which will be split roughly 50/50 between freight and passenger transport, with a large growth expected in the number of private cars.
- The total amount of collected and uncollected waste is projected to increase. From 2030 a slight decrease is expected in the open burning of waste, which implies a change in waste management towards greater collection, increased resource-use efficiency, adoption of circular economy and disposal of absolute waste in sanitary landfills.

This section details sector-specific drivers used in the Assessment to develop the baseline scenario. The population, economic and urbanization trends (Section 2.3) informed sector-specific projections for agriculture, energy, and waste in the baseline scenario. In addition to the results of drivers per sector, a summary of the methods and sources of data used are presented per sector and sub-sector in the energy sector; a more detailed technical description of the inputs and assumptions per sector is given in Annex 2.3. It is important to note that the development of all of the scenarios in this Assessment followed a participatory and consultative approach that included discussions and feedback on methods applied, data sources used, and assumptions applied.

2.4.1 AGRICULTURE

SUMMARY OF METHODS USED AND SOURCES OF DATA

The method and historical data used to quantify GHG, SLCP and air pollutant emissions from the agriculture sector is an application of the modelling framework presented in Malley *et al.* (2021). The agricultural GHG, SLCP and air pollutant emission sources covered include:

i. livestock – CH_4;
ii. manure management, application and deposition – CH_4, N_2O, NOx and NH_3;
iii. synthetic fertiliser application – N_2O, NOx and NH_3;
iv. agricultural residue burning;
v. fuel combustion in agricultural machinery.

The modelling framework is a demand driven model. Therefore, the food demand is the key variable that determines the level of livestock and crop production necessary to meet this demand, accounting for food imports and food exports (Malley *et al.* 2021).

RESULTS

Across Africa, between 2014 and 2018, the average person had approximately 2 600 kilocalories per day available for consumption – i.e., the food actually consumed plus the food wasted at the point of consumption (Figure 2.6a). This is equivalent to more than a million billion (1015) kilocalories consumed per year (Figure 2.6b). Approximately half of this food demand was met by cereals, with roots and pulses making up other significant fractions of food intake from crops (Figure 2.6a). Consumption of livestock products contributed approximately 200 kilocalories per person per day to the average African diet, less than 10 per cent of food intake available. Beef and dairy from cattle contributed approximately half of all livestock products consumption, with pork, poultry (meat and eggs), sheep and goats contributing the remainder.

In the baseline scenario, the key driver, projected into the future to understand the changing emissions in the agricultural sector, was food demand. Future food demand in the baseline scenario reflects changes in the total number of kilocalories consumed and changes in the types of food products that are consumed. The future population and income (GDP per person) (shown in Section 2.3, Figures 2.3 and 2.4) are used to estimate future food demand. Increases in population reflect the larger number of people in Africa consuming food in the future, while increases in income show strong relationships with i) increases in overall daily kilocalorie intake, and ii) increases in the consumption of specific food products, such as meat. Gouel and Guimbard (2019) calculate elasticities between changes in income levels and consumption of different food categories, which have been applied in this work with GDP per person projections from SSP2 to assess how changes in income will affect diets in Africa between 2019 and 2063. In general, this leads to increased consumption of meat and dairy, oils and fats, and sugar and other sweeteners as incomes rise, while the proportion of diet met by cereals, pulses, root crops and other staples decreases (Gouel and Guimbard 2019). As seen in Figure 2.3 the African population is projected to increase from 1.3 billion people in 2018, to 1.7 billion by 2030, and 3.0 billion people in 2063. Meanwhile, average incomes are projected in the baseline to increase from US$ 2 100 per person per year in 2018, to US$ 3 000 in 2030, and US$ 7 600 per person per year in 2063.

As a result of these increases in population and income levels, total food demand (Figure 2.6b) is also projected to increase substantially, with an almost 50 per cent increase between 2018 and 2030, and more than 2.5 times larger by 2063 compared to 2018 levels. This equates to an average daily kilocalorie intake across Africa of 2 900 kilocalories per person per day in 2063 (Figure 2.6a).

The composition of the average diet is also expected change in the baseline scenario. This Assessment found that an increase in meat and dairy consumption is projected, with this category contributing 250 kilocalories of food demand per day in 2030, around 10 per cent of average daily kilocalorie intake, and 493 kilocalories per day in 2063, about 17 per cent of average daily kilocalorie intake (Table 2.2). This consumption of meat and dairy remains well below consumption levels in high-income countries', the average United States food intake, for example, has 1 000 kilocalories of meat and dairy available per person per day.

Compared to 2018, the consumption of vegetable oils, sugar, fruit and vegetables is also projected to make a larger proportional contribution to the average African daily food consumption in 2063 (Table 2.2). Despite a proportional decrease in the contribution of cereals, pulses and root crops to the diet composition in the baseline scenario, these crops still constitute the largest overall fraction of the average African diet in 2063 – about 51 per cent of average daily kilocalorie intake. This, combined with the substantial increase in population, means that the overall demand increases for these staple crops (Figure 2.6b), along with the overall demand for meat and dairy, and other crops.

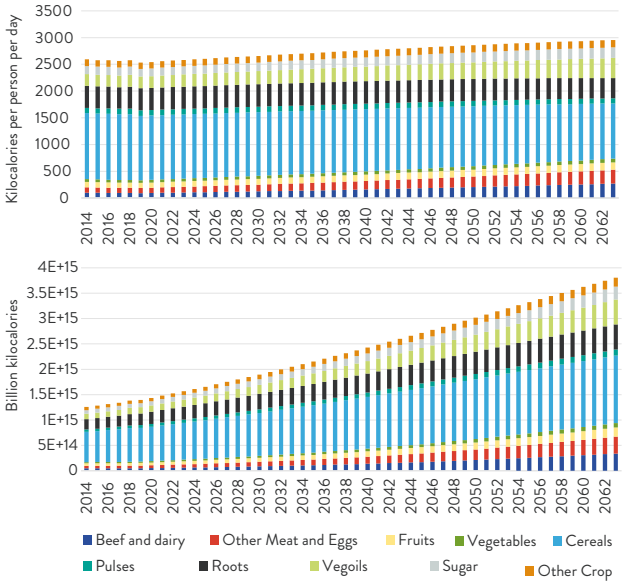

Figure 2.6 Africa, (a) average daily kilocalorie intake, 2014–2018 (historical data) and 2019–2063 for the baseline scenario, (b) total number of kilocalories consumed by Africa's population, 2014–2018 (historical data) and 2019–2063 for the baseline scenario

Table 2.2 Africa, average consumption per food group of daily food consumption, 2018, 2030 and 2063, per cent

MAJOR FOOD GROUPS	PER CENT		
	2018	2030	2063
BEEF AND DAIRY	3.56	4.57	8.91
OTHER MEAT AND EGGS	3.74	4.74	8.77
FRUITS	3.78	4.16	4.75
VEGETABLES	1.93	2.06	2.29
CEREALS	47.64	44.59	34.87
PULSES	4.01	3.80	3.17
ROOTS	16.18	16.08	13.02
VEGETABLE OILS	8.76	9.39	12.89
SUGAR	5.78	5.95	6.69
OTHER CROPS	4.62	4.66	4.65

2.4.2 ENERGY

SUMMARY OF METHODS USED AND SOURCES OF DATA

Energy consumption is modelled in the baseline scenario by assessing likely trends in economic activities; energy intensities, energy per unit activity; and emission factors, emissions per unit energy consumption, in each of the main energy consuming sectors: industry, transport, households, services, agriculture and fishing, and the non-energy use of fuels.

Historical energy consumption statistics for the period 2000–2018 are used to establish trends and to overall levels of energy consumption in 2018 for calibrating the more detailed bottom-up calculations used in the projections for the period 2019-2063. Energy consumption statistics are taken from the International Energy Agency's (IEA) World Energy Balances (IEA 2020) where available, or from the UN Energy Statistics Database (UN 2018) for countries not covered by IEA data. For each country, these data are used to establish overall levels of historical consumption and fuel shares for each major fuel in each sector for the period 2000–2018.

Activity levels in the industry, agricultural and services sectors for each country are taken directly from the value-added projections described in Section 2.3.2. In the household sector, the number of households in each country is used as the main indicator of energy use. Household numbers are calculated from the projection of population and household size –people per household. In the transport sector, a variety of methods are used to project activities depending on the mode (Section 2.4.2.3), but in each case the methods are tied to the change in average income seen in each country implied by the GDP and population projections described earlier.

Historical data on activity levels and overall energy consumption are combined to calculate historical energy intensity trends for the period 2000–2018 in all sectors. Two different approaches were adopted for projecting energy consumption into the future in the baseline scenario. For the industrial, services, agricultural and non-energy sectors where detailed data was not available, energy consumption is projected forward by extrapolating the trends in energy intensities and normalized fuel shares in combination with the previously described activity-level projections for value added and GDP for each country. For the transport and household sectors, a more detailed bottom-up end-use oriented approach was adopted, providing greater insights into the end uses and technologies used in each sector and enabling assessment of important trends such as urbanization, transport-mode shifts, and the role of passenger *versus* freight transport.

RESULTS

Energy demand for all types of fuels were modelled using the baseline scenario results show that for the entire African continent there will be an increase in energy demand of about 37 per cent in 2030 compared to 2018. This increase in energy demand will continue and reach 164 per cent of 2018 levels between 2030 and 2063 (Figure 2.7a). Also, main sectors, such as the residential sector identified as high energy consuming in 2018 (IEA 2019), will continue to be significant in the baseline scenario. In terms of total energy consumption, however, there is a slight decrease as the result of income increasing due to the transition tow cleaner and more efficient fuel use. In addition, sectors, such as industry and transport, will record the largest increase in the energy demand between 2018 and 2030. By 2063, the transport sector will stand as the largest energy consuming sector followed by the industrial sector.

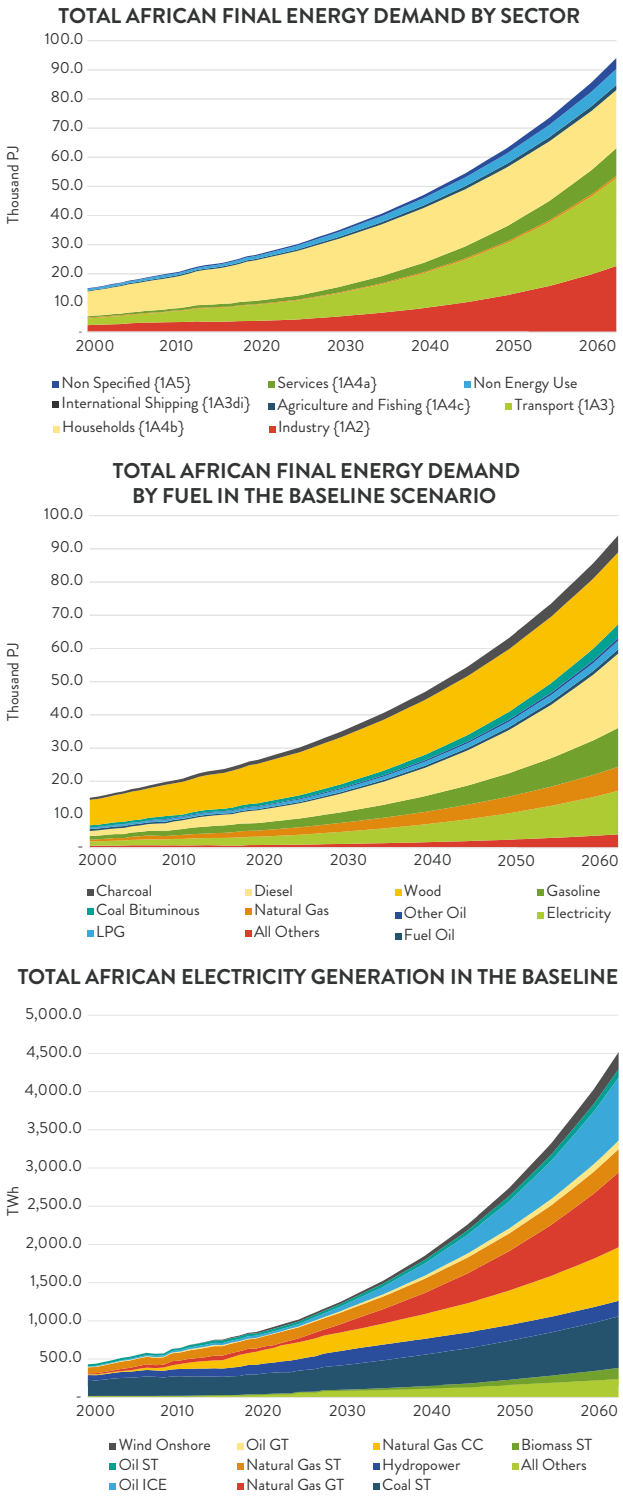

Figure 2.7 Africa, (a) total final energy demand disaggregated by sector, 2000–2063, thousand petajoules; (b) total final energy demand disaggregated by fuel, 2000–2063, thousand petajoules; and (c) electricity generation disaggregated by fuel, 2000–2063, '000 terawatt hours.

The analysis of trends in the energy consumption of different sectors emphasizes the expected changes of different fuel types over the entire period considered, 2000–2063. Demand for oil and gas are projected to increase substantially (Figure 2.7b). This is true especially for diesel and gasoline fuel types. Concerning the use of biomass, it remains constant in the model as the result of a balance between the increase in the number of households and a larger fraction of households switching to the use of cleaner fuels – away from wood and increases in the use of charcoal and LPG – and a change in cooking technology.

Finally, electricity demand is also projected to increase substantially as a result of a significant increase in electricity generation (Figure 2.7c). Electricity generation will be mainly met through increases in natural gas and diesel, while coal, hydro and other renewable energy sources are projected to have more limited increases.

2.4.2.1 INDUSTRY

The industrial sector emissions were estimated based on their historical energy consumption, with their projection based on the growth in the GDP from industry (Figure 2.4b). It is important to underline the lack of data that would have contributed to providing individual growth projections for the industrial sector and associated sub-sectors. Thus, in this Assessment, it is assumed that the industrial growth rate remains the same for all industrial and associated sub-sectors. This implies that, when potential changes occur in major economic sectors, such as agricultures and services, and are represented in the modelling, these changes do not reflect in the modelling of the industrial sector.

It is projected that the African economy's size as a whole will increase by 64 per cent by 2030 compared to the 2018 level, and this increasing trend will continue to 2063, by when it will be more than seven times higher than in 2018 (Figure 2.4b). In 2018, African industry accounted for 29 per cent of GDP, equivalent to 2007 PPP US$ 1.75 billion. The absolute value of the industrial sector is projected to increase by 47 per cent and 559 per cent, respectively, by 2030 and 2063. The relative contribution of industry is, however, projected to decrease slightly, to 26 per cent of Africa's economy by 2030, and 25 per cent by 2063, as result of the important increases in the service sector's contribution to GDP.

2.4.2.2 RESIDENTIAL/HOUSEHOLDS

SUMMARY OF METHODS USED AND SOURCES OF DATA

For the household sector, a bottom-up model was established that separately estimates the energy consumption in urban and rural households in each country for each major end use, i.e., cooking, lighting, refrigeration, air conditioning and other uses. The model was based on a variety of databases and models including the WHO's cooking and lighting databases (WHO 2019) that describe the main fuels used for cooking and lighting in different countries, the BUENAS modelling methodology used to estimate air conditioning and refrigerator stocks as a function of national income levels and, in the case of air conditioning, average national climate conditions as measured by cooling degree days (McNeil *et al.* 2012), and the Global Data Labs (GDL) database of development indicators (Smits and Permanyer 2019)

This bottom-up model was calibrated to closely match the top-down historical energy-consumption data taken from the IEA and UN energy databases for the first scenario year (2018) and then the bottom-up model was used as the basis for projections for the period 2019–2063. In the baseline scenario, these projections took into account overall trends in population growth, urbanization, declining average household sizes, growing average income levels and increasing air conditioning needs due to climate change. The model also took account of the gradual transition away from traditional fuels, wood, charcoal, kerosene, coal, dung, etc., and toward the use of cleaner fuels (LPG, natural gas, electricity) for cooking and lighting driven by these income trends. It is assumed that these trends will occur in the baseline scenario to some extent, even in the absence of active policies promoting clean cooking and lighting, as has happened in most regions of the world. Specifically, in the baseline scenario it is conservatively assumed that the transition to modern fuels will be completed in urban areas once average per person incomes reach PPP US$ 30 000 and PPP U$ 35 000 in rural areas.

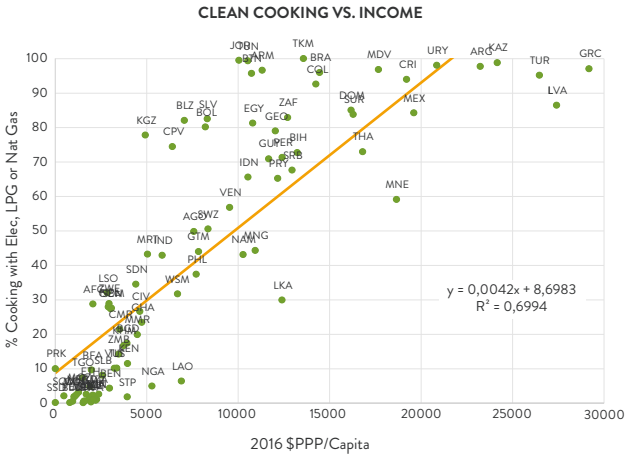

Figure 2.8 Multi-country regression showing predominance of clean cooking fuels *versus* average income levels, per cent and 2016 PPP US$ per person

Source: WHO cooking database (WHO 2019) World Bank Development Indicators (WDI 2022).

The model assumes that as countries average per person income approaches these values, so the share of clean fuels used approaches 100 per cent (Figure 2.8). Most African countries are not projected to reach these average income levels in the study period – the median per person average income level in 2063 is PPP US$ 13 300 – and thus the baseline scenario shows only a partial transition from traditional to cleaner fuel use.

Another important factor is urbanization. Urban households tend to have greater access to cleaner fuels for cooking and lighting, but they also tend to make greater use of charcoal compared to rural ones, in which wood fuel is more common. Thus, in the baseline scenario, urbanization trends tend to emphasize the transition to cleaner fuels but they also tend to prolong the use of charcoal, which in turn tends to increase the use of wood as a fuel due to the inefficiency of charcoal making processes.

RESULTS

Some of the overall energy demand results of the modelling in the household sector are illustrated in Figure 2.9 for Africa as a whole. There is a close correlation of results between the historical period (2000–2018) and the bottom-up projections for the period 2019–2063. Note also that final consumption of wood and dung (primary biomass) peaks in 2045, while charcoal consumption continues to grow until 2060. Figure 2.9c illustrates the projected end use of the fuels. It can be seen that a majority of the use is for cooking in both rural and urban areas.

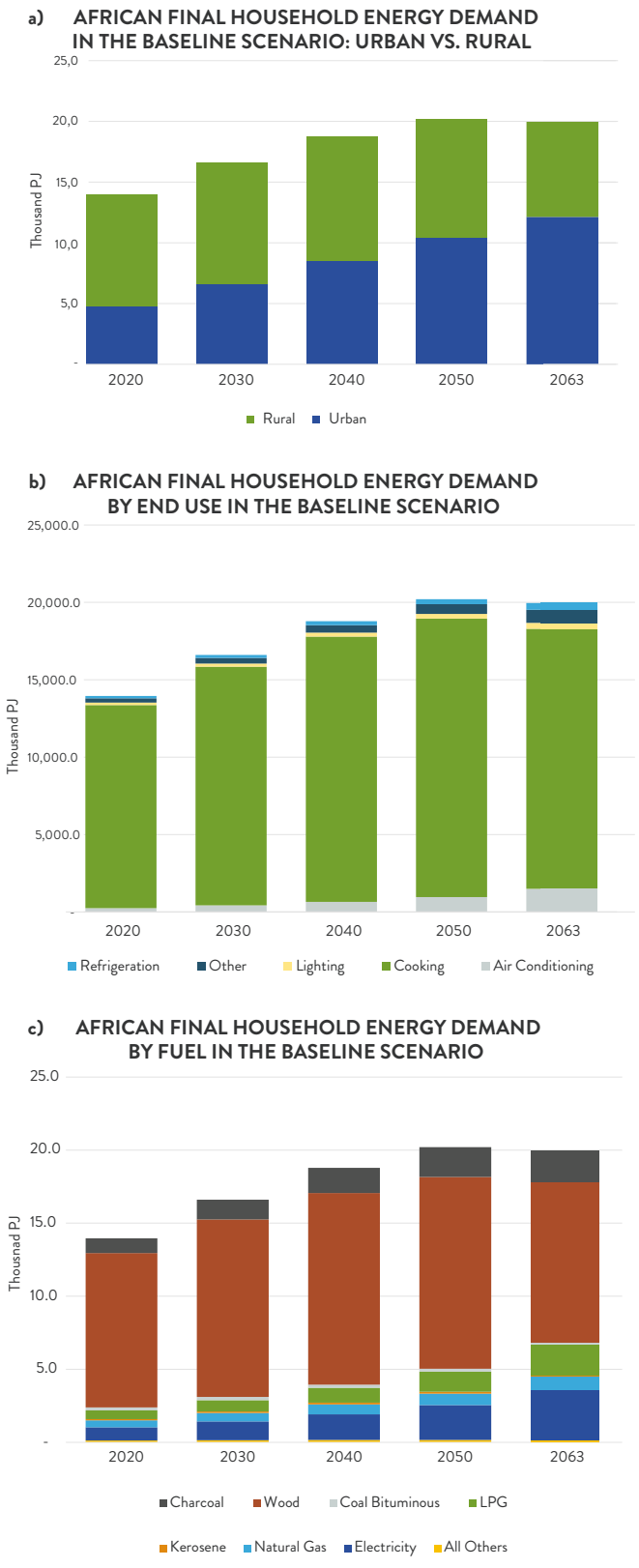

Figure 2.9 Africa final household energy demand in the baseline scenario: 2000–2063 (a) urban versus rural, (b) by fuelend use, and (c) total final energy consumption scenario,by fuel, 202019–2063, million tonnes of oil equivalent

Many households across Africa use multiple fuels for cooking, even when electricity is the primary one (Masera *et al.* 2000; Madubansi and Shackelton 2007; Uhunamure *et al.* 2017). The number of households disaggregated by fuel type used for cooking is shown in Figure 2.10. The number of households is estimated to increase from around 200 million in 2020 to more than 450 million in 2063 (Figure 2.10). It is also projected that there will be a gradual shift to the use of gas (light red) and electricity (dark red) for cooking. The electricity used for cooking will increase in 2063 compared to the current period. This increase in electricity use is not homogenous everywhere in Africa (Annex 2.3). While, for example, the use of electricity for cooking does not increase in the central part of Africa, where gas remains the major clean fuel that increases penetration in the baseline, or in Southern Africa as there is currently a substantial fraction of the population already using electricity. Therefore, the baseline scenario reflects a larger proportion of population using electric cooking over Southern Africa compared to other parts of the continent, currently and in the future. In addition, in North Africa, gas, which currently is the dominant fuel for cooking, will remain predominant in the baseline scenario. Overall, despite the use of cleaner fuels, gas and electricity, increasing over the continent, there will still be an important absolute number of households using biomass, wood and charcoal. The technology for cooking using wood and charcoal in the baseline is assumed to remain as the traditional lower-efficiency biomass stoves.

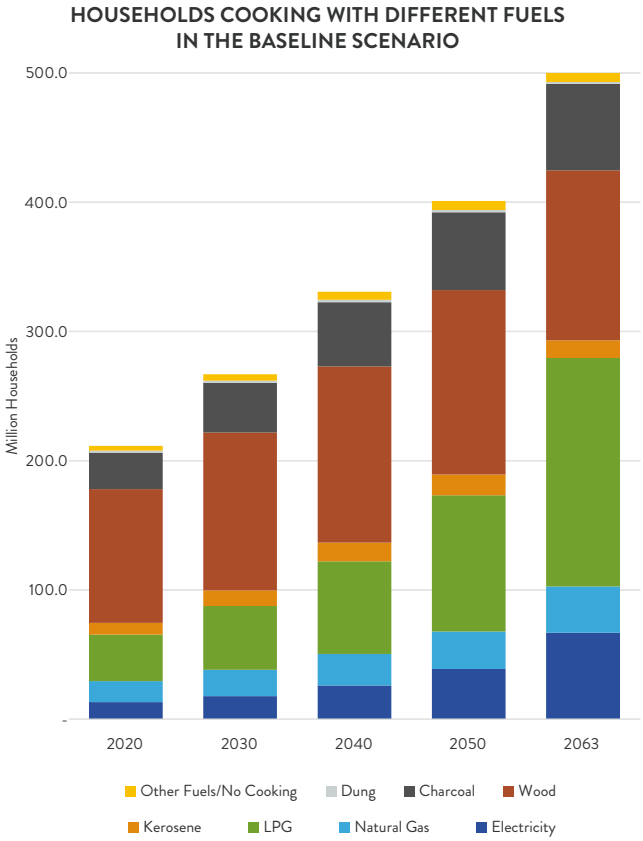

Figure 2.10 Africa, households cooking using different fuels and technologies in the baseline scenario, 2019–2063, millions

2.4.2.3 TRANSPORT SUMMARY OF METHODS USED AND SOURCES OF DATA

As in the household sector, modelling of transport sector was also based on a bottom-up model that took account of different modes, road, rail, aviation, shipping and pipelines, where possible differentiated between passenger and freight transport. It also considered different vehicle types – cars and taxis, buses, motorcycles and non-motorized transport passenger transport, and light- and heavy-duty road freight. The modelling also took into account different technologies, such as internal combustion engines, hybrid and pure electric vehicles, and fuels, including diesel, gasoline and electricity. Finally, the modelling also considered different emission-control technologies. In particular, for internal combustion engine vehicles technologies with no emissions controls were considered, as well as the possibility of moving to basic, European Emission Standard II) and then more advanced emissions controls (European Emission Standard V).

The detailed bottom-up projections by mode and technology were based on a variety of data sources, which were used to develop activity-level projections. For transport estimates of vehicles, vehicle-kilometres (number of vehicles x average length of distance travelled) and passenger-kilometres (number of passengers transported x average distance travelled) were developed based on such sources as the International Organisation of Motor Vehicle Manufacturers (OICA[6]) for vehicle numbers by country, the International Council on Clean Transport (ICCT) Transport Roadmap (ICCT 2013) for data on load factor and annual average distance travelled for road transport. For rail transport, passenger-kilometres and tonne-kilometres (mass of freight transport x average distance travelled) data compiled in the World Bank WDI (WDI 2022) were used, which in turn draw upon data from the International Union of Railways (UIC). Similarly, for air transport, WDI data for freight- and passenger-kilometres drawn from the International Civil Aviation Organization (ICAO), civil aviation statistics were used. Fuel economy estimates for different modes and vehicles were drawn from a variety of past LEAP analyses for Ethiopia, Ghana, Kenya, South Africa and Uganda. Energy intensities for other modes are based on a variety of sources, such as the 2012 IEA/UIC Railway Handbook or are calculated endogenously, based on the energy consumption statistics from the IEA and UN Energy Statistics database.

6. https://www.oica.net/

As in the household sector, the bottom-up model was calibrated to match with the top-down historical energy consumption data within each country, mode and fuel. These data were taken from the IEA and UN energy databases for the first scenario year, 2018, and then the bottom-up model was used as the basis for projections for the period 2019–2063. For road transport, future vehicle numbers were projected as the product of population and the number of vehicles per person. Vehicles per person for each country were estimated based on a multi-country regression of vehicle ownership and average income per person (Figure 2.11).

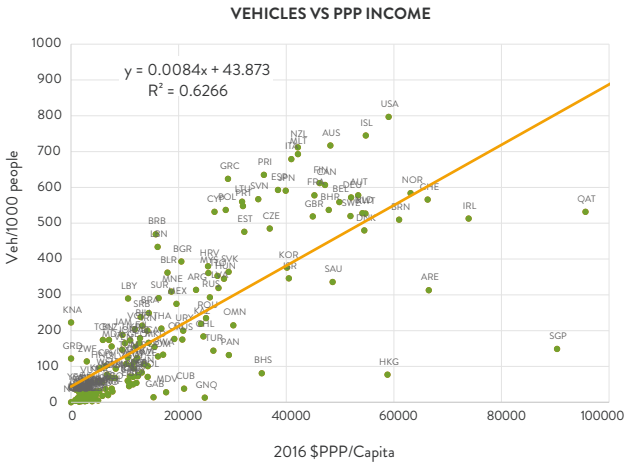

Figure 2.11 Multi-country regression of vehicle ownership and average income, vehicles per '000 people and PPP US$ per person

Source: OICA, ICCT and World Bank (see Section 2.4.2.3 for details).

This regression indicates that ownership approaches roughly one vehicle per person as average annual incomes approach 2016 PPP US$ 120 000 per person. No African countries approach such income levels over the study period; thus, in the model, it is assumed that vehicle ownership will increase based on the growth in average income in each country. The result is that median levels of vehicle ownership in Africa increase from 40 vehicles per 1 000 people today to about 122 vehicles per 1 000 people in 2063. Some countries do see vehicle ownership in 2063 above 600 vehicles per 1 000 people, which is similar to levels seen today in some high- income countries. Growth in other modes is assumed to follow the national GDP growth rate.

The transport sector is modelled in the LEAP based on the demand for passenger and freight transport. This demand used the number of passenger- and tonnes-kilometres. Since it is expected that the population and economy in Africa will increase substantially, it is also expected that transport demand for both passengers and freight will increase. Therefore, for transport, the number of passenger-kilometres is projected to increase by about 51 per cent between 2018 and 2030, and by 2063 it is projected to be almost four times 2030 levels (Figure 2.12a). Similarly, for freight transport, the number of tonnes-kilometres will increase about 49 per cent between 2018 and 2030 and in 2063 will be 3.6 times 2030 levels (Figure 2.12b).

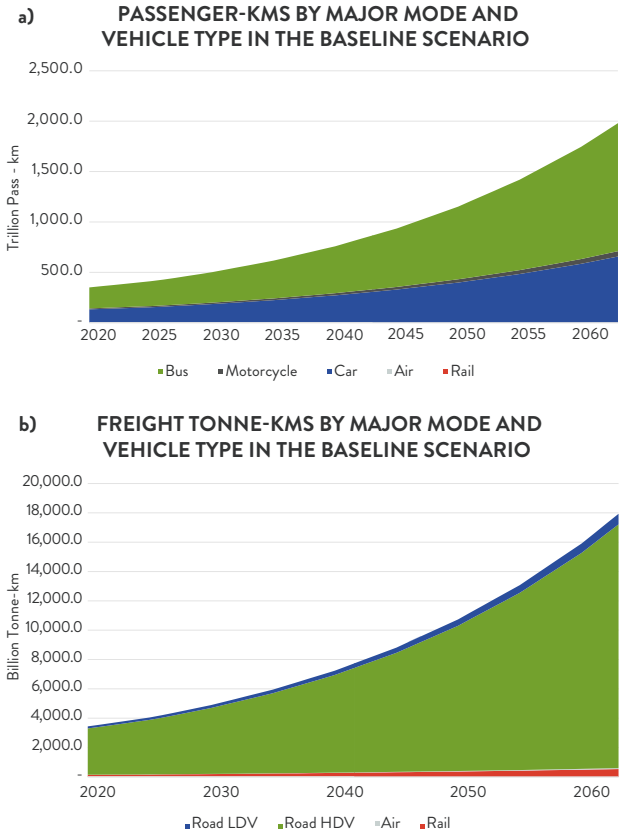

Figure 2.12 Africa, (a) total passenger transport demand disaggregated by transport mode, trillion passenger-kilometres and (b) total freight transport demand disaggregated by transport mode, billion tonnes-kilometres, 2000–2063 (see Section 2.4.2.3 for data sources behind projections)

RESULTS

The baseline scenario assumes very little change in terms of fuel, technology, modal shifts or transport-demand management. In particular, it assumes no significant electrification of transport and measures to improve fuel economy or reduce tailpipe transport emission factors.

The resulting energy consumption trends in the baseline scenario for the transport sector are shown for Africa as a whole in Figures 2.13 a, b and c. The baseline scenario reflects a future with tremendous growth in transport energy demand, which is met overwhelmingly by road transport (Figure 2.13a). Transport fuel use is dominated by gasoline and diesel consumption (Figure 2.13b) with electricity consumption in the baseline scenario remaining insignificant in 2063. Energy consumption for road transport is split roughly 50/50 between freight and passenger transport, with significant growth expected in the number of private cars and their energy use (Figure 2.13c).

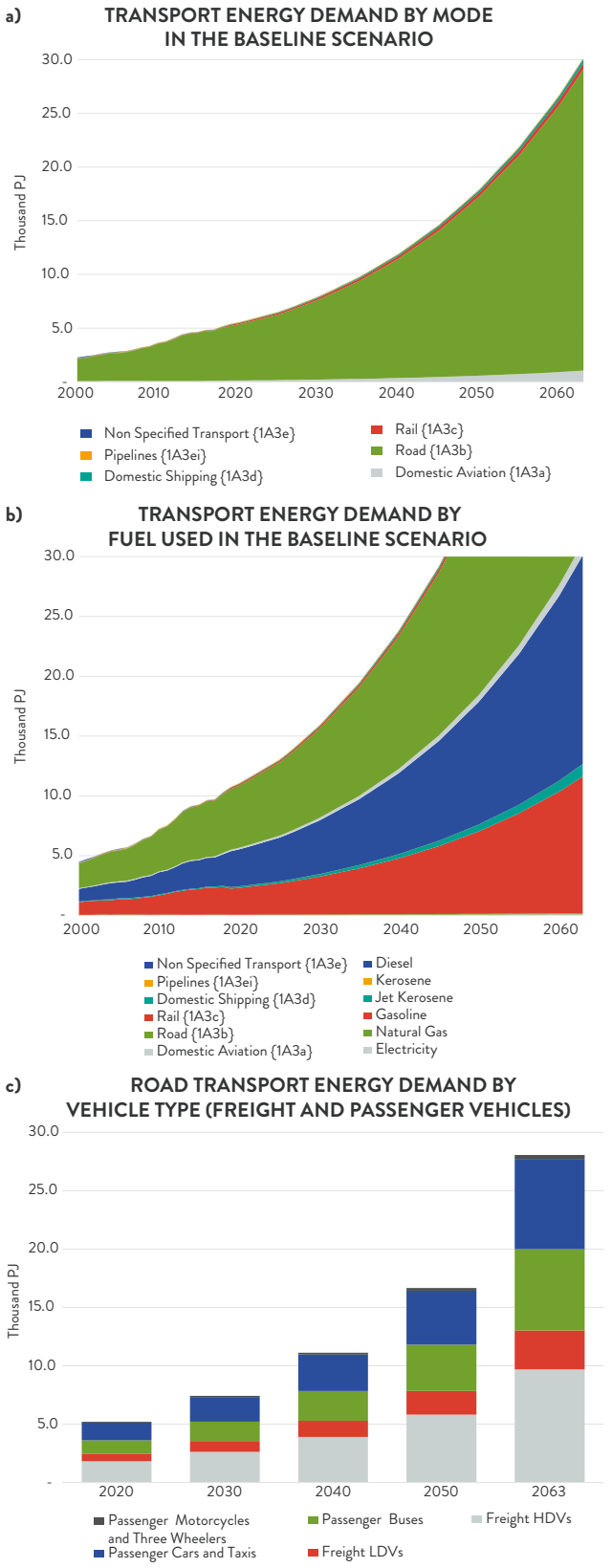

Figure 2.13 Africa, total energy consumption for road transport by (a) mode of transport, 2000–2063, (b) fuel used, 2000–2063, and (c) vehicle type in freight and passenger, 2019–2063, thousand petajoules.

2.4.2.4 ENERGY SECTOR TRANSFORMATION

To ensure the energy-sector modelling comprehensively covered all energy-sector emissions of GHGs and SLCPs the LEAP model for Africa also covered all major energy-transformation sectors – i.e., transmission, distribution and conversion. The model was based on the sectoral structure adopted by the IEA for its reporting of national energy balances and included modelling of the following basic sectors: transfers; transmission and distribution; energy sector own use; electricity generation; oil refining; coal and gas liquefaction, only important in Nigeria and South Africa; charcoal making; coal mining; and oil and gas extraction. Using this structure allows standard format energy balances to be produced for each country and region, and the continent as a whole, as well as also helping to ensure that emissions reporting matches the standards adopted by the IPCC and UNFCCC.

Most of these sectors were modelled in a relatively simple fashion based on high-level historical energy statistics maintained by the IEA in its World Energy Balances data (IEA 2021) or the UN in its Energy Statistics database (UN 2021) for countries not covered by the IEA database. These data were used to calculate inputs, outputs, high level conversion efficiencies, and levels of fuel imports to and exports from each country. In some cases, data gaps, mainly for smaller countries, were filled by calculating Africa-wide average values.

For most sectors, the baseline scenario assumed no future changes in energy efficiencies and the energy trade, and a gradual increase in production driven by growing demands for energy calculated previously. This reflects the baseline scenario's assumed absence of explicit new energy and emissions policies.

Some sectors, such as electricity generation, were modelled in more detail reflecting their importance as sources of GHGs and SLCPs. Modelling of the electricity-generation sector included both historical and forward-looking modelling of its generation capacity data for different types of power plants and simplified modelling of the likely production of those power plants. Accurate modelling of this is important for improving the accuracy of emission calculations, since many of most polluting fossil-fuel power plants are used primarily to meet peak electricity demands in some African countries, which otherwise rely on hydropower for much of their baseload. Twenty types of power plants were modelled reflecting different feedstocks – coal, oil, natural gas, biomass, nuclear, hydropower, wind, solar, geothermal, municipal solid waste, etc.; and different technologies – steam turbine, gas turbine, combined cycle, internal combustion engine, onshore and offshore wind, photovoltaics, etc.

Historical modelling of the generating capacity of these plants was based on data aggregated from the Global Power Plants Database (WRI GPPDB 2020), supplemented by the S&P World Electric Power Plants Database (WEPP 2020) and the IEA World Energy Balances (IEA 2021). Additional sources were used to estimate technical characteristics of electric generating systems, such as plant efficiencies and capacity factors. These sources included the National Renewable Energy Laboratory (NREL) Annual Technology Baseline (ATB 2020), the Energy Technology Systems Analysis Program (ETSAP) Technology Briefs (2010-2013), the IEA's World Energy Balances, and SEI's own estimates from past LEAP-based studies of African national energy systems.

The GPPDB and WEPP, which include data describing planned future additions and retirements of power plants, were used as the basis for estimating likely future capacity additions of each different power plant type for the period 2018–2024. For the period 2025–2063, further capacity additions in the baseline scenario were assumed to follow the patterns of additions made in each country for the period 2010–2025. In the case of hydropower, geothermal, wind and solar energy, these levels of additions were cross-checked, and where necessary constrained against estimates of the total maximum economic potential for those technologies to ensure that the extrapolated additions did not exceed the total resource base. The resource base for these technologies was estimated from a variety of resources including the World Energy Council's Survey of World Energy Resources (WEC, 2013) and the International Renewable Energy Agency (IRENA) report *Estimating the Renewable Energy Potential in Africa* (IRENA 2014, 2021).

Another very important transformation sector for Africa is charcoal making. For this sector, current and more advanced charcoal kilns were separately modelled. The efficiency of existing kilns was calculated from the IEA's World Energy Balances (IEA 2021). Charcoal making efficiency varies by country but on average is only about 26.9 per cent efficient, on an energy basis, for the continent. To reduce the growth in demand for primary biomass, it will be vital both to transition away from charcoal consumption and to improve the efficiency of charcoal making. Therefore, the possibility of switching to more efficient charcoal kilns, which are assumed to have an energy efficiency of 47 per cent, is included. These kilns are not, however, employed in the baseline scenario, in which the efficiency of kilns remains constant.

The Stockholm Environment Institute's standard sets of emission factors for GHGs and SLCPs were employed to calculate both combustion- and process-related emissions from each sector. It should be noted that, in some sectors such as electricity generation, emissions are calculated in proportion to the energy content of the feedstock fuels used in each process. In other sectors, such as oil refining, emissions calculations are based on the auxiliary fuel consumption in the refinery, rather than the quantity of crude oil it processed. In other sectors, such as charcoal making, sector-specific emissions factors were utilised from a variety of sources. The Institute's standard set of emission factors used in these analyses are those of Vallack and Rypdal (2019).

2.4.3 WASTE

SUMMARY OF METHODS USED AND SOURCES OF DATA

The waste emissions modelling framework was developed using the methodologies and approaches outlined in IPCC guidelines (IPCC 2019). Emission factors are taken from the IPCC guidelines and European Monitoring and Evaluation Programme /European Environment Agency (EMEP/EEA) guidebook (EMEP/EEA 2019). These emissions include municipal solid waste, which includes CH_4 emissions from landfill sites and domestic wastewater as well as emissions associated with waste incineration and open burning of waste.

To estimate these emissions, the solid waste generated is estimated from 1960–2018 historical data for urban and rural populations separately, by multiplying the urban and rural population by waste generation rates from IPCC Guidelines and Refinement. The composition of the waste generated in urban and rural areas is then split into the IPCC waste categories, including food, garden waste, paper and cardboard, disposable diapers, plastic, metal, glass, wood, textiles, rubber and leather, and others. The per centage of each type of waste in the total generated was based on IPCC Guidelines and Refinement (IPCC 2019).

RESULTS

The results reveal that between 1990 and 2063, the amount of waste increased across all categories (Figure 2.14a) as the result of increases in both the population and GDP. Waste can be openly burned at home or in informal sites only when it is not collected, or at open dump sites that are not properly managed (Wiedinmyer *et al.* 2014). The increasing trend in waste being burned between 1990 and 2020 slightly decreases around 2030 and continues as more waste is expected to be collected (Figure 2.14b) as the consequence of GDP increasing. This implies an expected change in practices of waste disposal which projects more waste collected and disposed in landfills. In addition, there will be more waste generated, particularly food and plastic waste due to increases in GDP.

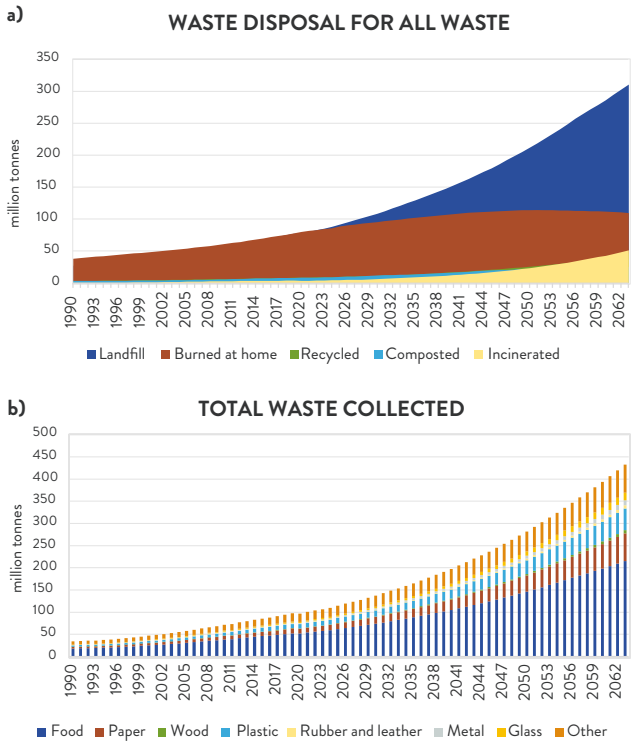

Figure 2.14 Africa, (a) waste disposal and management, by type, collected and uncollected, and (b) total waste collected, type, 1990–2063, million tonnes

2.4.4 SUMMARY

Large increases across sectoral drivers are seen in the baseline scenario. This is unsurprising as they are driven in part by the population, economic and urbanization trends (Section 2.3) with no changes in policies or plans to manage and decrease emissions. This scenario does capture projected shifts from historical trends, including changes in the composition of average diets, moves towards cleaner fuels, gas and electricity, in households, and small increases in the collection of waste. The impacts of the increases in all sectors are discussed in sections 2.5 and 2.6.

2.5 MODELLING THE PROGRESSION OF AFRICA'S ANTHROPOGENIC EMISSIONS IN THE BASELINE CASE

MAIN MESSAGES

- The baseline scenario shows large increases in emissions of GHGs, SLCPs and air pollutants. The total GHG emissions are projected to increase from 4 billion tonnes in 2018 to 14 billion tonnes of carbon dioxide equivalent (CO_2-eq) emissions in 2063. The agriculture, forestry and other land use (AFOLU) sector contributes the most to GHG emissions across the period studied in the Assessment and is responsible for large increases in CH_4 and N_2O emissions, while the power generation and transport sectors are responsible for the increase in CO_2 emissions between 2018 and 2063.
- Emissions of air pollutants and SLCPs are projected to increase in the baseline scenario. The largest emitting sector varies by pollutant, with household energy, charcoal making, and transport sectors contributing considerably to the emissions of different pollutants.
- At the regional level, the largest increases in GHG emissions are expected in the eastern and western parts of the continent, while the smallest, in ascending order, are expected in Northern, Southern and Central Africa.
- A benchmarking of the emissions estimated in the Assessment to other applicable inventories, that have their own baseline scenario, was performed. In general, the Assessment's emissions are within the range of other inventories. The largest differences between this Assessment and other inventories are for NOx, NMVOC and CO, all of which are higher in this Assessment. These differences are mainly due to the uncertainties in activity data and emission factors, which leads to different choices of these in the studies. This highlights the need for further research on locally applicable emissions information.
- The average GHG emissions per person does not change greatly over the time period studied and will continue to be lower than current levels in the high-income countries of Europe and North America.

- The ratio of GHG emissions to GDP is projected to decrease substantially. Thus, even in this baseline scenario, the GDP increases projected to 2063 do not lead to an equal increase in emissions.

The projections of activity per sector shown in Section 2.4 were used to estimate emissions of pollutants and GHGs at a national level under the baseline scenario. The emission results are presented in this section for the whole of Africa (Section 2.5.2) and a summarized view is presented per region (Section 2.5.3) with a detailed analysis in Chapter 4. The emissions estimated in the Assessment are compared to available inventories, where possible, to provide some benchmarking of the results (Section 2.5.4). The relationships between emissions and their growth factors are discussed to examine the evolution of emissions by factor in Section 2.5.5.

2.5.2 ANTHROPOGENIC EMISSIONS TREND IN AFRICA

This section focusses on emission trends from the reference emissions and simulated trajectories described in Section 2.4. Emissions of GHGs, SLCPs and air pollutants were evaluated using the LEAP model over the period 2018-2063 and the results are presented in Table 2.3.

Table 2.3 Africa, total emissions of greenhouse gases, short-lived climate pollutants and air pollutants for the baseline scenario, 2018 and 2063, thousand tonnes

GHG/SLCP/ POLLUTANT	EMISSIONS PER POLLUTANT ('000 TONNES)		
	2018	2030	2063
CO_2	2 460	3 020	6 700
CO	129 657	172 067	377 790
CH_4	48 449	69 069	207 805
NMVOCs	42 510	55 682	111 298
NO_x	9 741	15 506	51 583
N_2O	902	1 456	5 592
PM_{10}	11 552	14 228	23 834
$PM_{2.5}$	7 747	10 026	18 567
SO_2	5 469	7 011	20 519
NH_3	8 991	13 211	47 342
BC	1 225	1 401	2 738
OC	3 621	4 343	8 094
HFC-134a	23.1	16.6	39.4
HFC-125	10.1	7.3	17.2
HFC-143a	5.2	3.8	9
HFC-32	5.7	5.1	12

Note: additional years shown in Annex 2.6

As shown by Table 2.3, emissions of all species are projected to increase. In the following sections, the results will be presented by type of pollutant, GHGs, SLCPs and air pollutants; sectors; and regions of Africa.

2.5.2.1 TOTAL GREENHOUSE EMISSIONS

The total GHG emissions are projected to increase to 14 billion tonnes CO_2-eq emissions in 2063, compared to 4 billion tonnes in 2018, representing more than three times current levels (Figure 2.15). By 2030, the GHG emissions are projected to increase to 5.4 billion tonnes CO_2-eq, an increase of 35 per cent as compared to 2018 levels.

Disaggregation of these emissions by sector reveals that the AFOLU sectors will be the largest emitters of GHGs, followed respectively by electricity generation and transport (Figure 2.15).

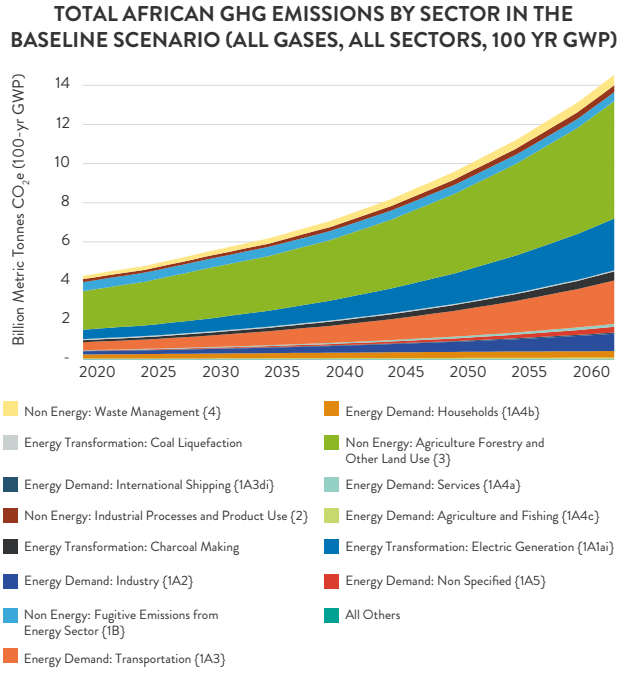

Figure 2.15 Africa, total greenhouse gas emissions in the baseline scenario, 2000–2063, billion metric tonnes of carbon dioxide equivalent (100-yr GWP)

2.5.2.2 GREENHOUSE GAS EMISSIONS PER MAIN SPECIES

It can be seen that CO_2 emissions are projected to increase by 23 per cent by 2030 compared to 2018 and are 2.7 times 2018 levels by 2063 (Figure 2.16a). It is also projected that CH_4 emissions will increase over Africa by about 21 per cent by 2030 compared to the 2018 level; while reaching more than 4 times 2018 levels by 2063 (Figure 2.16b). Nitrous oxide levels are also projected to increase between 2018 and 2063 to about five times 2018 levels (Figure 2.16c).

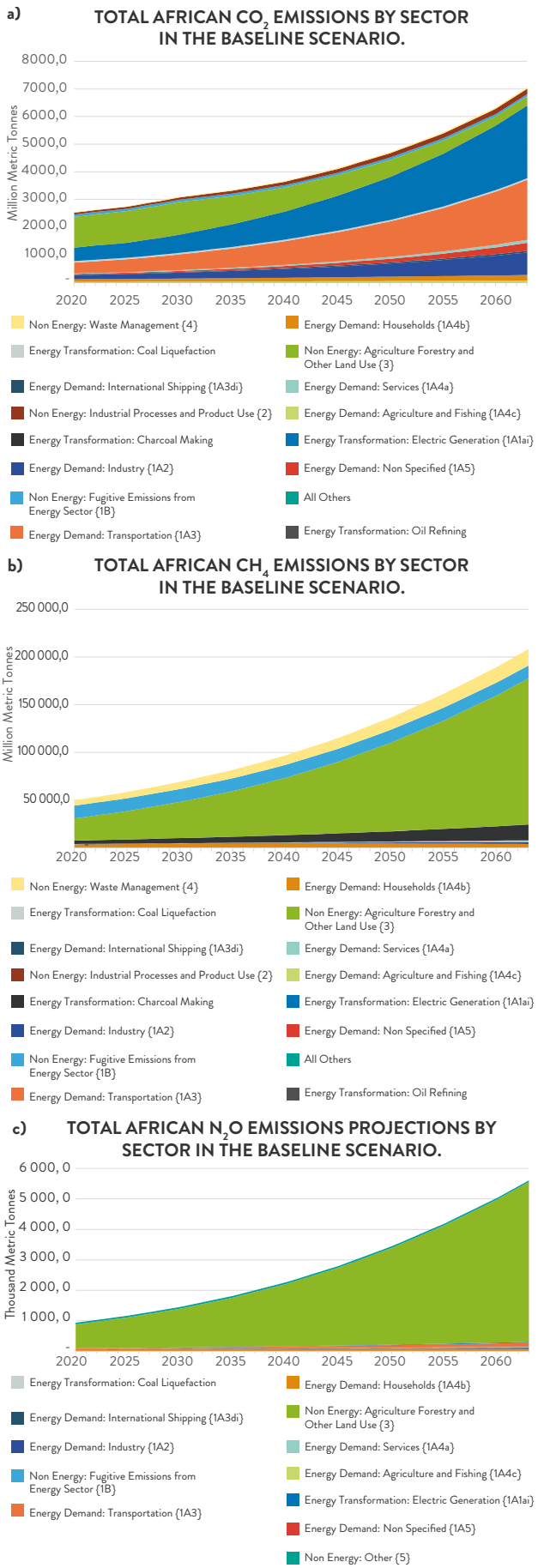

Figure 2.16 Africa, (a) total carbon dioxide emissions, million tonnes, (b) total methane emissions, million tonnes and (c) total nitrous oxide emissions, thousand tonnes, in the baseline scenario, 2000–2063

The growth in the agricultural sector drives large increases in CH_4 and N_2O. In the baseline scenario, the CH_4 and N_2O emissions from agriculture are expected to grow due to the large population growth and socioeconomic development driving increased meat consumption. There will therefore be a large increase in the projected demand for food and livestock in response to these populations' needs, implying more CH_4 emissions from enteric fermentation and manure management. In contrast, electricity generation and transport sectors drive the increase in CO_2 emissions between 2018 and 2063.

2.5.2.3 SHORT-LIVED CLIMATE POLLUTANTS AND AIR POLLUTANT EMISSIONS UNTIL 2063

The historical data and projections of SLCP emissions and their precursors are shown in Figure 2.17. Black carbon emissions will substantially increase between 2018 and 2063 (Figure 2.17a), by about 14 per cent by 2030 and about 123 per cent by 2063 compared to the 2018 levels. Similar patterns will also be observed for $PM_{2.5}$ (Figure 2.17b), NOx (Figure 2.17c), and NMVOC (Figure 2.17d); as they will all substantially rise by 2063. It should be noted that the apparent decrease of emissions in 2019 is an artefact from matching the historical data, which lacked information on vehicle type and emissions-control standards, to the projected results that explicitly model the vehicle fleet.

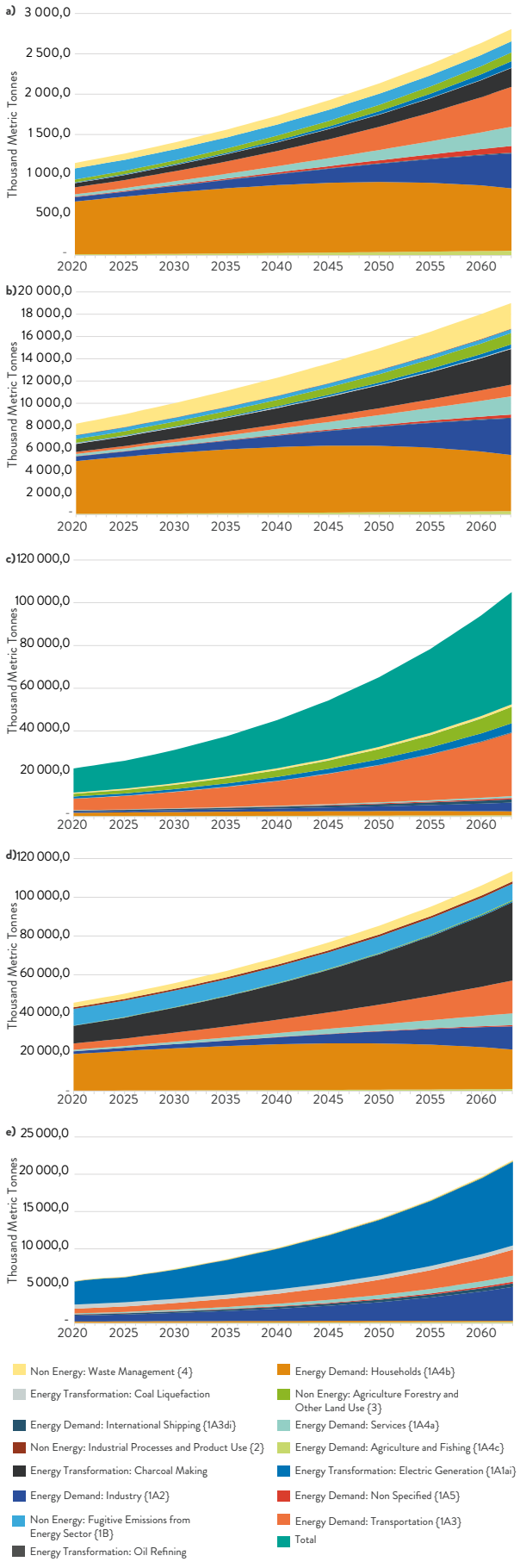

Figure 2.17 Africa, (a) total black carbon emissions (b) total fine particulate matter emissions (c) total nitrogen oxide emissions and (d) total non-methane volatile organic compounds (e) sulphur dioxide emissions in the baseline scenario, 2000–2063, million tonnes

Particulate matter, including BC and $PM_{2.5}$, emissions from households, which in 2018 are the largest emitters, are projected to decrease between 2018 and 2063. As noted in Section 2.4, a slight decrease in energy consumption is projected in the household sector due to the transition to cleaner and more efficient fuels use. However, PM emissions from charcoal production are projected to increase substantially because of the need to meet urban households' demand for cooking fuel. Also, a minor portion of PM and BC emissions are expected from the industrial sector, which will gradually increase and become more substantial by 2063. The transport sector drives the increase in NO_x emissions.

2.5.3 EMISSIONS PER AFRICAN REGION

2.5.3.1 TOTAL EMISSIONS AND MAIN GREENHOUSE GAS SPECIES EMISSIONS

Total GHGs emission per species and per African region are shown in Figure 2.18. Growth of GHGs, SLCPs and air pollutants to 2063 will be lowest over Northern Africa as a result of the combination of its smaller population and GDP growth compared to the remaining regions of Africa. Moreover, Southern Africa will undergo lower growth emissions, compared to the West, Central and East Africa, driven by its economy, which is relatively more developed, will grow less with smaller population growth. The Central Africa will record lower growth in GHGs compared to the West and East of Africa, which is mainly due to the assumed increase in carbon sequestration in the baseline scenario that offsets the increases in GHG emissions from other sources. Thus, the largest increases in GHG emissions are expected over East and West Africa.

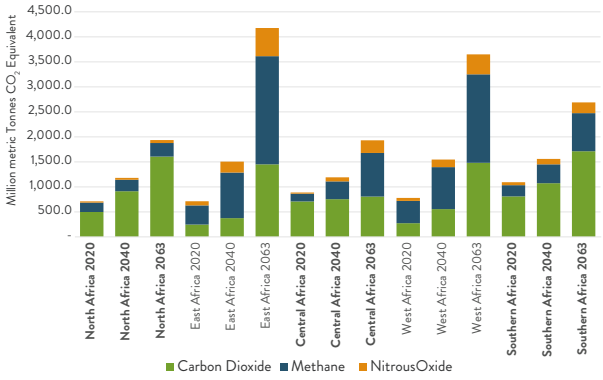

Figure 2.18 Total African carbon dioxide, methane and nitrous oxide emissions disaggregated by geographic region, 2018–2063, million tonnes CO_2 equivalent

2.5.3.2 EMISSIONS OF SHORT-LIVED CLIMATE POLLUTANTS AND AIR POLLUTANTS

For SLCPs and air pollutants, there are substantial increases in, for example, BC, $PM_{2.5}$ and SO_2 emissions to 2063 in West, Central and East Africa (Figure 2.19), reflecting increases in population and socioeconomic development that is driven by increases in fossil-fuel consumption and more intensive agricultural production to meet future food demand.

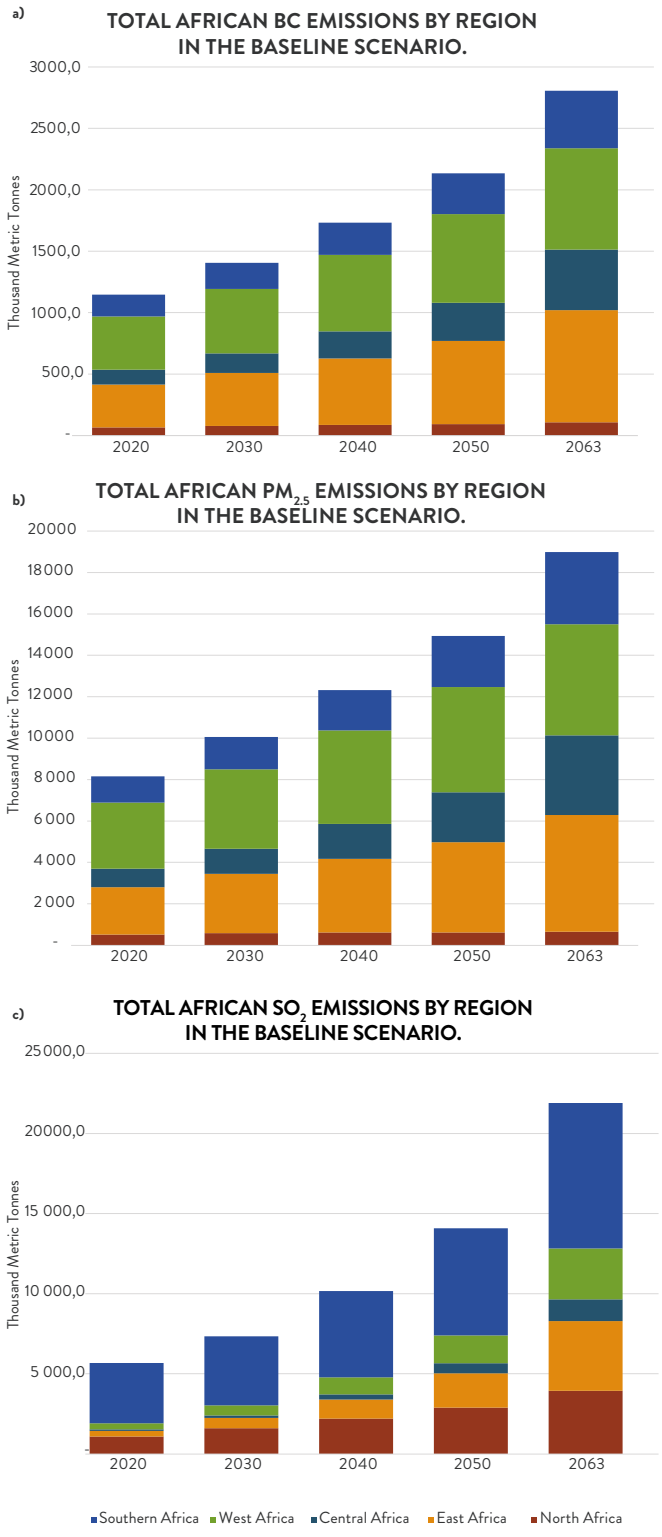

Figure 2.19 Africa, (a) total black carbon (b) total $PM_{2.5}$ and (c) sulphur dioxide emissions disaggregated by geographic sub-region, 2018–2063, thousandetric tonnes

2.5.4 COMPARISON WITH OTHER EXISTING REGIONAL INVENTORIES

The emissions simulated in the baseline are compared to emissions from other regional and global emission inventories that include Africa under a baseline scenario, specifically, DACCIWA (Keita *et al.* 2021) for regional inventories and the Community Emissions Data System (CEDS) (McDuffie *et al.* 2020), the Copernicus Atmosphere Monitoring Service (CAMS) (Granier *et al.* 2019), which is based on the Emissions Database for Global Atmospheric Research (EDGAR), and EDGAR v6 (Crippa *et al.* 2021) (Figure 2.20). As the Assessment's baseline scenario was developed specifically for it, the other inventories' scenarios are not exactly the same. Comparing the Assessment's baseline scenario with the other inventories, however, provides an important benchmark for its results. Except for NOx, NMVOC and CO emissions, the Assessment's scenarios are within the range of the other inventories. The largest differences between this Assessment and the others were highest for NOx, NMVOC, and CO, respectively 135 per cent, 175 per cent and 29 per cent. These differences are, however, relatively smaller in the regional DACCIWA inventory at 20 per cent, 139 per cent and 18 per cent higher respectively for NOx, NMVOC and CO. These differences are mainly due to the uncertainties in activity data and emission factors, which led to different choices made in those studies. For CO_2 and CH_4, the relative difference between the emissions in this Assessment and the other inventories is relatively smaller, with a maximum difference of 20 per cent, compared to the air pollutants as shown by Figure 2.21. This can be partly explained by the use of the IPCC default emission factors by all inventories in general.

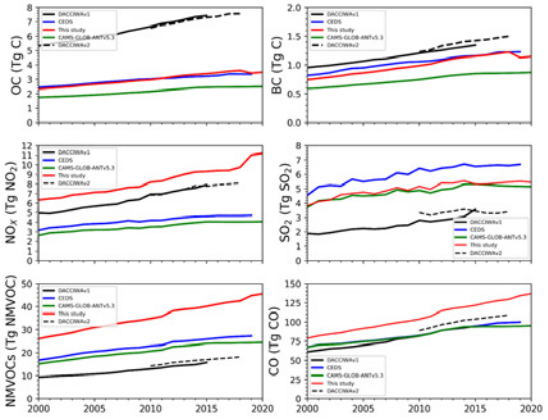

Figure 2.20 Africa, comparison of emissions of selected air pollutants in this Assessment (red line) and other regional and global inventories, 2000–2020, million tonnes /teragrams (Tg)

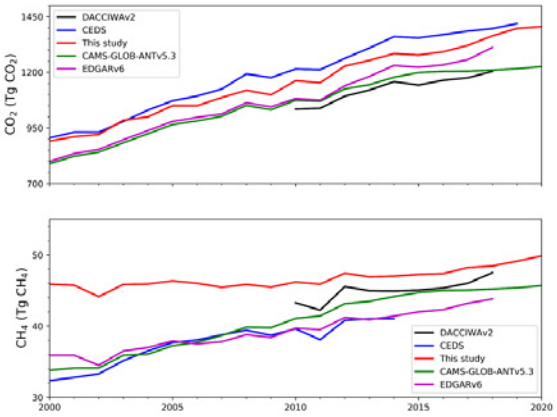

Figure 2.21 Africa, comparison of carbon dioxide and methane emissions in this study (red line) and other regional and global inventories, 2000–2020, million tonnes /teragrams (Tg)

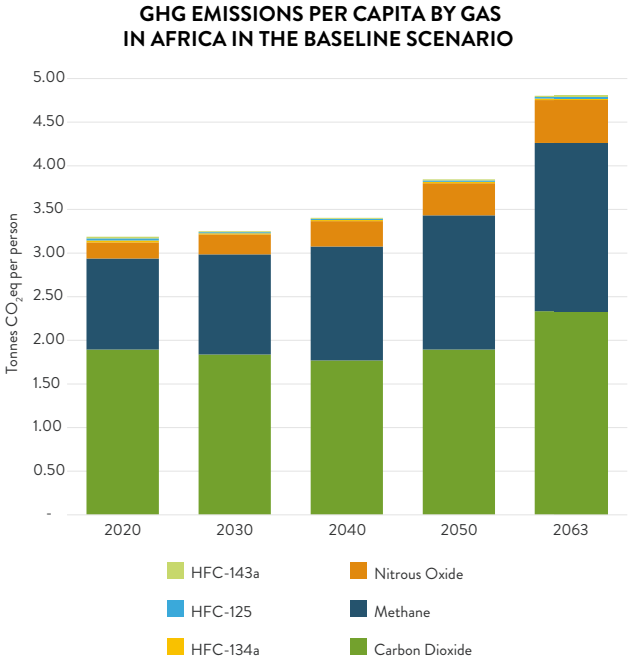

Figure 2.22 Africa, emissions in the baseline scenario of greenhouse gases, carbon dioxide, nitrous oxide and methane, 2020–2063, tonnes per person

2.5.5 EMISSIONS CHANGE IN RELATION TO DIFFERENT SOCIOECONOMIC METRICS

Overall, in Africa there will be substantial increases in GHG, SLCP and air pollutant emissions in absolute terms under the baseline scenario. This would be expected as, when the drivers of emissions grow, such as population, GDP, urbanization, transport demand, energy production and use, etc., the emissions generally grow as well – unless emission reduction measures and policies are enacted. To disentangle these relationships, it is helpful to investigate the change in emissions per driver.

The emissions per person in Africa in this Assessment's baseline scenario are lower than the current levels in high-income countries of Europe and North America. The 2018 level of GHG emission per person in Africa is estimated at just over 3 tonne CO_2-eq per person, and these GHGs emissions are expected to increase to around 4.7 tonnes CO_2-eq by 2063 (Figure 2.22). For comparison, in 2018, emissions in the European Union were 8.6 tonnes CO_2-eq per person (EEA 2022).

Considering the ratio of emissions to GDP, the emissions intensity, i.e. tonnes of CO_2 -eq emitted per PPP$ of GDP) is projected to decrease substantially (Figure 2.23). Thus, even in this baseline scenario, the GDP increases projected to 2063 do not lead to an equal increase in emissions, similarly to global trends (World Bank 2022c).

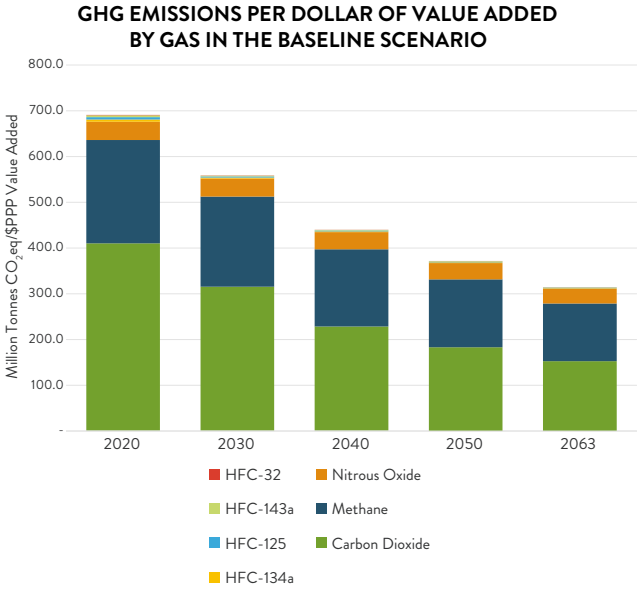

Figure 2.23 Africa, emissions intensity in the baseline scenario, 2000–2063, tonnes CO_2-eq per 2007 PPP US$ million

2.5.6 SUMMARY

The baseline scenario showed large increases in GHG, SLCPs and air pollutant emissions, as shown in the projections of activity data by sector in Section 2.4. The AFOLU sector is the largest contributor to CH_4 and N_2O emissions over the 2020–2063 period, while the power generation and transport sectors are responsible for the increase in CO_2 emissions. For air pollutants and SLCPs, the highest emitting sector varies by pollutant, with the domestic-energy, charcoal-making and transport sectors making large contributions for all pollutants. Per person GHG emissions in Africa will also continue to be lower than current levels in high-income countries in Europe and North America. Finally, a comparison of the emissions estimated in this Assessment with those of other inventories show some differences due mainly to uncertainties in the activity data and emission factors used, which highlights the need for further research on local emissions.

2.6 AIR POLLUTION AND CLIMATE CONSEQUENCES IN AFRICA FOLLOWING A BASELINE TRAJECTORY

MAIN MESSAGES

- Under the baseline scenario, Africa mean near-surface air temperatures will be 2 °C (range 1.8–2.1 °C) warmer by the 2060s than the present day. Precipitation also changes, including a drying of West Africa during June to August, although there is lower confidence in these projections.
- In the baseline scenario, increased pollutant emissions expose all populations to higher surface concentrations of PM2.5 and O3. The higher PM2.5 levels are estimated to result in more than 50 million premature deaths in the period 2015–2063. Increased pollution also means a reduction in crop yields, with 20 per cent reductions projected for wheat by 2063.
- A transition to cleaner fuels for cooking under the baseline scenario, coupled with a decreasing mortality rate, mean that deaths from household air pollution decrease by 40 per cent to 150 000 deaths/year by 2063.

This section focusses on the projected climate and air pollution changes as simulated for the baseline emissions and development trajectory, as described in Section 2.5. It draws on global chemistry-climate modelling experiments completed with the GISS-E2.1-G model (Kelley *et al.* 2020) to present projected changes in the African climate (Section 2.6.1) and human health (Section 2.6.2) and crop yield (Section 2.6.3) under the baseline scenario for 2015–2063. Details of GISS-E2.1-G and its configuration for the baseline simulations are presented in Annex 2.2. One aspect to note is that these model runs are global and include emissions from all sectors. Thus, emission futures are needed for the rest of the world as well as natural sources not included in this Assessment, such as wildfires, desert dust and sea salt. The GISS model generates emission estimates for natural emission sources and those were used here. The Assessment's anthropogenic emission estimates for Africa (Section 2.5) were aligned with the emission levels prescribed as in CMIP6 simulations for the SSP3-7.0 scenario (Eyring *et al.* 2016; Fujimori *et al.* 2017). As such, this emission scenario was used for the rest of the world, as well as sources not estimated in this Assessment or GISS, such as wildfires.

There are caveats from presenting results from a single chemistry-climate model, chiefly that the results do not have an estimate of the structural uncertainty, i.e., the fact that given the same inputs, different models give different results (IPCC 2021). Nevertheless, where there is evidence that the results presented here are robust, meaning that other models show similar magnitudes and directions of change, this is highlighted below. The reader is directed to the wider literature for more detailed examinations and discussions of differences between models (Young *et al.* 2013; 2018).

Finally, this section also presents calculations of the human health impacts from changes in household air pollution (Section 2.6.4), applying household air pollution health impact assessment methodologies (Pillarisetti *et al.* 2016; Kuylenstierna *et al.* 2020).

2.6.1 NEAR SURFACE TEMPERATURE AND RAINFALL CHANGES

The baseline scenario shows 2.0 °C (ensemble 95 per cent confidence interval, 1.9–2.1 °C) of near surface warming by the 2060s (2059–2063) relative to 2015–2019 for the Africa mean (Figure 2.24). This projection is virtually identical to GISS-E2.1-G simulations of the SSP3-7.0 scenario performed for CMIP6, a medium-to-high-end forcing scenario (O'Neill *et al.* 2016). This is not surprising as the SSP3-7.0 scenario was used for the GHG and air pollutant emissions outside Africa (Annex 2.2). As Africa's GHG emissions are a small proportion of the global total, the warming signal over the continent will be dominated by the rest of the world's emissions, irrespective of changes in African

emissions. Under SSP3-7.0 and in this Assessment's baseline scenario, the global mean near surface temperature change compared to the pre-industrial period (1850–1900) will very likely exceed 2 °C by mid-century (IPCC 2021), which is above the 1.5°C global warming level outlined in the 2015 Paris Agreement. There is a large body of work that describes the different global impacts at different global warming levels, with the risks of extreme heat and impacts to humans and ecosystems growing with each degree of warming (IPCC, 2018; 2021).

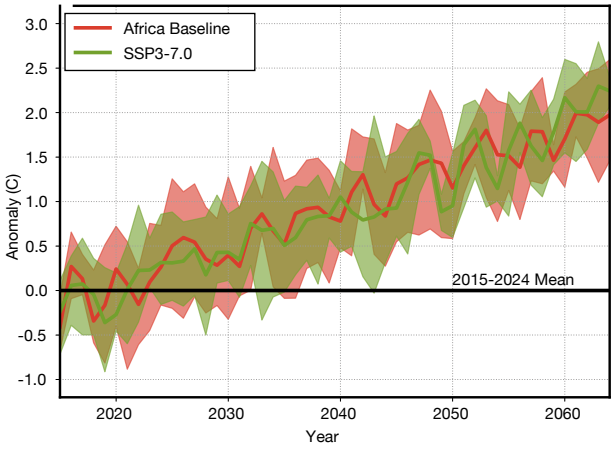

Figure 2.24 Africa, mean annual average near-surface air temperature anomalies for this Assessment's baseline scenario (black) and SSP3-7.0 (red) as simulated by the GISS-E2.1-G model, 2015-2063, degrees centigrade

Note: solid lines show the ensemble mean whereas shaded areas show the range across the ensemble (n=5). Anomalies are calculated relative to the 2015–2024 mean.

There is a spatial and seasonal structure to the warming under the baseline scenario, with year-round stronger warming across much of the northern and southern (i.e. subtropical) parts of the continent and a comparatively weaker warming in the centre of the continent by the 2050s (Figure 2.25). The stronger warming in the subtropics is most evident in the June–August average, which also has the strongest warming overall. For the June–August average, the 2050s near surface warming exceeds 2 °C in the subtropics in Africa compared to the present day, with a 1–1.5 °C warming over much of the remainder of the continent (Figure 2.25c). The 2050s warming is around 0.25–0.5 °C less for the December–February average in northern and southern Africa and is similarly weaker over the Congo Basin. The increased warming over the subtropical parts of the continent and the stronger northern warming in June–August are robust features across climate model simulations (IPCC 2021), giving confidence to the results presented here.

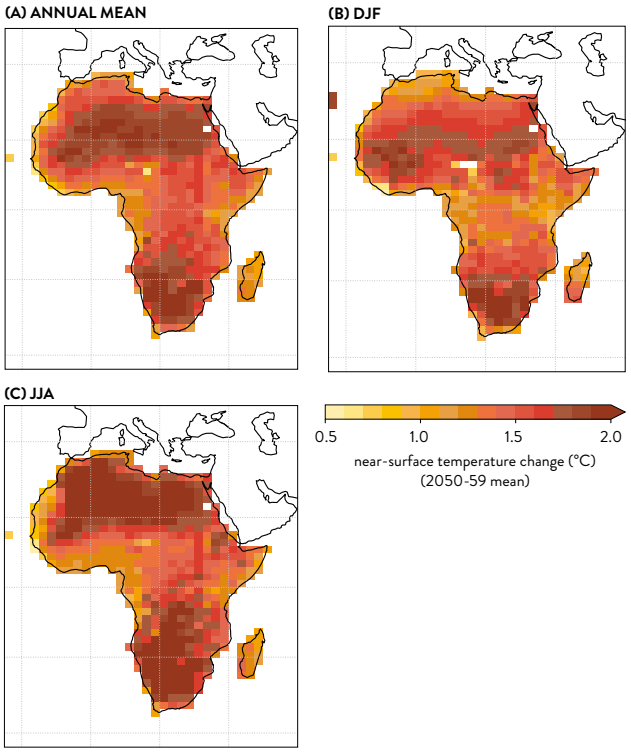

Figure 2.25 Africa, near-surface air temperature changes in the baseline scenario as simulated by the GISS-E2.1-G model, for the (a) the annual mean, (b) the December–February mean, and (c) the June–August mean, 2050–2059 minus 2015–2024 mean, degrees centigrade

There are changes in precipitation with the baseline scenario, with both simulated drying and wettening depending on the location and season (Figure 2.26). There are often, however, substantial differences between climate models in terms of projected precipitation changes (Hawkins and Sutton 2011; IPCC 2021) and agreement between climate models is particularly low in tropical regions (IPCC 2021). The drying over subtropical Southern Africa is a feature of global warming that has medium confidence in the latest IPCC report (IPCC 2021). The boreal summer, June–August, drying in westernmost West Africa seen here is a fairly robust feature of climate models across warming scenarios. So too is the boreal winter, December–February, pattern of wetting over southern tropical Africa, centred over Angola, and drying over most of the land southward of that (Almazroui *et al.* 2020; IPCC 2021). Therefore, these aspects of the response have relatively higher confidence than changes in other areas/seasons.

Finally, unlike the temperature changes, there are some differences with the simulated baseline changes in precipitation compared to the otherwise similar SSP3-7.0 simulations in the GISS-E2.1-G model (not shown). In particular, the SSP3-7.0 simulations show

enhanced precipitation across northern tropical Africa whereas there is a weak decrease/no change in this Assessment's baseline simulations. This difference is driven by the different SLCP emissions from Africa in the baseline simulation compared to the SSP3-7.0 global scenario, which impact aerosol concentrations, which in turn impact rainfall. While these changes are explainable in terms of plausible physical processes, there is low confidence in these results due to uncertainties in the representation of aerosol and cloud microphysics in the model and the aforementioned uncertainties in the overall climate change/precipitation signal.

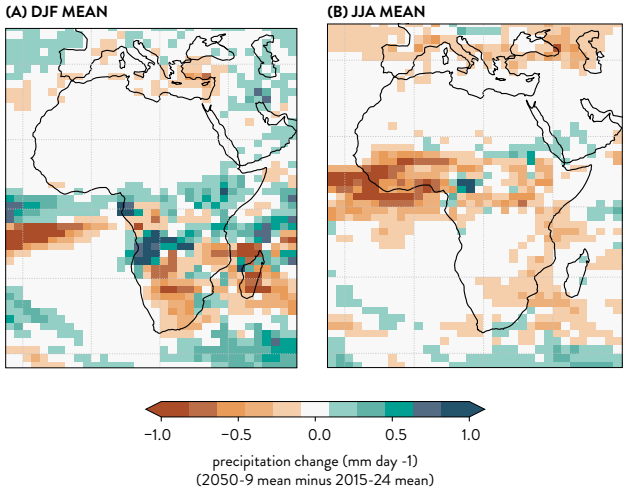

Figure 2.26 Africa, precipitation change in the baseline scenario as simulated by the GISS-E2.1-G model for the (a) December–February mean and (b) June–August mean, 2050–2059 minus 2015–2024 mean, millimetres per day

2.6.2 IMPACTS OF OUTDOOR AIR POLLUTION ON HUMAN HEALTH

The very large increases in emissions of aerosols, aerosol precursors and O_3 precursors, including SO_2, NH_3, NOx, CO and OC projected to occur under the baseline scenario (Section 2.5) results in increases of outdoor O_3 and $PM_{2.5}$ concentrations. Both of these air pollutants have well-known and documented negative impacts on human health (Nuvolone,et al., 2018; Romanello *et al.* 2021).

Between the start (2015–2024 mean) and end (2050–2059 mean) of the simulations, both annual average surface $PM_{2.5}$ and daily maximum 8-hour average O_3 increase mostly strongly over the Niger Delta and Ethiopia, Uganda and parts of Kenya, which are places where levels of these pollutants are already high (Figure 2.27). The increases in O_3 in these regions are apparent over a large area, highlighting the strong regional nature of O_3 pollution. Higher levels of O_3 are also simulated for the populated regions of coastal North, East and West Africa, and the industrialized regions of Angola and South Africa. There are similar hot spots for $PM_{2.5}$, a large contribution to which comes from dust over the Sahara. Also apparent from these simulations is that a very large proportion of the continent exceeds, or is projected to exceed, the latest WHO guideline (WHO 2021) of an annual average of 5 µg/m³ for $PM_{2.5}$ and a 6-month mean[7] of 60 µg/m³, about 30 ppbv, for O_3, respectively light yellow and light orange areas in Figure 2.27.

The impact on human health can be deduced from changes in the population-weighted pollutant concentrations in the baseline scenario, which is related to people's exposure to pollution. Figure 2.28 shows the population-weighted increases in $PM_{2.5}$ and daily maximum 8-hour average O_3 exposure for the five different African regions. The population-weighted impact is calculated using the same method as Shindell *et al.* (2022), using population data for 2015 from the Gridded Population of the World (GPWv3, updated from the *Center for International Earth Science Information Network (CIESIN)* 2005; Annex 2.2) and the projected changes in population appropriate to the SSP3 scenario (Samir and Lutz 2017).

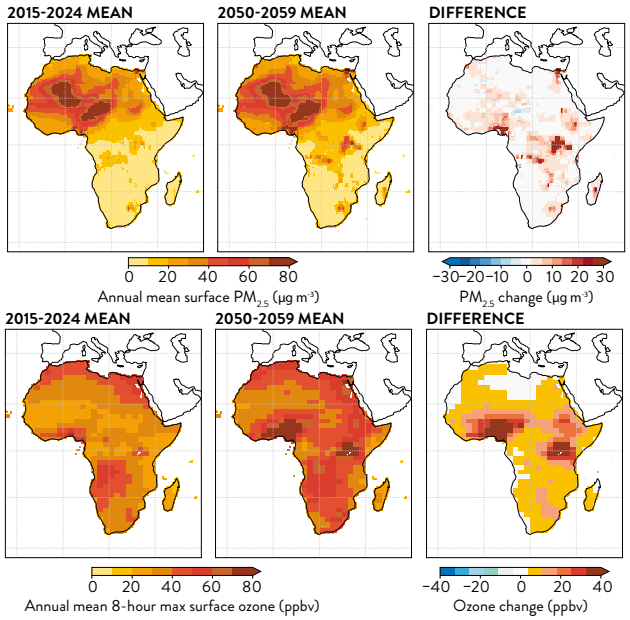

Figure 2.27 Africa, annual mean levels and changes in the baseline scenario as simulated by the GISS-E2.1-G model for (top) surface fine particulate matter, micrograms per cubic metre and (bottom) daily maximum 8-hour average ozone precipitation, parts per billion by volume, decadal mean values for (left) 2015–2024, (centre) 2050–2059, and (right) the difference

7. The limit for O_3 is stipulated for a 6-month mean, so the annual mean present here is conservative.

For population-weighted $PM_{2.5}$ levels, the relative order of the different regions is preserved over the 2015–2063 period of the simulations, with Southern Africa having the lowest population-weighted $PM_{2.5}$ levels and West Africa having the highest, albeit more closely matched by North Africa by the end of the period. Saharan dust contributes strongly to West Africa's high $PM_{2.5}$ levels. The relative changes differ in each region over the period, however, with population-weighted $PM_{2.5}$ levels increasing by around 30 per cent in West Africa, about 50 per cent in Southern Africa, nearly doubling in Central Africa, and more than doubling in North Africa. As similarly noted previously, the population-weighted $PM_{2.5}$ levels for all regions exceed the latest WHO (2021) guideline of 5 µg/m³ throughout the simulations, although the latest research points to there being no safe threshold (WHO 2021).

Population-weighted 8-hour daily maximum O_3 levels also increase over the course of the simulation for the baseline scenario. Again, all regions begin and end with population-weighted O_3 levels above the WHO (2021) guideline of about 30 ppbv. Population-weighted O_3 levels more than double for West and East Africa and increase by about 65 per cent over Central Africa, by around 30 per cent over Southern Africa, and by 10 per cent over North Africa.

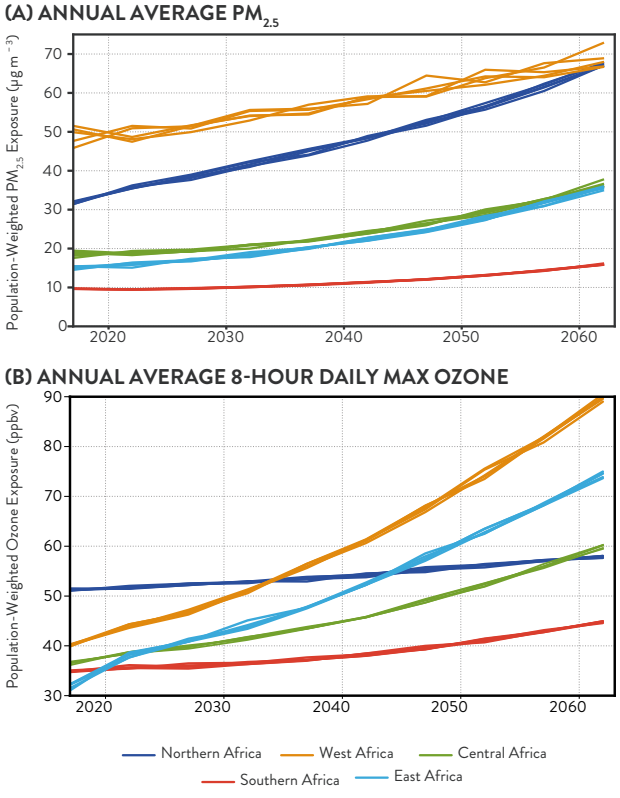

Figure 2.28 Africa, regional annual mean, population-weighted exposure in the baseline scenario as simulated by the GISS-E2.1-G model for (top) fine particulate matter, micrograms per cubic metre and (bottom) daily maximum 8-hour average ozone precipitation, parts per billion by volume, 2015–2063. Individual lines for each region represent the five ensemble members

The impacts of $PM_{2.5}$ and O_3 exposure on premature death can be evaluated by combining the GISS-E2.1-G output with exposure-response functions produced by the Global Exposure Mortality Model for $PM_{2.5}$, which draws from cohort studies from around the world including locations with high-exposures comparable to those in Africa (Burnett *et al.* 2018), and exposure-response functions for O_3 (Turner *et al.* 2016). The method to calculate mortality estimates from exposure follows that outlined of Shindell *et al.* (2021; 2022). It considers different risks for 5-year age increments for adults above 25 and projections of both the future population and baseline mortality rates but does not consider changes in the age profile. The uncertainty in the exposure-response relationship is estimated as ±16 per cent (Burnett *et al.* 2018), which is not included here.

Mortality estimates from $PM_{2.5}$ and O_3 exposure increase for all regions throughout the simulation period in the baseline scenario (Figure 2.29). Between 2015 and 2063, mortality rates attributable to both $PM_{2.5}$ and O_3 exposure more than double for West, East, Central and Southern Africa; for North Africa, there is a 25 per cent and 50 per cent increase in mortality rates for $PM_{2.5}$ and O_3, respectively. Particularly strong increases in the estimated mortality rates are seen for O_3, increasing by around 8 times for West Africa and more than doubling in East Africa. Integrating over 2015–2063 suggests that $PM_{2.5}$ alone would result in 50 million premature deaths over the whole continent over this 48-year period[8].

Given the challenges in projecting populations and baseline health, evaluating exposure-response functions, and the fact that these results are based on the output of realizations from a single model, the exposure and impact assessments come with substantial uncertainties. It is noted, however, that, at least for $PM_{2.5}$, the GISS-E2.1-G model matches the ground-based observations well (Shindell *et al.* 2022; Annex 2.2). Moreover, simulated changes in $PM_{2.5}$ exposure in GISS-E2.1-G are well within the range and on the low end of values produced by the CMIP6 models (Shindell *et al.* 2022). The comparison of results from this Assessment's model with those from a broad suite of models suggests that the impact estimates presented here are probably conservative, at least in terms of model-projected changes.

8. O_3 deaths cannot be directly added to this, since they are not separable

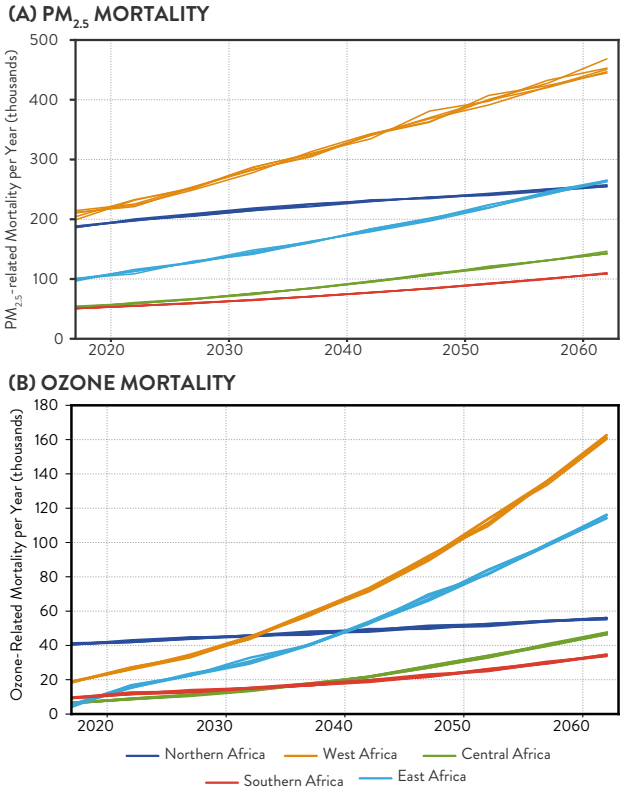

Figure 2.29 Africa, regional annual total premature deaths in the baseline scenario, as simulated by the GISS-E2.1-G model due to (top) fine particulate matter and (bottom) ozone exposure, 2015–2063, thousands.

Note: mortality calculations include the projected changes in population and vulnerability under the scenario. Individual lines for each region represent the five ensemble members. Note the different scales on the vertical axes

2.6.3 IMPACTS OF HOUSEHOLD AIR POLLUTION ON HUMAN HEALTH

Impacts on human health were also estimated for changes in household air pollution under the baseline scenario, using the method explained in detail in Annex 2.4. Briefly, exposure to household air pollution – annual average $PM_{2.5}$ concentration associated with cooking using different fuels and technologies – was estimated separately for household cooking using traditional wood stoves, efficient wood stoves, traditional charcoal stoves, efficient charcoal stoves, other biomass, LPG/natural gas and electricity. Exposure was estimated separately for the primary household cook, other adults and children, using global average exposure values for different population groups as there are very few studies for Africa (Shupler *et al.* 2018). The population assigned to each household $PM_{2.5}$ exposure value was based on the total national historical and future populations from the UN WPP (UN 2019) used throughout this Assessment. In the baseline scenario, there is a gradual shift to cleaner fuels for cooking between 2018 and 2063 (Section 2.4.2.2).

The impact on human health was quantified as the number of premature deaths attributable to household air pollution exposure for six diseases: ischaemic heart disease, stroke, lung cancer, chronic obstructive pulmonary disease, Type-2 diabetes, and LRTIs in children. The baseline mortality rates for these diseases, disaggregated by sex and age, were extracted from the GBD (2019) and used for years before 2020. To estimate future mortality rates, the change in overall death rate projected by the UN WPP (2019) between 2019 and future years was applied to the GBD disease-specific mortality rates for 2019 to estimate future disease-specific mortality rates. At the same time, the UN WPP (2019) death rates for all countries and population groups in Africa are projected to decrease, i.e., life expectancy is expected to increase. As a result, the mortality rates for the diseases associated with air pollution are also expected to decrease over time (Annex 2.4).

In 2018, approximately 250 000 premature deaths are estimated to be attributable to cooking using solid fuels across Africa (Figure 2.30), the largest proportions of which are in East and West Africa. Over a third of the total number of premature deaths from household air pollution are children under five, with the remainder adult premature deaths (Figure 2.31).

Despite an increasing population across Africa, the gradual transition of households to cleaner fuels (Figure 2.8) and reduction in baseline mortality rates (Annex 2.4), especially for children, results in a reduction in the number of premature deaths attributable to household air pollution into the future (Figure 2.31) in the baseline scenario. By 2063, the number of premature deaths attributable to household air pollution is estimated to reduce by 40 per cent compared to 2018 levels, to around 150 000 per year (Figure 2.30). The dramatic reduction in infant mortality rates is estimated to reduce child mortality from household air pollution by 79 per cent in 2063 compared to 2018 levels (Figure 2.31). These reductions are consistent with historical trends. Between 1999 and 2019, for example, the number of premature deaths attributable to household air pollution across Africa decreased by 22 per cent (GBD 2019). The largest number of premature deaths attributable to household air pollution occur now and into the future in West and East Africa (Figure 2.30), with the smallest number in North Africa, where the majority of households cook using gas.

The Africa-wide historical disease burden estimated for household air pollution here is substantially lower than the GBD's (2019) estimate of 696 000 premature deaths. One likely reason for this difference is the lower $PM_{2.5}$ exposure estimates used in the Assessment (from Schupler *et al.* 2018), which are based on cooking fuel/technology, compared to the GBD (2019) exposure estimates, which are based on socioeconomic status and have assigned higher

exposure in lower socioeconomic-status households. A second reason for the Assessment's lower estimate is the exclusion of maternal and neonatal disorders attributable to household air pollution, for example, as a result of preterm or low birth weight resulting from maternal exposure to $PM_{2.5}$. These are included in the GBD (2019) estimates, which attribute 146 000 premature deaths to maternal and neonatal disorders due to household air pollution.

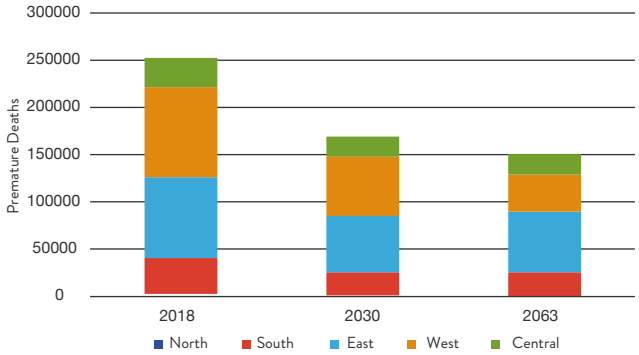

Figure 2.30 Africa, premature deaths attributable to household air pollution exposure disaggregated by region, 2018 and as in the baseline scenario for 2030 and 2063

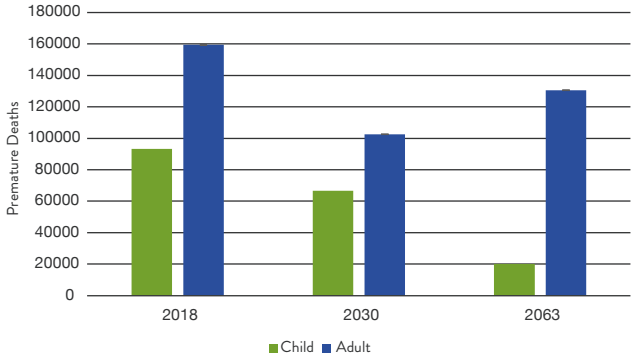

Figure 2.31 Africa, premature deaths attributable to household air pollution exposure, 2018 and as in the baseline scenario for 2030 and 2063, children under five and adults

2.6.4 CROP-YIELD IMPACTS FROM CHANGES IN CLIMATE AND OUTDOOR AIR POLLUTION

Crop yields are impacted by climatic conditions and atmospheric composition. In this Assessment, impacts are evaluated for four staple crops for which data on their response to O_3 and CO_2 exposure and climate change are available. Output from the GISS-E2.1-G simulations was used to calculate yield changes across Africa under the baseline scenario for maize, rice, soy and wheat (Figure 2.32). These calculations include the influence of temperature and precipitation change, and changes in exposure to CO_2 and O_3 (Shindell *et al.* 2019; UNEP and CCAC 2021); additional details are provided in Annex 2.2. These four crops provide the majority of the world's food energy intake, though many other crops are important in Africa and elsewhere (FAO 2022).

Yields for all four crops are all negatively affected in the baseline scenario, with around 2-6 per cent decreases by 2030, about 7 per cent losses by 2060 for maize and soy, and around 15 per cent and 20 per cent losses by 2060 for wheat and rice, respectively (Figure 2.32). Spatially, the pattern of crop cultivation plays the largest role in the geographic patterns of yield changes, followed by precipitation, with changes in temperature, O_3 and CO_2 being relatively evenly distributed across the continent. Under the baseline scenario, O_3, CO_2 concentrations and temperatures are all projected to increase substantially everywhere across Africa, whereas precipitation changes differ regionally (Sections 2.6.1 and 2.6.2). The increases in O_3 and temperature reduce yields, with the largest impacts in the near term, and temperature over the longer term, except for maize, for which the impact of O_3 increases is always the more significant. Changes in CO_2 are beneficial for yields in the modelling, through the CO_2 fertilization effect, and the changes in precipitation can sometimes lead to improved yields, but these are overall outweighed by the damage from the other factors. It then follows that despite precipitation changes being more variable between models (IPCC 2021), it is not a large driver of structural uncertainty in the assessment of the impacts on crops.

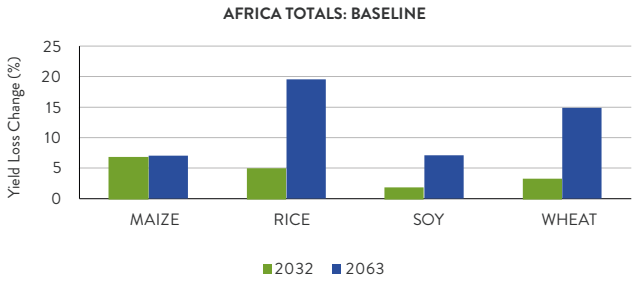

Figure 2.32 Africa, simulated maize, rice, soy and wheat yield-loss changes due to changes in O_3, CO_2, temperature, and precipitation in the baseline scenario using data from the GISS-E2.1-G simulations, 2032 and 2063, per cent

Uncertainty bars reflect the variability in climate and O_3 across the five ensemble simulations completed for the baseline scenario and indicate when the modelled changes are statistically significant. There are additional uncertainties in the CO_2 atmospheric concentration response to CO_2 emissions and in the crop impact-response functions, which are not included here.

2.6.5 SUMMARY

This Assessment's baseline scenario highlights the potential pathway for Africa if the current trajectories and policies in the energy, agricultural and waste sectors continue with no further policy development. This pathway leads to large increases in emissions of SLCPs and other air pollutants, which will have significant negative impacts on air quality. The impacts of the growth in emissions are seen strongly in the increased concentrations of $PM_{2.5}$ and O_3, which leads to serious negative impacts on human health and agriculture. The higher $PM_{2.5}$ levels are estimated to result in more than 50 million deaths between 2015 and 2063. Increased pollution also leads to a reduction in crop yields, with a 20 per cent reduction projected for wheat by 2063.

In the scenario, there is a 40 per cent decrease in premature mortality caused by household emissions of $PM_{2.5}$ from cooking. As described in Section 2.4.2, this is due in part to a transition to the use of cleaner and more efficient fuels as the result of increasing incomes. Even with this decrease, however, there are still an estimated 150 000 premature deaths per year from household pollution.

There are large increases in GHG and SLCP emissions in the baseline scenario, which are similar to those in the SSP3.0-7 scenario. Despite these increases, Africa's GHG emissions remain a small proportion of the global total. Under the baseline scenario, Africa mean near-surface air temperatures are 2 °C (range 1.8–2.1 °C) warmer than the present day by the 2060s. Precipitation also changes, including a drying in West Africa during June– August, although there is lower confidence in these projections. Local emissions can impact precipitation, and there are differences between the changes in future precipitation this baseline scenario and the SSP3-7.0 global scenario, though there are large uncertainties.

ANNEXES

ANNEX 2.1 STATE OF AIR QUALITY MONITORING INFRASTRUCTURE IN AFRICA (FROM SECTION 2.2)

Given the scale of air pollution emissions apportioned to the African continent through the use of model simulations, it is crucial to examine the status of *in-situ* measurement of them. This section gives an overview of the current state of air quality monitoring networks, dedicated field campaigns and future implementation plans across the five African Regional Integrations Communities.

WEST AFRICA: THE ECONOMIC COMMUNITY FOR WEST AFRICAN STATES (ECOWAS)

While continuous air-quality monitoring stations/ networks are scarce in West African countries (Petkova *et al.* 2013; Amegah 2018; Fayiga *et al.* 2018; Agbo *et al.* 2020), a number of dedicated large-scale initiatives aimed at characterizing and understanding air quality in the region have been implemented. Such initiatives include the Aerosol Robotic Network (AERONET), the African Monsoon Multidisciplinary Analysis (AMMA) (Redelsperger *et al.* 2006), the POLlution de Capitales Africaines (POLCA) (Liousse and Galy-Lacaux 2010), the International Network to study Deposition and Atmospheric chemistry in AFrica (INDAAF) and, more recently, DACCIWA (Knippertz *et al.* 2015b).

The INDAAF is a long-term program for monitoring atmospheric composition and atmospheric fluxes. The INDAAF measurement network spans rural areas across 13 stations on the African continent; eight in West and Central Africa, Benin, Cameroon, Côte d'Ivoire, Congo, Mali, Niger, and Senegal; and five partner sites, of which four are in South Africa and one in Tunisia. The objective of the programme is to document and understand the different steps of the lifetime of gaseous and particulate species from their emission, transport and chemical evolution to their deposition on continental surfaces. To achieve these objectives, the INDAAF long-term monitoring network performs measurements of: (1) the chemical composition of the atmosphere in Africa, to document the temporal and spatial evolution of trace gas and aerosol concentrations; and (2) wet and dry atmospheric deposition fluxes using quality-controlled measurements at the regional-ecosystem scale. Passive samplers based on molecular diffusion of gas molecules and developed after the work of Fermi are being used to monitor HNO_3, NH_3, NO_2, O_3 and SO_2 at each of the sites (Adon *et al.* 2016; Conradie *et al.* 2016). Aerosol measurements are carried out in two phases; monitoring and chemical speciation of PM_{10} and $PM_{2.5}$, and aerosol optical depth measurement. PM fractions are measured with a low-volume sampler operating at 5 litres per minute along two sampling inlets. One inlet collects samples on Teflon filters and the other on quartz filters for mineral and carbonaceous analysis respectively. Aerosol optical depth is measured with an AERONET CIMEL sun photometer. Data collection at most of the sites started in 1995 and are still ongoing.

The DACCIWA project conducted an extensive field-monitoring campaign in three southern West African countries, Benin, Ghana and Nigeria, in June/July 2016. The overall goal of DACCIWA is to significantly improve monitoring capacities and

the scientific understanding of key interactions between surface-based emissions, atmospheric dynamics and chemistry, clouds, aerosols and the climate of West Africa, and to integrate the findings into the next generation of weather and climate models (Knippertz *et al.* 2015 a, b). Three research aircraft were flown along demarcated flight paths for horizontal and vertical profiling of the atmosphere. Also, a wide range of surface-based instrumentation was deployed at the three designated supersites at Ile-Ife, Save and Kumasi. DACCIWA produced the most comprehensive observational dataset of the atmosphere over the region to date (see Flamant *et al.* 2018 for detailed description of the activities during the campaign) and used this dataset to foster scientific understanding of atmospheric processes, and evaluate dynamic models and satellite data. Some findings from the field campaign have been reported (Adon *et al.* 2010; Val *et al.* 2013; Adon *et al.* 2016; Bahino *et al.* 2018; Brito *et al.* 2018; Deroubaix *et al.* 2019). The comprehensive dataset is freely available on request at the Base Afrique de l'Ouest Beyond AMMA Base (http://baobab.sedoo.fr/DACCIWA/).

Presently, there is an ongoing World Bank project on air quality monitoring in Lagos, Nigeria. The project deployed arrays of air quality monitors (Federal Reference Method (FRM) and Near FRM Monitors) at six locations in Lagos Metropolis. The measurement is intended to last for a period of one year and combines chemical characterization, source apportionment modelling, emission inventory development and dispersion modelling.

EAST AFRICA: EAST AFRICAN COMMUNITY (EAC)

As in other African regions, there is a paucity of air-quality monitoring networks and data in East Africa. In effect, this has been a major hinderance to efforts to build an understanding air quality in the region. An ongoing effort to ensure that air quality is monitored in East Africa is being carried out by A Systems Approach to Air Pollution – East Africa (ASAP-East Africa, 2020) Project. This seeks to provide support for existing monitoring facilities and capacity building at selected locations in three East African countries – Ethiopia, Kenya and Uganda. Air-quality monitoring is one of three key elements, the other two being air-quality modelling and management, and is focussed on indoor and outdoor monitoring.

Likewise, there has been a franchise of Clean Air Engineering projects – Clean Air Engineering for Cities (CArE-Cities) and Clean Air Engineering for Homes (CArE-Homes). These included 12 cities in overseas development assistance (ODA) countries including Addis Ababa, Ethiopia: Akure, Nigeria; Blantyre, Malawi; Dar-es-Salaam, Tanzania; Kampala, Uganda; and Nairobi, Kenya. CArE-Cities measured in-car exposure across these cities (Kumar *et al.* 2021a; 2021b) while the CArE-Homes focussed on in-kitchen exposure in low-income homes (Kumar *et al.* 2022b).

Addis Ababa, Ethiopia: there is one long-term monitoring station in Addis Ababa that was established by the US Embassy in 2017 (airnow.gov). The ASAP-East Africa has also carried out similar spot measurements in Addis Ababa to supplement existing data.

Kampala, Uganda: Unlike Addis Ababa and Nairobi, the city of Kampala has an extensive air-quality monitoring network. The Greater Kampala Area, for instance, is reported to have more than 15 active monitoring sites. Nevertheless, the city does not have a long-term air-quality dataset.

Nairobi, Kenya: although the city of Nairobi has one long-term monitoring station at Alliance Girls High School (https://aqicn.org/city/nairobi/), the ASAP-East Africa has supplemented the available data with spot measurement campaigns. The outdoor monitoring was carried out in three locations with characteristic urban-background, urban-roadside and rural-background air quality. Visibility data from the city's two airports have also been analyzed to fill historical data and used to infer the air-quality status of the city.

CENTRAL AFRICA: ECONOMIC COMMUNITY OF CENTRAL AFRICAN STATES (ECCAS)

Air-quality monitoring, either nationally coordinated or independent investigations, is almost non-existent in ECCAS. Studies conducted in the Republic of Cameroon are limited to those of Pelassy (1978), Doumbia *et al.* (2012) and Antonel and Chowdhury (2014). A recent update of the adverse effects of air pollution by Sousa *et al.* (2022) reiterated the lack of an air-quality monitoring network in Angola but pointed at the initiatives of Campos *et al.* (2021) in Luanda. Only recently has the first air-quality data been reported for two locations, Libreville and Port Gentil, in Gabon (Ngo *et al.* 2019). This trend is the same across other countries in the region.

SOUTH AFRICA: SOUTHERN AFRICAN DEVELOPMENT COMMUNITY (SADC)

Southern Africa, as is the case across the African continent, is faced with the challenge of air pollution and a lack of an operational monitoring network. Unlike the other regions, however, coordinated efforts to monitor and understand the region's air-pollution is much advanced in the SADC. One of the earliest and ongoing efforts in the region is the Air Pollution Information Network for Africa (APINA) (Simukanga

et al. 2003). Seven countries in the region are said to have documented their air-quality status in a report commissioned by APINA in 2002 (Simukanga *et al.* 2003), but the extent of air-quality monitoring reported is not clear. Available information indicated that most of the SADC countries, except South Africa, have a limited number of air quality monitoring stations (Mapoma and Xie, 2013; Akinola *et al.* 2017). According to the South African government website (https://saaqis.environment.gov.za/home/index), there are more than 100 government-managed outdoor air quality monitoring stations across 278 municipalities in South Africa that that have been reporting to the South African Air Quality Information System (SAAQIS) since 2009, when the system was launched. The SAAQIS is an online platform providing all air-quality information including policies, legislation and guidelines all across the country. Pollutants measured by these stations are $PM_{2.5}$ and $P.M_{10}$, NO_2, CO, O_3 and SO_2 as well as meteorological parameters such as temperature, rainfall and humidity. The aim of SAAQIS is both to provide enough information on air quality for the public, stakeholders and decision makers and to ensure that air-quality management decisions are taken based on accurate and complete information. Data can be requested based on the user's preference although the years of coverage vary from station to station.

NORTH AFRICA DEPLOYMENT OF LOW-COST AIR-QUALITY MONITORING SENSORS IN AFRICA

The recent deployment of low-cost air-quality monitoring sensors has gathered tremendous momentum globally. With new technologies being introduced, low-cost sensors range from commonly-known passive sensors to more sophisticated micro-electrochemical and mechanical ones. The capability of the sensors to monitor a wide range of gaseous and particulate pollutants makes them even more attractive in addition to being affordable, easy to use and light weight. Although concerns exist about the performance and accuracy of low-cost sensor measurement, their repeatability and reproducibility, stability against weather parameters, data quality, etc., a number of independent and coordinated studies have been carried out in Africa, while some are still ongoing. A brief overview is presented in the following section

A review by Amegah (2018) indicated the limited deployment of low-cost sensors in Sub-Saharan Africa. Only five independent studies across three countries were identified to have used low-cost CO sensors for either outdoor or personal exposure monitoring: Kume *et al.* (2010) in Ethiopia, Balogun *et al.* (2014) and Alexander *et al.* (2018) in Nigeria, Naidoo *et al.* (2013) and Mentz *et al.* (2018) in South Africa. In addition to the CO monitor, Alexander *et al.* (2018) also deployed a $PM_{2.5}$ low-cost sensor.

In 2017, de Souza *et al.* reported on a collaborative experiment between six partners led by UNEP was conducted in Nairobi, Kenya, starting in May 2016, using low-cost sensors at six locations. The sensor units consisted of an optical-particle counter for measuring PM1, $PM_{2.5}$ and PM_{10}, and electrochemical (amperometric) gas sensors which measured NO_2, NO and SO_2. The study suggested that, while low-cost sensors have high potential in bridging the air-quality data gap, they were not yet suitable as substitutes for high-end monitoring systems due to unresolved quality-assurance and quality-control issues.

Through a collaborative field experiment between Obafemi Awolowo University, Nigeria and University of Cambridge, UK, two pilot studies were conducted to monitor size-segregated PM, gas-phase pollutants and meteorological parameters in Ile-Ife, Osun State in June–July 2018, and Lagos Metropolis in November 2018–March 2019), and state measurements were carried out at six locations in each state within the Sensor Network for Air Quality (SNAQ) project. Each SNAQ unit utilizes an optical particle counter. Results of the study in Ile-Ife have been published (Omokungbe *et al.* 2020). The main objective of the study was to collect baseline air-quality data and assess the influence of weather parameters on PM loading and it concludes by pointing at the huge potential of low-cost sensors in providing continuous *in-situ* measurements.

According to Amegah (2018), a yet to be published study deployed low-cost sensors at two locations in Ghana, Abuesi and Cape Coast Metropolis in 2016 to monitor $PM_{2.5}$, CO and O_3. The study was said to be part of the Air Sensors Everywhere project of Massachusetts Department of Environmental Health Science, US. It was designed to evaluate the performance of low-cost sensors in a tropical environment and measure occupational exposures.

A wide study by Awokola *et al.* (2020) conducted pilot study of $PM_{2.5}$ monitoring across 13 sites in seven Sub-Saharan Africa countries – the Republic of Benin, Burkina Faso, Cameroon, The Gambia, Kenya, Nigeria and Uganda. The study was able to provide continuous data for outdoor $PM_{2.5}$ concentrations over a period of one month. During the time of the study, the study experienced some challenges that affected the data recovery as some of the data were missing. One of the issues encountered was the power supply and this is an issue common to countries in Sub-Saharan Africa. Although, a power bank was purchased to alleviate the effect of power shortages, in the process of switching to the power bank, some data were lost as a result of the break in transmission. Moreover, the project implementation had problems in terms of identifying

suitable locations for the placement of the devices. Accessibility was a factor since the sensors require regular maintenance checks but there was also fear that devices might be stolen or tampered with in the selected locations. Work with the local communities, however, helped ensure that the devices were not sabotaged in the long run. Key recommendations of the study include the need for future studies to carefully take note of the supply of electricity. Furthermore, the location to be used for the placement of the device should be selected to avoid vandalization. The study then concluded that it is practical and feasible for several Sub-Saharan African countries to make use of low-cost air-quality sensors to produce an air-quality monitoring network.

There have also been on-road monitoring campaigns using the low-cost sensors in the car environments. For example, Kumar *et al.* (2021a) successfully assessed the feasibility of low-cost sensors in understanding the $PM_{2.5}$ and PM_{10} exposure to car users across 10 global cities, including cities in Ethiopia, Malawi and Tanzania. They later used the data to extrapolate and assess the health risk and associated economic burdens in these cities (Kumar *et al.* 2021b). Their recent work used the low-cost sensors for monitoring exposure to aerosols inside kitchens of 60 homes across cities in Ethiopia, Kenya, Malawi, Nigeria and Tanzania (Kumar *et al.* 2022).

It is important to note the existence of a fast-growing network of low-cost sensors across Africa. The network is a cohort of independently managed PM sensors, such as the Purple Air PA-II-SD[9], by individuals or organizations. In West Africa, for instance, the network is supported through the collaboration of Pennsylvania State University, US, with the Centre for Atmospheric Research of the National Space Research and Development Agency in Nigeria as well as other partners from other countries in the region.

ANNEX 2.2 SIMULATIONS IN THE GISS-E2.1-G MODEL

This Annex provides brief details on the GISS-E2.1-G global Earth system model, its configuration for the baseline scenario, and some information on the model performance for the key climate and air pollution aspects explored here.

MODEL DESCRIPTION

The GISS-E2.1-G model is an Earth system model developed at the NASA Goddard Institute for Space Studies (GISS). The GISS series of models have been developed over many decades (Hansen *et al.* 1983; Hansen 2002; Schmidt *et al.* 2006; Hansen *et al.* 2007) and the GISS-E2.1-G version used here is part of the most recent ModelE incarnation (Kelley *et al.* 2020). This model consists of equations representing the basic physical and chemical processes that take place in the atmosphere, ocean and land systems. The Earth's atmosphere and ocean are divided into regular grids with these equations solved within, e.g., evaporation, or across, e.g., winds, each grid along the simulation. The model incorporates representations of many processes, including radiative transfer through the atmosphere; the hydrological cycle; the chemical and physical processes affecting gases, including O_3, GHGs and aerosols, particulates; ocean circulation and heat uptake; sea-ice; vegetation; and groundwater. Such models have been developed over several past decades to better represent many characteristics of the real world, but now require supercomputing systems due to their complexity and relatively high spatial and temporal resolution.

Complete technical details of this model are described by Kelley *et al.* (2020). In brief, GISS-E2.1-G represents the atmosphere on a 2° × 2.5° latitude/longitude grid with 40 vertical levels (surface to 0.1 hectopascal (hPa)), coupled to a 1° × 1.25° latitude/longitude ocean model also with 40 vertical levels. Whereas most quantities are evaluated only at this standard resolution, the simulations conducted for this Assessment include a previously developed method to provide $PM_{2.5}$ output at a resolution of 0.5° × 0.5°, incorporating within grid-box emissions information to alter constituent gradients that are then preserved during transport (Shindell *et al.* 2018). The model simulates aerosols (particulate matter) using a mass-based scheme that includes representations of sulphate, black and organic carbonaceous aerosols, nitrate, NH_4, dust, and sea-salt, with fixed-size distributions other than for dust and sea-salt (Bauer *et al.* 2020). The atmospheric chemistry scheme has around 200 reactions simulating approximately 40 species (Kelley *et al.* 2020). Most relevant to this study is the chemistry involving tropospheric O_3, for which the model simulates basic NOx-(HOx)-Ox-CO-CH_4 chemistry as well as peroxyacyl nitrates, isoprene, alkyl nitrates, aldehydes, alkenes, paraffins and terpenes. The model generates its own meteorology,

9. https://www2.purpleair.com/products/purpleair-pa-ii (accessed 12 October 2022)

which is fully interactive with the gaseous and aerosol species so that they are affected by a changing climate. Changes in all chemical parameters are evaluated using 15-minute time steps throughout the simulations. This version of the model also contributed simulations for CMIP6 (Eyring *et al.* 2016) in support of the most recent IPCC report (IPCC 2021).

CONFIGURATION FOR THE BASELINE SIMULATIONS

Simulations were performed from 2015 through 2063 for the baseline scenario. Five ensemble members were used to better distinguish the climate and air pollution response to the emissions changes from unforced, natural internal variability in the climate system. Individual ensemble members began from starting conditions at the end of 2014 taken from five independent historical simulations with the GISS-E2.1-G model, which in turn began from starting conditions taken from widely spaced years of a long preindustrial control simulation (Miller *et al.* 2021).

Anthropogenic emissions for Africa for the baseline scenario were taken from the LEAP model (Section 2.5). For natural emissions, the GISS-E2.1-G model includes internally generated climate-sensitive emissions from several sources, including NOx from lightning, biogenic VOCs, windblown dust and sea-salt emissions. Emissions not produced by the LEAP model, for example, wildfires, nor generated by the GISS model were prescribed as in CMIP6 simulations for the SSP3-7.0 scenario, including those outside of Africa (Eyring *et al.* 2016; Fujimori *et al.* 2017). The concentrations of well-mixed GHGs are prescribed throughout the atmosphere, CO_2 and N_2O, or at the surface, CH_4, which is then adjusted for chemical changes aloft, rather than input as emissions. Input concentrations for these that result from the LEAP African and SSP3-7.0 non-African emissions were evaluated using box models.

As noted in Section 2.6.1, the global and Africa mean near surface temperature projections of the baseline simulation are virtually identical to those in the GISS-E2.1-G simulations of the SSP3-7.0 scenario performed for CMIP6. In addition, while the simulations end in 2063, the global mean net radiation at that time is ~1.5 watts per square metre (W/m2). This means that even if atmospheric concentrations of all pollutants were to stay constant beyond then, the warming would continue until the energy balance was restored, resulting in another 0.8–0.9 °C of warming globally, based on the model's sensitivity (Kelley *et al.* 2020).

MODEL EVALUATION AND BENCHMARKING

This model and others like it have been used extensively for both attribution of past changes and projections of future ones. Peer-reviewed literature has documented how this model realistically captures many observed physical quantities and trends (Seltzer *et al.* 2017; Bauer *et al.* 2020; Kelley *et al.* 2020). This section presents an Africa-focussed evaluation and benchmarking of near surface temperature, rainfall and PM. Due to a relative lack of observations, it is not possible to conduct a similarly detailed evaluation of the model for surface O_3 levels over Africa. Nevertheless, evaluations for other regions do indicate high biases for O_3 relative to surface observations (Seltzer *et al.* 2017), emphasizing that caution should be exercised when estimating impacts.

One exercise for climate data is to compare the projected temperature and rainfall from GISS-E2.1-G against the other models driven with the same emissions scenario. While not an evaluation of the projections, it does allow the GISS-E2.1-G projections to be placed in the context of the climate model literature, including results reported in the most recent IPCC report (IPCC 2021). Figure 2.33 compares the simulated near-surface temperature and precipitation changes between the 2050–2059 and 2015–2024 decadal means for the GISS-E2.1-G model and the CMIP6 multi-model mean, where all models have been driven by the SSP3-7.0 scenario, which has similar climate changes to this assessment's baseline scenario, as noted above. The spatial patterns of warming, namely the maxima in northern and southern Africa, are similar in the GISS-E2.1-G simulations and the CMIP6 mean. Warming in Sub-Saharan Africa is stronger in GISS-E2.1-G, particularly for Southern and West Africa, where it exceeds the mean projected warming of around1.5 °C by 0.25–0.5 °C, i.e., by about 16–33 per cent. Similarly, while the overall tropical wettening in the GISS-E2.1-G simulations is similar to the CMIP6 mean, the precipitation increase in central Africa is less marked. Additionally, there is a stronger drying signal in West Africa in the GISS-E2.1-G simulations. At the same time, the dominant source of uncertainty for projected tropical and West African rainfall changes is model, or structural, uncertainty over this coming century, with conflicting signals noted for different models despite the same scenario (Lee *et al.* 2021, Figure 4-24; Douville *et al.* 2021, Figure 8.23).

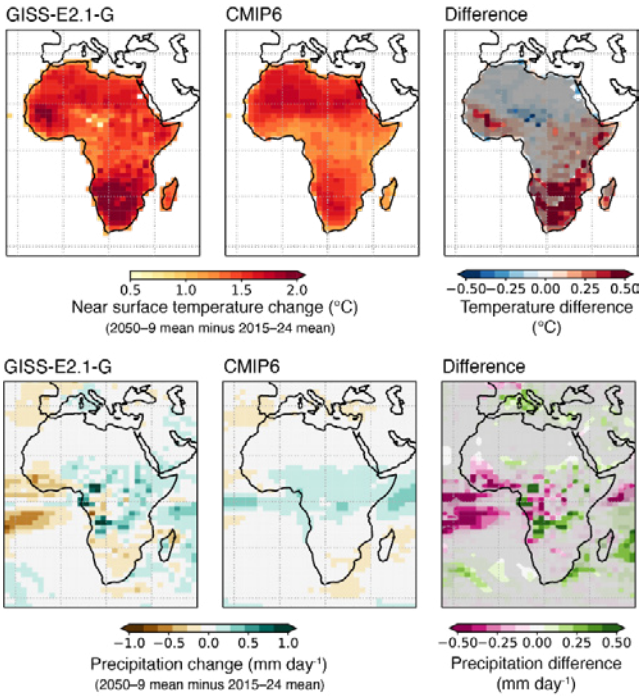

Figure 2.33 Africa, change in decadal mean (top) near-surface air temperature and (bottom) precipitation between 2015–2024 and 2050–2059 for the SSP3-7.0 scenario as simulated by (left) the GISS-E2.1-G model, (middle) the CMIP6 models (ensemble mean; n=29). Also shown is (right) the difference between the decadal changes (GISS-E2.1-G minus the CMIP6 ensemble mean) with greyed out areas indicating grid squares where the differences are not statistically significant (95 per cent confidence; Mann-Whitney U test).

Note: as this statistical testing was done on a grid-square basis, rather than accounting for field significance, this is a conservative indication of the differences in the climate signals between the GISS-E2.1-G simulations and the CMIP6 ensemble mean.

GISS-E2.1-G $PM_{2.5}$ levels over Africa have recently been evaluated by Shindell *et al.* (2022) and are summarize here. That study compared simulated $PM_{2.5}$ levels against ground-based monitoring sites and a satellite-derived product, weighting the observed and simulated $PM_{2.5}$ by population to reflect human exposure, using population data for 2015 from the Gridded Population of the World (GPWv3; updated from CEISIN, 2005). Ground-based monitoring data cover 2013–2015 and are from 53 locations. This includes data from 42 sites as assembled by the WHO (2016), 29 sites of which measured $PM_{2.5}$ directly and 13 from which $PM_{2.5}$ is inferred from PM_{10} measurements, and 13 monitors located at US embassies in Africa, of which two are located within the same grid box as data points in the WHO dataset – adding this data to the WHO dataset provides 11 new locations and changes the average for two existing locations. The satellite-based product consists of $PM_{2.5}$ levels for 2014–2016 estimated from a chemistry-transport model where simulated $PM_{2.5}$ has been adjusted so that the modelled column aerosol optical depth matches satellite aerosol optical-depth measurements (Shaddick *et al.* 2018a and b).

For the ground monitors, the population-weighted average exposure is 43.8 μg/m^3 (Figure 2.34). The simulated mean with GISS-E2.1-G (five ensemble members) is very similar at 45.4 μg/m^3, so that the mean bias is 1.6 ± 0.5 μg/m^3. Without population-weighting, the mean bias is 0.2 μg/m^3, which indicates that the good match is not a result of the dominance of a few locations. The satellite-based dataset has 10 641 data points over Africa and has a mean population-weighted value of 63.8 μg/m^3. In comparison with that data, the simulated data have a population-weighted bias of –36.5 ± 0.8 μg/m^3. At the same time, however, comparing the satellite-based dataset to the 53 ground monitor locations indicates that the satellite-based dataset has a population-weighted average bias of +20.7 μg/m^3. Therefore, the comparison against ground observations is likely the most useful in validating the simulated $PM_{2.5}$ levels. On the other hand, the broader coverage of the satellite-based data makes them more useful in evaluating the spatial distribution in the model, and the R2 correlation between the model and the satellite-based data is 0.7. Overall, additional ground monitoring would obviously be very useful to better evaluate the model's $PM_{2.5}$. It should be noted that the analysis for this Assessment uses the model's simulation of small dust particles and assumes dry aerosol mass, whereas Shindell *et al.* (2022) used a fixed fraction, 10 per cent, of all dust mass as small to match other CMIP6 models and included the weight of absorbed water to align with reporting in some regions outside Africa. Africa-wide averages are only weakly sensitive to these choices, for example, by a few μg/m^3, though individual station values can vary substantially.

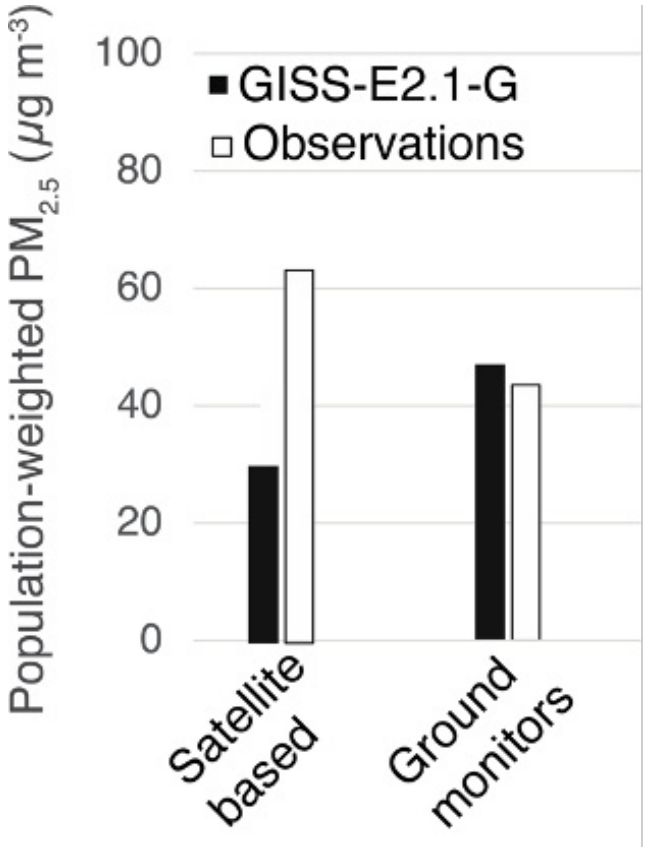

Figure 2.34 Observed population-weighted $PM_{2.5}$ from the model plus satellite AOD estimates ("Observations"; N=10641) over Africa (Shaddick *et al.* 2018) and ground monitors in Africa (N=53) compared with the values simulated by the GISS-E2.1-G model, after unbiasing and sampling at the same locations

Source: Adapted from Shindell *et al.* (2022).

ESTIMATING HEALTH AND CROP IMPACTS

In order to estimate the health impacts from exposure to $PM_{2.5}$, projections of future baseline mortality are taken from the International Futures model (Hughes *et al.* 2011), using the version 7.45 base scenario. This model projects cause- and country-specific baseline mortality rates through 2100. The projected changes in baseline mortality rates between future years and 2015 are applied to the grid-level 2015 GBD baseline mortality dataset (Stanaway *et al.* 2018).

Crop-yield impacts are evaluated using an empirical crop model based on statistical relationships for the impacts of temperature, precipitation, CO_2 concentrations, and O_3 (Shindell *et al.* 2019). Maize, rice and wheat responses to changes in meteorological variables are based on a meta-analysis of more than 1 000 modelling studies (Challinor *et al.* 2014), incorporating relationships observed in field studies. Responses for soy to temperature are based on a separate study (Zhao *et al.* 2017) as they were not included in the meta-analysis. Separate temperature response coefficients for maize, rice and wheat are included according to temperate or tropical conditions. For O_3, the mean 7- or 12-hour daylight exposure during the growing season, i.e., M7 and M12 metrics, respectively, depending on the crop, are used. These affect yields based on the response reported in field studies (Wang and Mauzerall 2004). For CO_2, fertilization effects are included based on relationships described previously (Tebaldi and Lobell 2018). Changes in all factors are taken from the baseline, SLCPs and Agenda 2063 simulations performed for this Assessment. Crop distributions are those for 2010 from the FAO and are maintained at those levels in all calculations of impacts, i.e., no projected changes in crop areas are included.

ANNEX 2.3 LOW EMISSIONS ANALYSIS PLATFORM (LEAP)

The LEAP system is a widely used software tool for integrated planning of energy policy, emissions abatement and climate change mitigation assessment (Heaps 2021). This scenario-based planning tool, developed by SEI, was originally configured to track energy consumption, transformation and resource extraction in all sectors of the economy (SEI 2017). It is able to quantify total national emissions of GHGs – CO_2, CH_4, N_2O, and HFCs; SLCPs – BC, CH_4 and HFCs; and other air pollutants – NOx, NMVCs, SO_2, NH_4, $PM_{2.5}$ and PM_{10}, made up of OC, BC and mineral dust, and CO – from both the energy and non-energy sectors. Emissions inventory is calculated from activity data of specific sources and emission factors which can be country specific if available, or from default datasets available from the IPCC Guidelines for National Greenhouse Gas Inventories, EMEP/EEA (2016) and other sources. Emissions results produced in LEAP for Africa for the three scenarios, the baseline, SLCPs and Agenda 2063, for the period 2000–2063 are used as one of the inputs to the global atmospheric circulation calculations of the GISS model (Figure 2.35).

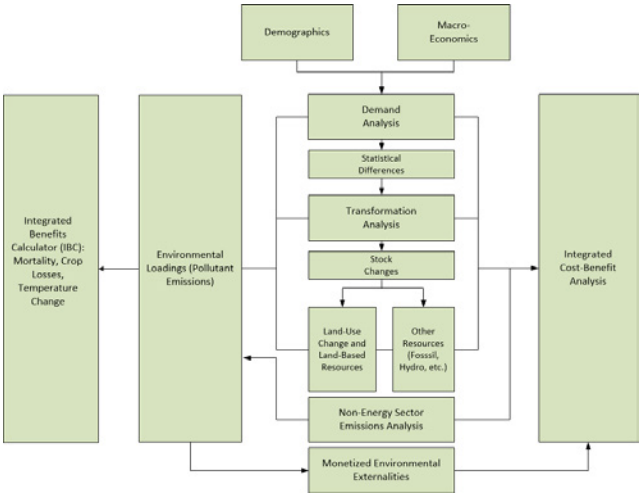

Figure 2.35 Structure of the LEAP planning framework
Source: Heaps (2021)

GEOS-CHEM ADJOINT MODEL

GEOS-Chem is a global three dimensional (3D) chemical transport model of tropospheric chemistry driven by assimilated meteorological observations from the Goddard Earth Observing System (GEOS) of the NASA Data Assimilation Office (Bey *et al.* 2001). The model transports 24 chemical tracers to describe tropospheric O_3-NOx-hydrocarbon chemistry while advection is computed every 15 minutes (2° x 2.5° horizontal resolution) or 30 minutes (4o x 5o horizontal resolution) with a flux-form semi-Lagrangian method (Bey *et al.* 2001). Standard GEOS-Chem tropospheric chemical mechanism comprises 87 species and 307 reactions integrated using the SMVGEARII solver of Jacobson (Henze *et al.* 2007). The adjoint of GEOS-Chem is presently the only such model to include gas-phase chemistry, heterogeneous chemistry, black and organic primary aerosol, and sulphate-ammonium-nitrate formation chemistry and thermodynamics (Henze *et al.* 2012). GEOS-Chem Adjoint model output quantifies the relationship between emissions of a particular pollutant that contributes directly to $PM_{2.5}$ – BC, OC or other PM; or is a precursor to $PM_{2.5}$ – NOx, SO_2 and NH_3 – in any location; and the associated change in $PM_{2.5}$ in the target country (Kuylenstierna *et al.* 2020).

GISS model - see Annex 2.2

ANNEX 2.4 HOUSEHOLD INDOOR AIR POLLUTION METHOD

The health impact assessment for exposure to household pollution used methods outlined by Pillarisseti *et al.* (2016) and Kuylenstierna *et al.* (2020). Exposure to household air pollution –annual average $PM_{2.5}$ concentrations associated with cooking using different fuels and technologies – was estimated separately for households cooking using traditional wood stoves, efficient wood stoves, traditional charcoal stoves, efficient charcoal stoves, other biomass LPG/natural gas and electricity. Exposure was also estimated separately for the primary household cook, other adults and children. Shupler *et al.* (2018) reviewed studies on personal exposure to air pollution of different population groups living in households cooking using different fuels and developed average exposure values for females, males and children. The Shupler *et al.* (2018) personal $PM_{2.5}$ exposure estimates were estimated for different regions. For Africa, only four countries and five studies were identified and used in the Assessment. Due to the small sample size, the global average exposure values for different population groups were used. These values do not differ substantially from the Shupler *et al.* (2018) average exposure values for west and east Sub-Saharan Africa – studies were not identified from Central, North and Southern Africa. The average female $PM_{2.5}$ exposure was used as the primary-cook exposure, while the average male exposure was used as the average other-adult $PM_{2.5}$ exposure. The child $PM_{2.5}$ exposure values from Shupler *et al.* (2018) were used as the exposure for the child population categories.

The population assigned each household $PM_{2.5}$ exposure value was based on the total national historic and future population from the UN WPP (2019) used throughout this Assessment. The population in each country was disaggregated by 5-year age group and sex, and then separated into urban and rural population and into households cooking using different fuels/technologies. The population in each geographic region and household was then disaggregated into primary cooks, assuming one adult per household is the primary cook, and that 95 per cent of primary cooks are women, other adults and children. Each of these groups was assigned a different exposure estimate. In the baseline scenario, there is a gradual shift to cleaner fuels for cooking between 2018 and 2063, and this is reflected in the number of people assigned exposures consistent with households cooking using electricity and gas (Section 2.4.2.2).

The impact of household air pollution on human health was quantified as the number of premature deaths attributable to household air-pollution exposure for six diseases: ischaemic heart disease, stroke, lung cancer, COPD, Type-2 diabetes, and LRTI in children. The baseline mortality rates for these diseases, disaggregated by sex and age, were extracted from the GBD (2019) and used for years before 2020. To estimate future mortality rates, the change in overall death rates projected by UN WPP (2019) between 2019 and future years was applied to the GBD disease-specific mortality rates for 2019 to estimate future disease-specific mortality rates. The death rates for all countries and population groups in Africa are projected to decrease, i.e. life expectancy is expected to increase (UN WPP 2019).

Given the projected increase in life expectancy (UN WPP 2019), the mortality rates for the diseases associated with air pollution are also expected to decrease over time. Figure 2.36 shows the overall change in average mortality rates for children and adults across Africa –country-specific death rates were used to project disease-specific mortality rates in the household air-pollution impact assessment. Figure 2.36 shows that, on average across Africa, between 2020 and 2030, mortality rates of under five-year-olds and adults are expected to reduce by around 22 per cent and 5 per cent, respectively, and between 2020 and 2060, they are projected to decrease by 54–62 per cent and 10 per cent, respectively. Hence, especially for child mortality, UN WPP (2019) envisions a substantial reduction in child-mortality rates, which will consequently reduce the number of premature deaths attributable to household air pollution, even without changes in household air-pollution exposure.

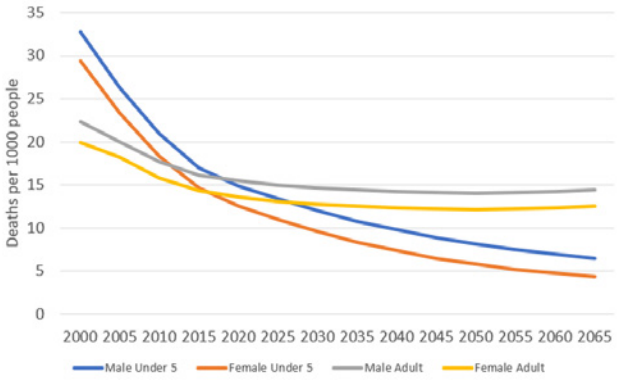

Figure 2.36 Africa, historic and projected overall mortality rates, 2000–2020 and 2020–2065, deaths per thousand people

These data are used to project changes in disease-specific mortality rates for the assessment of household air-pollution mitigation.

ANNEX 2.5 SOURCES OF DATA

The data sources used for economic growth are as follows.

- GDP PPP (constant 2017 international $) with projections to 2100 for each country based on Shared Socioeconomic Pathway: SSP2: Middle of the Road. (For more on the SSPS, see: https://en.wikipedia.org/wiki/Shared_Socioeconomic_Pathways).
- Historical data (World Bank WDI GDP PPP): NY.GDP.MKTP.PP.KD (1990–2019) GDP PPP (constant 2017 international $) https://data.worldbank.org indicator/NY.GDP.MKTP.PP.KD
- IMF World Economic Outlook (IMF WEO - April 2021) and UN Population data used to fill data gaps in WDI statistics (https://www.imf.org/en Publications/WEO/weo-database/2021/April).
- Short-term projections use growth rates from IMF WEO (2020-2024) to capture estimated impact of COVID-19.
- Long-term projections based on growth rates in the five SSPs (OECD model versions) (2025-2100) SSP Public Database Version 2.0 (https://tntcat.iiasa.ac.at/SspDb). All five scenarios are the same through 2025 for each economy.

ANNEX 2.6 ESTIMATED EMISSIONS OF GHGS, SLCPS AND AIR POLLUTANTS IN THE BASELINE

(units: thousand metric tonnes)

POLLUTANT	2018 ('000 TONNES)	2020 ('000 TONNES)	2025 ('000 TONNES)	2030 ('000 TONNES)	2040 ('000 TONNES)	2050 ('000 TONNES)	2060 ('000 TONNES)	2063 ('000 TONNES)
CO_2	2 459 408	2 495 391	2 699 078	3 024 205	3 528 642	4 495 031	6 003 543	6 698 463
CO	129 657	136 924	152 784	172 067	217 675	275 660	350 510	377 790
CH_4	48 449	49 852	58 459	69 069	96 636	136 317	188 981	207 805
NMVOCs	42 510	45 587	50 183	55 682	68 380	84 144	104 117	111 298
NO_x	9 741	11 202	13 009	15 506	22 251	32 076	46 165	51 583
N_2O	902	936	1 167	1 456	2 262	3 439	5 022	5 592
PM_{10}	11 552	12 052	13 077	14 228	16 724	19 547	22 776	23 834
SO_2	5 469	5 455	6 030	7 011	9 478	13 127	18 413	20 519
NH_3	8 991	8 945	10 838	13 211	19 817	29 548	42 640	47 342
$PM_{2.5}$	7 747	8 162	9 037	10 026	12 194	14 689	17 599	18 567
BC	1 225	1 147	1 264	1 401	1 713	2 095	2 570	2 738
OC	3 621	3 502	3 900	4 343	5 311	6 415	7 682	8 094
HFC-134a	23.1	23.0	17.6	16.6	21.0	29.4	37.2	39.4
HFC-125	10.1	10.1	7.7	7.3	9.2	12.9	16.3	17.2
HFC-143a	5.2	5.2	4.0	3.8	4.8	6.7	8.5	9.0
HFC-32	5.7	7.0	5.4	5.1	6.4	9.0	11.4	12.0

REFERENCES

Abiye, O.E., Obioh, I.B. and Ezeh, G.C. (2013). Elemental characterization of urban particulates at receptor locations in Abuja, north-central Nigeria. *Atmospheric Environment* 81, 695-701. https://doi.org/10.1016/J.ATMOSENV.2013.08.042.

Adon, M., Galy-Lacaux, C., Yoboue, V., Delon, C., Lacaux, J.P., Castera, P. et al. (2010). Long-term measurements of sulfur dioxide, nitrogen dioxide, ammonia, nitric acid and ozone in Africa using passive samplers. *Atmospheric Chemistry and Physics* 10(15), 7467–7487. https://doi.org/10.5194/acp-10-7467-2010.

Adon, M., Yoboue, V., Galy-Lacaux, C., Liousse, C., Diop, B., Doumbia, E.H.T. *et al.* (2016). Measurements of NO_2, SO_2, NH_3, HNO_3 and O_3 in West African urban environments. *Atmospheric Environment* 135, 31-40. https://doi.org/10.1016/j.atmosenv.2016.03.050.

Agbo, K.E., Walgraeve, C., Eze, J.I., Ugwoke, P.E., Ukoha, P.O. and Van Langenhove, H.A. (2020). Review on ambient and indoor air pollution status in Africa. *Atmospheric Pollution Research* 12(2), 243-260. doi: .https://doi.org/10.1016/j.apr.2020.11.006

Akinola, M.O. and Lekonpane, M. (2017). Air quality management in Botswana. *Clean Air Journal* 27(1), 43-43.

Alexander, D.A., Northcross, A., Karrison, T., Morhasson-Bello, O., Wilson, N., Atalabi, O. M. *et al.* (2018). Pregnancy outcomes and ethanol cook stove intervention: A randomized-controlled trial in Ibadan, Nigeria. *Environment international* 111, 152-163. https://doi.org/10.1016/j.envint.2017.11.021.

Almazroui, M., Saeed, F., Saeed, S., Islam, M.N., Ismail, M., Klutse, N.A.B. *et al.* (2020). Projected Change in Temperature and Precipitation Over Africa from CMIP6. *Earth Systems and Environment* 4, 455–475. https://doi.org/10.1007/s41748-020-00161-x.

Alvarado, M.J., McVey, A.E., Hegarty, J.D., Cross, E.S., Hasenkopf, C.A., Lynch, R. *et al.* (2019). Evaluating the use of satellite observations to supplement ground-level air quality data in selected cities in low-and middle-income countries. *Atmospheric Environment* 1 (218), 117016.

Amegah, A.K. (2018). Proliferation of low-cost sensors. What prospects for air pollution epidemiologic 967 research in Sub-Saharan Africa? *Environmental Pollution* 241, 1132-1137

Amegah, A.K., Quansah, R. and Jaakkola, J.J. (2014). Household air pollution from solid fuel use and risk of adverse pregnancy outcomes: a systematic review and meta-analysis of the empirical evidence. *Plos One* 9(12), p.e113920. https://doi.org/10.1371/journal.pone.0113920.

Antonel, J. and Chowdhury, Z. (2014). Measuring ambient particulate matter in three cities in Cameroon, Africa. *Atmospheric Environment* 95, 344-354.

ASAP (2020). *A Systems Approach to Air Pollution – East Africa: Synthesis Report*. https://assets.publishing.service.gov.uk/media/5eb16ef186650c4356562f91/ASAP_-_Air_Pollution_in_East_Africa_-_Synthesis_Report.pdf.

Assamoi, E.M. and Liousse, C. (2010). A new inventory for two-wheel vehicle emissions in West Africa for 2002. *Atmospheric Environment* 44(32), 3985–3996. https://doi.org/10.1016/j.atmosenv.2010.06.048.

Awokola, B., Okello, G., Mortimer, K. and Semple, S. (2020). Measuring Air Quality for Advocacy in Africa (MA3): Feasibility and Practicality of Longitudinal Ambient PM2.5 Measurement Using Low-Cost Sensors. International journal of environmental research and public health. 17. 10.3390/ijerph17197243.

Bahino, J., Yoboué, V., Galy-Lacaux, C., Adon, M., Akpo, A., Keita, S. *et al.* (2018). A pilot study of gaseous pollutants' measurement (NO2, SO2, NH3, HNO3 and O3) in Abidjan, Côte d'Ivoire: contribution to an overview of gaseous pollution in African cities. *Atmospheric Chemistry and Physics* 18, 5173–5198.

Balogun, I.A., Balogun, A.A. and Adegoke, J. (2014). Carbon monoxide concentration monitoring in Akure - A comparison between urban and rural environment. *Journal of Environmental Protection* 266, 273.

Bauer, S.E., Tsigaridis, K., Faluvegi, G., Kelley, M., Lo, K.K., Miller, R.L. et al. (2020). Historical (1850–2014) Aerosol Evolution and Role on Climate Forcing Using the GISS ModelE2.1 Contribution to CMIP6. *Journal of Advances in Modeling Earth Systems* 12. https://doi.org/10.1029/2019MS001978.

Bey, I., Jacob, D.J., Yantosca, R.M., Logan, J.A., Field, B.D., Fiore, A.M. *et al.* (2001). Global modeling of tropospheric chemistry with assimilated meteorology: Model description and evaluation. Journal of Geophysical Research Atmospheres 106, 23073–23095. https://doi.org/10.1029/2001JD000807.

Bockarie, A.S., Marais, E.A. and MacKenzie, A. R. (2020). Air Pollution and Climate Forcing of the Charcoal Industry in Africa. *Environmental Science and Technology* 54(21), 13429–13438. https://doi.org/10.1021/acs.est.0c03754.

Borbely-Kiss, I., Kiss, A. Z., Koltay, E., Szabo, G. and Bozó, L. (2004). Saharan dust episodes in Hungarian aerosol: elemental signatures and transport trajectories. Journal of Aerosol Science 35(10), 1205–1224.

Brito, J., Freney, E., Dominutti, P., Borbon, A., Haslett, S.L., Batenburg, *et al.* (2018). Assessing the role of anthropogenic and biogenic sources on PM1 over southern West Africa using aircraft measurements, *Atmos. Chem. Phys*. 18, 757–772.

Buchholz, R.R., Worden, H.M., Park, M., Francis, G., Deeter, M.N., Edwards, D.P. (2021). Air pollution trends measured from Terra: CO and AOD over industrial, fire-prone, and background regions. *Remote Sensing of Environment* 1, 256:112275.

Burnett, R., Chen, H., Szyszkowicz, M., Fann, N., Hubbell, B., Pope, C.A. *et al.* (2018). Global estimates of mortality associated with long-term exposure to outdoor fine particulate matter. *Proceedings of the National Academy of Sciences of the United States of America,* 115, 9592-9597.

Campos, P.M., Esteves, A.F., Leitão, A.A. and Pires, J.C. (2021). Design of air quality monitoring network of Luanda, Angola: Urban air pollution assessment. *Atmospheric Pollution Research* 12(8),101128.

Challinor, AJ, Watson, J, Lobell, DB, Howden, SM, Smith, DR and Chhetri, N (2014) A meta-analysis of crop yield under climate change and adaptation. Nature Climate Change, 4. 287- 291. ISSN 1758-678X http://dx.doi.org/10.1038/nclimate2153

Chirisa, I. (2008). Population Growth and Rapid Urbanization in Africa: Implications for Sustainability. *Journal of Sustainable Development in Africa* 10(2), 361-394.

Conradie, E.H., Van Zyl, P.G., Pienaar, J., Beukes, J.P., Galy-Lacaux, C., Venter, A.D et al. (2016). The chemical composition of fluxes of atmospheric wet deposition at four sites in South Africa. *Atmospheric Environment* 146, 113-151.

Crippa, M., Guizzardi, D., Muntean, M., Schaaf M., Lo Vullo, E., Solazzo, E., *et al.* (2021). EDGAR v6.0 Greenhouse Gas Emissions. *European Commission, Joint Research Centre (JRC) [Dataset].* http://data.europa.eu/89h/97a67d67-c62e-4826-b873-9d972c4f670b.

D'Almeida, G.A. (1986). A model for Saharan dust transport. *Journal of Climate and Applied Meteorology* 25(7) 903–916.

Deroubaix, A., Menut, L., Flamant, C., Brito, J., Denjean, C., Dreiling, V. (2019). Diurnal cycle of coastal anthropogenic pollutant transport over southern West Africa during the DACCIWA campaign. *Atmospheric Chemistry and Physics* 19, 473–497.

deSouza, P., Nthusi, V., Klopp, J., Shaw, B.E., Ho, W., Saffell, J. *et al.* (2017). A Nairobi experiment in using low-cost air quality monitors. *Clean Air Journal* 27(2), 12. https://doi.org/10.17159/2410-972X/2017/v27n2a6.

Doumbia, E.H., Liousse, C., Galy-Lacaux, C., Ndiaye, S.A., Diop, B., Ouafo, M. (2012). Real time black carbon measurements in West and Central Africa urban sites. *Atmospheric Environment* 54, 529-537. http://dx.doi.org/10.1016/j.atmosenv.2012.02.005.

Douville, H., Raghavan, K., Renwick, J., Allan, R.P., Arias, P.A., Barlow, M. (2021). The Physical Science Basis. Contribution of Working Group I to the Sixth Assessment Report of the Intergovernmental Panel on Climate Change, In *Climate Change*. Masson-Delmotte, V., P. Zhai, A. Pirani, S.L. Connors, C. Péan, S. Berger, N. Caud, Y. Chen, L. Goldfarb, M.I. Gomis, M. Huang, K. Leitzell, E. Lonnoy, J.B.R. Matthews, T.K. Maycock, T. Waterfield, O. Yelekçi, R. Yu, and B. Zhou (eds.), Cambridge University Press, Cambridge, UK, 1055–1210. https://doi.org/10.1017/9781009157896.010.

Duncan, B.N., Lamsal, L.N., Thompson, A.M., Yoshida, Y., Lu, Z., Streets, D.G. (2016). A space-based, high-resolution view of notable changes in urban NOx pollution around the world (2005–2014). *Journal of Geophysical Research: Atmospheres* 121(2), 976-996.

EEA - European Environment Agency (2022). *Greenhouse gas emissions per capita.* https://ec.europa.eu/eurostat/databrowser/view/t2020_rd300/default/table.

Ellouz, F., Masmoudi, M., Medhioub, K. and Azri, C. (2014). Temporal evolution and particle size distribution of aerosol constituents collected in Northern Tunisia (Boukornine) under sirocco wind circulations. *Arabian Journal of Geosciences* 7(10), 4399-4406.

EMEP/EEA (2016). *EMEP/EEA air pollutant emission inventory guidebook 2016: Technical guidance to prepare national emission inventories*. European Environment Agency. Copenhagen.

EMEP/EEA (2019). EMEP/EEA air pollutant emission inventory guidebook 2019: Technical guidance to prepare national emission inventories. European Environment Agency. EEA Report No 13/2019. https://www.eea.europa.eu/publications/emep-eea-guidebook-2019

Eyring, V., Bony, S., Meehl, G.A., Senior, C.A., Stevens, B., Stouffer, R. J. (2016). Overview of the Coupled Model Intercomparison Project Phase 6 (CMIP6) experimental design and organization. *Geoscientific Model Development* 9(5), 1937-1958.

FAO (2022). CROP PROSPECTS and FOOD SITUATION - Quarterly Global Report. https://www.fao.org/3/cc3233en/cc3233en.pdf

Fayiga, A.O., Ipinmoroti, M.O. and Chirenje, T. (2018). Environmental pollution in Africa. *Environment, Development and Sustainability* 20(1), 41-73.

Feig, G., Garland, R. M., Naidoo, S., Maluleke, A., & Van der Merwe, M. (2019). Assessment of changes in concentrations of selected criteria pollutants in the Vaal and Highveld priority areas. Clean Air Journal, 29(2). https://doi.org/10.17159/caj/2019/29/2.7464

Flamant, C., Deroubaix, A., Chazette, P., Brito, J., Gaetani, M., Knippertz, P. *et al.* (2018). Aerosol distribution in the northern Gulf of Guinea: local anthropogenic sources, long-range transport, and the role of coastal shallow circulations. *Atmospheric Chemistry and Physics* 18, 12363–12389.

Flaounas, E., Kotroni, V., Lagouvardos, K., Klose, M., Flamant, C., and Giannaros, T. M. (2017). Sensitivity of the WRF-Chem (V3.6.1) model to different dust emission parametrisation: assessment in the broader Mediterranean region. *Geoscientific Model Development* 10(8), 2925–2945. https://doi.org/10.5194/gmd-10-2925-2017.

Fujimori, S., Hasegawa, T., Masui, T., Takahashi, K., Silva H.D. and Dai, H. (2017). Implementation of shared socioeconomic pathways. *Global Environmental Change* 42, 268-283.

Garland, R.M., Naidoo, M., Sibiya, B. and Oosthuizen, R. (2017). Air quality indicators from the Environmental Performance Index: potential use and limitations in South Africa. *Clean Air Journal* 27(1), 33–33. https://doi.org/10.17159/2410-972X/2017/v27n1a8.

GBD (2019). Health effects of dietary risks in 195 countries, 1990–2017: a systematic analysis for the Global Burden of Disease Study 2017. *The Lancet*, 393(10184). https://doi.org/10.1016/S0140-6736(19)30041-8.

Ginoux, P., Prospero, J.M., Gill, T.E., Hsu, N.C., Zhao, M. (2012). Global-scale attribution of anthropogenic and natural dust sources and their emission rates based on MODIS Deep Blue aerosol products. *Reviews of Geophysics* 50.

Gordon, J., Bilsback, K., Fiddler, M., Pokhrel, R. P., Fischer, E. V., Pierce, J. F. (2021). The Effects of Trash, Residential Biofuel, and Open Biomass Burning Emissions on Local and Transported PM2.5 and its Attributed Mortality in Africa, *AGU Fall Meeting 2021*, New Orleans and online everywhere, 13-17 Dec 2021.

Gouel, C. and Guimbard, H. (2019). Nutrition transition and the structure of global food demand. *American Journal of Agricultural Economics* 101, 383–403. https://doi.org/10.1093/ajae/aay030.

Govender, K., & Sivakumar, V. (2019). A decadal analysis of particulate matter (PM2.5) and surface ozone (O3) over Vaal Priority Area, South Africa. Clean Air Journal, 29(2). https://doi.org/10.17159/caj/2019/29/2.7578

Granier, C., Darras, S., van der Gon, H.D., Doubalova, J., Elguinidi, N., Galle, B. *et al.* (2019). *The Copernicus Atmosphere Monitoring Service Global and Regional Emissions.*

Gueye, M. and Jenkins, G.S. (2019). Investigating the sensitivity of the WRF-Chem horizontal grid spacing on PM10 concentration during 2012 over West Africa. *Atmospheric Environment* 196, 152–163. https://doi.org/10.1016/j.atmosenv.2018.09.064.

Hansen, J. (2002). Climate forcing in Goddard Institute for Space Studies SI2000 simulations. *Journal of Geophysical Research* 107, 4347. https://doi.org/10.1029/2001JD001143.

Hansen, J., Russell, G., Rind, D., Stone, P., Lacis, A., Lebedeff, S. *et al.* (1983). Efficient three-dimensional global models for climate studies: Models I and II. *Monthly Weather Review* 111, 609–662.

Hansen, J., Sato, M., Ruedy, R., Kharecha, P., Lacis, A., Miller, R. *et al.* (2007). Climate simulations for 1880–2003 with GISS model Climate Dynamics 29, 661–696. https://doi.org/10.1007/s00382-007-0255-8.

Hawkins, E., and R. Sutton (2011), The potential to narrow uncertainty in projections of regional precipitation change, Clim. Dyn., 37, 407–418, doi:10.1007/s00382-010-0810-6.

Heaps, C.G. (2021). *New Developments with LEAP: The Low Emissions Analysis Platform* https://leap.sei.org.

Health Effects Institute (2020). *State of Global Air 2020*. Special Report. Boston.

Heft-Neal, S., Burney, J., Bendavid, E., Burke, M. (2018). Robust relationship between air quality and infant mortality in Africa. *Nature* 559(7713), 254-258.

Henze, D.K., Hakami, A. and Seinfeld, J.H. (2007). Development of the adjoint of GEOS-Chem. *Atmospheric Chemistry and Physics* 7 2413-2433. https://doi.org/10.5194/acp-7-2413-2007.

Henze, D.K., Shindell, D.T., Akhtar, F., Spurr, R.J.D., Pinder, R.W. and Loughlin, D. (2012). Spatially Refined Aerosol Direct Radiative Forcing Efficiencies. *Environmental Science and Technology* 46(17), 9511-9518.

Hersey, S.P., Garland, R.M., Crosbie, E., Shingler, T., Sorooshian, A., Piketh, S. *et al.* (2015). An overview of regional and local characteristics of aerosols in South Africa using satellite, ground, and modeling data. *Atmospheric Chemistry and Physics* 15(8), 4259-4278.

Hindy, K. and Abdelmaksoud, A. (2016). Air quality monitoring around the first ISCC power plant in Egypt. *Air, Water, Soil and Pollution* 227(2), 1-12.

Huang, Y., Hickman, J. E., and Wu, S. (2018). Impacts of enhanced fertilizer applications on tropospheric ozone and crop damage over sub-Saharan Africa. *Atmospheric Environment* 180, 117-125. https://doi.org/10.1016/j.atmosenv.2018.02.040.

Hughes, B.B., Kuhn, R., Peterson, C.M., Rothman, D.S., Solórzano, J.R. and Mathers, C.D. (2011). Projections of global health outcomes from 2005 to 2060 using the International Futures integrated forecasting model. *Bulletin of the World Health Organization* 89, 478-486.

CCT (2013). The International Council on Clean Transportation. TRANSPORTATION ROADMAP: ENERGY & CLIMATE. https://theicct.org/event/transportation-roadmap-energy-climate/

Inness, A., Ades, M., Agustí-Panareda, A., Barré, J., Benedictow, A., Blechschmidt, A-M. , Dominguez, J.J., R Engelen, R., Eskes, H., Flemming, J., Huijnen, V., Jones, L., Kipling, Z., Massart, S., Parrington, M., Peuch, V-H., Razinger, M., Remy, S., Schulz, M. and Suttie, M. (2019). The CAMS reanalysis of atmospheric composition. *Atmospheric Chemistry and Physics,* 19(6),3515-3556. https://doi.org/10.5194/acp-19-3515-2019

International Energy Agency (2019). *Africa Energy Outlook 2019. A focus on energy prospects in sub-Saharan Africa.* IEA, Paris. https://www.iea.org/reports/africa-energy-outlook-2019.

International Energy Agency (2020). *Clean Energy Transitions in North Africa*. IEA, Paris https://www.iea.org/reports/clean-energy-transitions-in-north-africa.

International Energy Agency (2021). IEA World Energy Balances. https://www.iea.org/data-and-statistics/data-product/world-energy-balances

Intergovernmental Panel on Climate Change (2018). Special Report: G*lobal Warming of 1.5 ºC*. Geneva. https://www.ipcc.ch/sr15/.

Intergovernmental Panel on Climate Change (2019). 2019 Refinement to the 2006 IPCC Guidelines for National Greenhouse Gas Inventories. https://www.ipcc.ch/report/2019-refinement-to-the-2006-ipcc-guidelines-for-national-greenhouse-gas-inventories/

Intergovernmental Panel on Climate Change (2021a). *The Physical Science Basis.* Contribution of Working Group I to the Sixth Assessment Report of the Intergovernmental Panel on Climate Change. Geneva. https://doi.org/10.1017/9781009157896.

International Renewable Energy Agency (2014). *Renewable Energy in Manufacturing: A technology roadmap for REmap 2030*.

International Renewable Energy Agency (2021). *The Renewable Energy Transition in Africa: Powering Access, Resilience and Prosperity.* https://www.irena.org/-/media/Files/IRENA/Agency/Publication/2021/March/Renewable_Energy_Transition_Africa_2021.pdf.

Israelevich, P. Ganor, L.E., Levin, Z. and Joseph, J.H. (2003). Annual variations of physical properties of desert dust over Israel. *Journal of Geophysical Research* 108(13), 4381,1-9.

Kaiser, J. W., Heil, A., Andreae, M. O., Benedetti, A., Chubarova, N., Jones, L., Morcrette, J.-J., Razinger, M., Schultz, M. G., Suttie, M., and van der Werf, G. R. (2012). Biomass burning emissions estimated with a global fire assimilation system based on observed fire radiative power, Biogeosciences, 9, 527–554, https://doi.org/10.5194/bg-9-527-2012.

Katoto, P.D., Byamungu, L., Brand, A.S., Mokaya, J., Strijdom, H., Goswami, N. *et al.* (2019). Ambient air pollution and health in Sub-Saharan Africa: Current evidence, perspectives and a call to action. *Environmental research* 173,174-188.

Keita, S., Liousse, C., Assamoi, E.M., Doumbia, T., N'Datchoh, E. T., Gnamien, S. *et al.* (2021). African anthropogenic emissions inventory for gases and particles from 1990 to 2015. *Earth System Science Data* 13, 3691–3705. https://doi.org/10.5194/essd-13-3691-2021.

Kelley, M., Schmidt, G.A., Nazarenko, L.S., Bauer, S.E., Ruedy, R., Russelet, G.L. *et al.* (2020). GISS-E2.1: Configurations and Climatology. *Journal of Advances in Modeling Earth Systems* 12, e2019MS002025.

Knippertz, P., Coe, H., Chiu, C., Evans, M. J., Fink, A. H., Kalthoff, N. *et al.* (2015a). The DACCIWA project: Dynamics-aerosol-chemistry-cloud interactions in West Africa. *American Meteorological Society* 96, 1451–1460.

Knippertz, P., Evans, M.J., Field, P.R., Fink, A.H., Liousse, C. and Marsham, J. H. (2015b). The possible role of local air pollution in climate change in West Africa. *Nature Climate Change* 5, 815– 822. https://doi.org/10.1038/nclimate2727.

Kok, J. F., Adebiyi, A. A., Albani, S., Balkanski, Y., Checa-Garcia, R., Chin, M. *et al.* (2021). Contribution of the world's main dust source regions to the global cycle of desert dust. *Atmospheric Chemistry and Physics* 21, 8169–8193. https://doi.org/10.5194/acp-21-8169-2021.

Koster, R. D., Darmenov, A. S., & da Silva, A. M. (2015). The quick fire emissions dataset (QFED): Documentation of versions 2.1, 2.2 and 2.4 (No. NASA/TM-2015-104606/Vol. 38).

Kuik, F., Lauer, A., Beukes, J. P., Van Zyl, P. G., Josipovic, M., Vakkari, V., *et al.* (2015). The anthropogenic contribution to atmospheric black carbon concentrations in southern Africa: a WRF-Chem modeling study. *Atmospheric Chemistry and Physics* 15(15), 8809-8830. https://doi.org/10.5194/acp-15-8809-2015.

Kumar, P., Hama, S., Nogueira, T., Abbass, R. A., Brand, V. S., Andrade, M. F. *et al.* (2021a). In-car particulate matter exposure across ten global cities. *Science of the Total Environment* 750, 141395.

Kumar, P., Hama, S., Abbass, R. A., Nogueira, T., Brand, V. S., Abhijith, K. V. *et al.* (2021b). Potential health risks due to in-car aerosol exposure across ten global cities. *Environment International* 155, 106688. https://doi.org/10.1016/j.envint.2021.106688.

Kumar, P., Hama, S., Abbass, R. A., Nogueira, T., Brand, V. S., Wu, H. W. *et al.* (2022a). In-kitchen aerosol exposure in twelve cities across the globe. *Environment International* 107155. https://doi.org/10.1016/j.envint.2022.107155.

Kumar, R., Cenlin H., Bhardwaj, P., Lacey, F., Buchholz, R.R., Brasseur, G.P. *et al.* (2022b). Assessment of regional carbon monoxide simulations over Africa and insights into source attribution and regional transport. *Atmospheric Environment* (277), 119075. https://doi.org/10.1016/j.atmosenv.2022.119075.

Kume, A., Charles, K., Berehane, Y., Anders, E. and Ali, A. (2010). Magnitude and variation of traffic air pollution as measured by CO in the City of Addis Ababa, Ethiopia. *Ethiopian Journal of Health Development* 24(3).

Kuylenstierna, J.C.I., Heaps C. G., Ahmed, T., Vallack, H. W., Hicks, W.K., Ashmore, M.R. *et al.* (2020). Development of the low emissions analysis platform -Integrated benefits calculation (LEAP-IBC) tool to assess air quality and climate co-benefits: Application for Bangladesh. *Environment International* 145, 1-21. https://www.sciencedirect.com/science/article/pii/S0160412020321103.

Lacey, F.G., Henze, D.K., Lee, C.J., van Donkelaar, A., and Martin, R.V. (2017). Transient climate and ambient health impacts due to national solid fuel cookstove emissions. *Proceedings of the National Academy of Sciences of the United States of America* 114(6), 1269–1274. https://doi.org/10.1073/pnas.1612430114.

Lacey, F.G., Marais, E.A., Henze, D.K., Lee, C.J., Donkelaar, A., Martin, R. V. *et al.* (2017). Improving present day and future estimates of anthropogenic sectoral emissions and the resulting air quality impacts in Africa. Faraday Discussions, 200(0), 397-412. https://doi.org/10.1039/C7FD00011A.

Laurent, B., Marticorena, B., Bergametti, G., Léon, J. F. and Mahowald, N. M. (2008). Modeling mineral dust emissions from the Sahara desert using new surface properties and soil database. *Journal of Geophysical Research* D 113(14) https://doi.org/10.1029/2007JD009484.

Lee, J.-Y., Marotzke, J., Bala, G., Cao, L., Corti, S., Dunne, J.P. *et al.* (2021). Future Global Climate: Scenario-Based Projections and Near-Term Information. In *Climate Change 2021: The Physical Science Basis*. Contribution of Working Group I to the Sixth Assessment Report of the Intergovernmental Panel on Climate Change, Masson-Delmotte. Zhai, V.P., Pirani, A., Connors, S.L., Péan, C., Berger, S., Caud, N. et al. (eds.). Cambridge University Press, Cambridge, UK, 553–672. https://doi.org/10.1017/9781009157896.006.

Liousse, C., Assamoi, E., Criqui, P., Granier, C. and Rosset, R. (2014). Explosive growth in African combustion emissions from 2005 to 2030. *Environmental Research Letters* 9(3), p. 035003. https://iopscience.iop.org/article/10.1088/1748-9326/9/3/035003.

Madubansi, M. and Shackleton, C. (2007). Changes in fuelwood use and selection following electrification in the Bushbuckridge lowveld, South Africa. *Journal of environmental management* 83, 416-26. 10.1016/j.jenvman.2006.03.014.

Malings, C., Westervelt, D. M., Hauryliuk, A., Presto, A. A., Grieshop, A., Bittner, A. (2020). Application of low-cost fine particulate mass monitors to convert satellite aerosol optical depth to surface concentrations in North America and Africa*. Atmospheric Measurement Techniques* 13, 3873-3892. https://doi.org/10.5194/amt-13-3873-2020.

Malley, C.S., Hicks, W.K., Kulyenstierna, J.C.I., Michalopoulou, E., Molotoks, A., Slater, J. *et al.* (2021). Integrated assessment of global climate, air pollution, and dietary, malnutrition and obesity health impacts of food production and consumption between 2014 and 2018. *Environmental Research Communications* 3. https://doi.org/10.1088/2515-7620/ac0af9.

Mapoma, H.W.T. and Xie, X. (2013). State of Air Quality in Malawi. *Journal of Environmental Protection* 4(11), 1258.

Marais, E.A., & Chance, K. (2015). A Geostationary Air Quality Monitoring Platform for Africa. Clean Air Journal, 25, 40-45.

Marais, E.A., Jacob, D.J., Wecht, K., Lerot, C., Zhang, L., Yu, K. (2014). Anthropogenic emissions in Nigeria and implications for atmospheric ozone pollution: A view from space, *Atmospheric Environment* 99, 32-40, ISSN 1352-2310. https://doi.org/10.1016/j.atmosenv.2014.09.055.

Marais, E.A. and Wiedinmyer, C. (2016). Air Quality Impact of Diffuse and Inefficient Combustion Emissions in Africa (DICE-Africa). *Environmental Science and Technology* 50(19), 10739–10745. https://doi.org/10.1021/acs.est.6b02602.

Marais, E.A., Silvern, R.F., Vodonos, A., Dupin, E., Bockarie, A.S., Mickley, L.J. (2019). Air Quality and Health Impact of Future Fossil Fuel Use for Electricity Generation and Transport in Africa. *Environmental Science and Technology* 53(22), 13524-13534. https://doi.org/10.1021/acs.est.9b04958.

Masera, O.R., Saatkamp, B.D. and Kammen, D.M. (2000). From Linear Fuel Switching to Multiple Cooking Strategies: A Critique and Alternative to the Energy Ladder Model. *World Development* 28 (12) https://doi.org/10.1016/S0305-750X(00)00076-0.

McDuffie, E. E., Smith, S. J., O'Rourke, P., Tibrewal, K., Venkataraman, C., Marais, E. A. *et al.* (2020). A global anthropogenic emission inventory of atmospheric pollutants from sector- and fuel-specific sources (1970–2017): an application of the Community Emissions Data System (CEDS). *Earth Systems Science Data* 12, 3413-3442. https://doi.org/10.5194/essd-12-3413-2020.

McNeil, M.A., Letschert, V.E., de la Rue du Can, S. et al. Bottom–Up Energy Analysis System (BUENAS)—an international appliance efficiency policy tool. Energy Efficiency 6, 191–217 (2013). https://doi.org/10.1007/s12053-012-9182-6

Mentz G, Robins TG, Batterman S, Naidoo RN. (2018). Acute respiratory symptoms associated with short term fluctuations in ambient pollutants among schoolchildren in Durban, South Africa. Environ Pollut. 2018 Feb; 233:529-539. doi: 10.1016/j.envpol.2017.10.108. Epub 2017 Nov 5. PMID: 29102883; PMCID: PMC5764788.

Miller, R., Schmidt, G.A., Nazarenko, L.S., Bauer, S.E., Kelley, M., Ruedy, R. *et al.* (2021) CMIP6 Historical Simulations (1850-2014) with GISS-E2.1. *Journal of Advances in Modeling Earth Systems* 13, e2019MS002034.

Moulin, C., Lambert, C. E., Dayan, U., Masson-Delmotte, V., Ramonet, M., Bousquetet, P. *et al.* (1998). Satellite climatology of African dust transport in the Mediterranean atmosphere. *Journal of Geophysical Research* D 103(11), 13137-13144.

Naidoo, R. N., Robins, T. G., Batterman, S., Mentz, G., and Jack, C. (2013). Ambient pollution and respiratory outcomes among schoolchildren in Durban, South Africa. *South African Journal of Child Health* 7(4), 127-134.

Ngo, N.S., Asseko, S.V.J., Ebanega, M.O., Allo'o, S.M.A.O. and Hystad, P. (2019). The relationship among PM2.5, traffic emissions, and socioeconomic status: Evidence from Gabon using low-cost, portable air quality monitors. *Transportation Research* Part D: Transport and Environment 68, 2-9.

Nuvolone, D., Petri, D. and Voller, F. (2018). The effects of ozone on human health. *Environmental Science and Pollution Research* 25, 8074-8088. https://link.springer.com/article/10.1007/s11356-017-9239-3.

Offor, I.F., Adie, G.U. and Ana, G.R. (2016). Review of particulate matter and elemental composition of aerosols at selected locations in Nigeria from 1985–2015. *Journal of Health and Pollution* 6(10),1-18.

Omokungbe, O. R., Fawole, O. G., Owoade, O. K., Popoola, O. A., Jones, R. L., Olise, F. S. *et al.* (2020). Analysis of the variability of airborne particulate matter with prevailing meteorological conditions across a semi-urban environment using a network of low-cost air quality sensors. *Heliyon* 6(6), e04207.

Owoade, O.K., Abiodun, P.O., Omokungbe, O.R., Fawole, O.G., Olise, F.S., Popoola, O.O. *et al.* (2021). Spatial-temporal Variation and Local Source Identification of Air Pollutants in a Semi-urban Settlement in Nigeria Using Low-cost Sensors. *Aerosol and Air Quality Research* 21, p.200598.

Paton-Walsh, C., Emmerson, K.M., Garland, R.M., Keywood, M., Hoelzemann, J.J., Huneeus, N. *et al.* (2022). Key challenges for tropospheric chemistry in the Southern Hemisphere. Elementa: *Science of the Anthropocene* 7, 10(1):00050.

Pelassy, P. (1978). First characteristics of particulate air pollution in Yaounde (Cameroon): Intertropical front influence. *Atmospheric Environment* 12(5),1187-1193.

Petkova, E. P., Jack, D. W., Volavka-Close, N. H. and Kinney, P. L. (2013). Particulate matter pollution in African cities. *Air Quality, Atmosphere and Health volume* 6, 603–614. https://doi.org/10.1007/s11869-013-0199-6.

Pillarisetti, A., Mehta, S. and Smith, K.R. (2016). HAPIT, the household air pollution intervention tool to evaluate the health benefits and cost-effectiveness of clean cooking interventions. In *Broken Pumps and Promises: Incentivizing Impact in Environmental Health*. https://doi.org/10.1007/978-3-319-28643-3_10.

Prospero, J.M., Collard, F.X., Molinié, J. and Jeannot, A. (2014). Characterizing the annual cycle of African dust transport to the Caribbean Basin and South America and its impact on the environment and air quality. *Global Biogeochemical Cycles* 28(7), 757-773.

Prospero, J.M. and Lamb, P. J. (2003). African droughts and dust transport to the Caribbean: climate change implications. *Science* 302(5647), 1024-1027.

Redelsperger, J., Thorncroft, C., Diedhiou, A., Lebel, T., Parker, D., and Polcher, J. (2006). African Monsoon Multidisciplinary Analysis (AMMA): An International Research Project and Field Campaign. B. *American Meteorological Society* 1739–1746.

Ridley, D.A., Heald, C.L. and Ford, B. (2012). North African dust export and deposition: A satellite and model perspective. *Journal of Geophysical Research: Atmospheres* 117(D2).

Romanello, M., McGushin, A., Di Napoli, C., Drummond, P., Hughes, N., Jamart, L., Kennard, H., Lampard, P., Solano Rodriguez, B., Arnell, N., Ayeb-Karlsson, S., Belesova, K., Cai, W., Campbell-Lendrum, D., Capstick, S., Chambers, J., Chu, L., Ciampi, L. , Dalin, C., Dasandi, N. et al (2021). The 2021 report of the Lancet Countdown on health and climate change: code red for a healthy future. The Lancet, 398 (10311). pp. 1619-1662. ISSN 0140-6736 doi: https://doi.org/10.1016/S01406736(21)01787-6 Available at https://centaur.reading.ac.uk/100869/

Rushingabigwi, G., Nsengiyumva, P., Sibomana, L., Twizere, C. and Kalisa, W. (2020). Analysis of the atmospheric dust in Africa: The breathable dust's fine particulate matter PM2.5 in correlation with carbon monoxide. *Atmospheric Environment* 224, 117-319.

Saidou, C.A.A., Ma, X., Kumar, K. R., Jia, H., Tang, Y. and Sha, T. (2020). Evaluation of dust extinction and vertical profiles simulated by WRF-Chem with CALIPSO and AERONET over North Africa. *Journal of Atmospheric and Solar-Terrestrial Physics* 199, 105213. https://doi.org/10.1016/j.jastp.2020.105213.

Samir, K.C. and W. Lutz, W. (2017). The human core of the shared socioeconomic pathways: Population scenarios by age, sex and level of education for all countries to 2100. *Global Environmental Change* 42, 181-192.

Schmidt, G.A., Ruedy, R., Hansen, J.E., Aleinov, I., Bell, N. and Bauer, M. (2006). Present-Day Atmospheric Simulations Using GISS ModelE: Comparison to In Situ, Satellite, and Reanalysis Data. *Journal of Climate* 19, 153-192. https://doi.org/10.1175/JCLI3612.1.

Seltzer, K.M., Shindell, D. T., Faluvegi, G. and Murray, L.T. (2017). Evaluating Modeled Impact Metrics for Human Health, Agriculture Growth, and Near-Term Climate. *Journal of Geophysical Research-Atmospheres* 122, 13506-13524.

Shaddick, G. et al. (2018a). Data integration model for air quality: a hierarchical approach to the global estimation of exposures to ambient air pollution. J. R. Stat. Soc. Ser. C. Appl. Stat. 67, 231–253. https://doi.org/10.1111/rssc.12227

Shaddick G, Thomas ML, Amini H, Broday D, Cohen A, Frostad J, Green A, Gumy S, Liu Y, Martin RV, Pruss-Ustun A, Simpson D, van Donkelaar A, Brauer M. (2018b). Data Integration for the Assessment of Population Exposure to Ambient Air Pollution for Global Burden of Disease Assessment. Environ Sci Technol. 2018 Aug 21;52(16):9069-9078. https://doi.org/10.1021/acs.est.8b02864

Shikwambana, L., Mhangara, P. and Mbatha, N. (2020). Trend analysis and first-time observations of sulphur dioxide and nitrogen dioxide in South Africa using TROPOMI/Sentinel-5 P data. *International Journal of Applied Earth Observation and Geoinformation* 91, 102130.

Shindell D, Faluvegi G, Seltzer K, Shindell C. (2018). Quantified, Localized Health Benefits of Accelerated Carbon Dioxide Emissions Reductions. Nat Clim Chang. 2018;8(4):291-295. doi: 10.1038/s41558-018-0108-y. Epub 2018 Mar 19. PMID: 29623109; PMCID: PMC5880221.

Shindell, D., Faluvegi, G., Kasibhatla, P. and Van Dingenen, R. (2019). Spatial patterns of crop yield change by emitted pollutant. *Earth's Future* 7, 101-112. https://doi.org/10.1029/2018EF001030.

Shindell, D., Ru, M., Zhang, Y., Seltzer, K., Faluvegi, G. and Nazarenko,, L. (2021). Temporal and Spatial Distribution of Health, Labor and Crop Benefits of Climate Change Mitigation in the US*. Proceedings of the National Academy of Sciences* 118, e2104061118. https://doi.org/10.1073/pnas.2104061118.

Shindell, D., Faluvegi, G., Parsons, L., Nagamoto, E. and Chang, J. (2022). Premature deaths in Africa due to particulate matter under high and low warming scenarios, *GeoHealth* 6, e2022GH000601. https://agupubs.onlinelibrary.wiley.com/doi/10.1029/2022GH000601.

Shupler M, Balakrishnan K, Ghosh S, Thangavel G, Stroud-Drinkwater S, Adair-Rohani H, Lewis J, Mehta S, Brauer M. (2018). Global household air pollution database: Kitchen concentrations and personal exposures of particulate matter and carbon monoxide. Data Brief. 2018 Oct 27;21:1292-1295. doi: 10.1016/j.dib.2018.10.120. PMID: 30456246; PMCID: PMC6231029.

Simukanga, S., Hicks, W. K., Feresu, S., and Kuylenstierna, J. C. I. (2003). The Air Pollution Information Network for Africa (Apina): *Activities Promoting Regional Co-Operation On Air Pollution Issues In Southern Africa.* https://www.umad.de/infos/cleanair13/pdf/full_292.pdf.

Smits, J., Permanyer, I. The Subnational Human Development Database. Sci Data 6, 190038 (2019). https://doi.org/10.1038/sdata.2019.38

Sousa, A.C., Pastorinho, M.R., Masjedi, M.R., Urrutia-Pereira, M., Arrais, M., Nunes, E. *et al.* (2022). Issue 1 - Update on adverse respiratory effects of outdoor air pollution (Part 2): Outdoor air pollution and respiratory diseases: Perspectives from Angola, Brazil, Canada, Iran, Mozambique and Portugal. *Pulmonology* 28(5):376-395. https://doi.org/10.1016/j.pulmoe.2021.12.007.

Stanaway, J.D., Afshin, A., Gakidou, E., Lim, S.S., Abate, D., Abate, K.H. (2018), Global, regional, and national comparative risk assessment of 84 behavioural, environmental and occupational, and metabolic risks or clusters of risks for 195 countries and territories, 1990–2017: A systematic analysis for the Global Burden of Disease Study. *The Lancet* 1923–1994.

Stockholm Environment Institute (2017). SEI. The Long-range Energy Alternatives Planning-Integrated Benefits Calculator (LEAP-IBC). Key features in LEAP-IBC. https://www.sei.org/publications/leap-ibc/

Swap, R., Garstang, M., Greco, S., Talbot, R. and P. Kallberg, P. (1992). Saharan dust in the Amazon Basin. *Tellus* B 44(2), 133-149.

Tahri, M., Bounakhla, M., Zghaïd, M., Benchrif, A., Zahry, F. and Noack, Y. (2013). TXRF characterization and source identification by positive matrix factorization of airborne particulate matter sampled in Kenitra City (Morocco). *X-Ray Spectrom* 42(4), 284-289.

Tanaka, T. Y., Kurosaki, Y., Chiba, M. Matsumura, T., Nagai, T., Yamazaki, A. *et al.* (2005). Possible transcontinental dust transport from North Africa and the Middle East to East Asia. Atmospheric Environment 39(21) 3901-3909.

Tang, W., Edwards, D. P., Emmons, L. K., Worden, H. M., Judd, L. M., Lamsal, L. N. *et al.* (2021). Assessing sub-grid variability within satellite pixels over urban regions using airborne mapping spectrometer measurements. *Atmospheric Measurement Techniques* 14, 4639–4655. https://doi.org/10.5194/amt-14-4639-2021.

Tebaldi, C. and Lobell, D. (2018) Environ. Res. Lett. 13 065001. https://doi.org/10.1088/1748-9326/aaba48

Teixeira, J. C., Carvalho, A. C., Tuccella, P., Curci, G. and Rocha, A. (2016). WRF-chem sensitivity to vertical resolution during a saharan dust event. *Physics and Chemistry of the Earth Parts A/B/C*, 94, 188-195. https://doi.org/10.1016/j.pce.2015.04.002.

Terrouche, A., Ali-Khodja, H., Kemmouche, A., Bouziane, M., Derradji, A., Charron, A. (2016). Identification of sources of atmospheric particulate matter and trace metals in Constantine, Algeria. Air Quality. *Atmosphere and Health* 9(1):69–82. https://doi.org/10.1007/s11869-014-0308-1.

Touré, N., Konaré, A. and Silué, S. (2012). Intercontinental transport and climatic impact of Saharan and Sahelian dust. *Advances in Meteorology* 2012(2). https://doi.org/10.1155/2012/157020.

Turner MC, Jerrett M, Pope CA 3rd, Krewski D, Gapstur SM, Diver WR, Beckerman BS, Marshall JD, Su J, Crouse DL, Burnett RT. (2016). Long-Term Ozone Exposure and Mortality in a Large Prospective Study. Am J Respir Crit Care Med. 15;193(10):1134-42. doi: 10.1164/rccm.201508-1633OC. PMID: 26680605; PMCID: PMC4872664.

Uhunamure, S., Nthaduleni, N. and Agnes M. (2017). Driving forces for fuelwood use in households in the Thulamela municipality, South Africa. *Journal of Energy in Southern Africa*, 28.

United Nations (2014). Department of Economic and Social Affairs, Population Division. (2014). World Urbanization Prospects: The 2014 Revision, Highlights (ST/ESA/SER.A/325).

United Nations (2021). United Nations Energy Statistics Database https://unstats.un.org/unsd/energystats/pubs/yearbook/

United Nations (2018). United Nations Energy Statistics Database https://unstats.un.org/unsd/energystats/pubs/yearbook/

United Nations Department of Economic and Social Affairs - Population Division. (2019). *World Population Prospects 2019*. Data Booklet. ST/ESA/SER.A/424.

United Nations Department of Economic and Social Affairs - UNDESA (2018). U.N. Department of Economic and Social Affairs, Population Division 2018 Revision of World Urbanization Prospects. https://www.un.org/development/desa/publications/2018-revision-of-world-urbanization-prospects.html

Val, S., Liousse, C., Doumbia, E.H.T., Galy-Lacaux, C., Cachier, H., Marchand, N. *et al.* (2013). Physico-chemical characterization of African urban aerosols (Bamako in Mali and Dakar in Senegal) and their toxic effects in human bronchial epithelial cells: description of a worrying situation. *Particle and Fibre Toxicology* 10(10). https://doi.org/10.1186/1743-8977-10-10.

United Nations Environment Programme and Climate and Clean Air Coalition (2021). *UNEP and CCAC. Global Methane Assessment: Benefits and Costs of Mitigating Methane Emissions.* Nairobi. https://www.ccacoalition.org/en/resources/global-methane-assessment-full-report.

Vallack, H. W. and Rypdal, K. (2019). The Global Atmospheric Pollution Forum Air Pollutant Emission Inventory Manual. Version 6.0 May 2019 revision. https://pure.york.ac.uk/portal/en/publications/the-global-atmospheric-pollution-forum-air-pollutant-emission-inv

van der Werf, G. R., Randerson, J. T., Giglio, L., van Leeuwen, T. T., Chen, Y., Rogers, B. M., Mu, M., van Marle, M. J. E., Morton, D. C., Collatz, G. J., Yokelson, R. J., and Kasibhatla, P. S. (2017). Global fire emissions estimates during 1997–2016, Earth Syst. Sci. Data, 9, 697–720, https://doi.org/10.5194/essd-9-697-2017.

Van Donkelaar, A., Martin, R.V., Brauer, M., Hsu, N.C., Kahn, R.A., Levy, R.C.*et al.* (2016). Global estimates of fine particulate matter using a combined geophysical-statistical method with information from satellites, models, and monitors. Environmental science and technology 50(7), 3762-3772. https://doi.org/10.1021/acs.est.5b05833.

van Marle, M.J.E., Kloster, S., Magi, B.I., Marlon, J.R., Daniau, A.L., Field, R.D. (2017). Historic global biomass burning emissions for CMIP6 (BB4CMIP) based on merging satellite observations with proxies and fire models (1750–2015). *Geoscientific Model Development* 10, 3329-3357. https://doi.org/10.5194/gmd-10-3329-2017.

van Vuuren, D.P., Kriegler, E., O'Neill, B.C. et al. A new scenario framework for Climate Change Research: scenario matrix architecture. Climatic Change 122, 373–386 (2014). https://doi.org/10.1007/s10584-013-0906-1

Velazco, V. A., Deutscher, N. M., Morino, I., Uchino, O., Bukosa, B., Ajiro, M. *et al.* (2019). Satellite and ground-based measurements of XCO2 in a remote semiarid region of Australia, *Earth System Science Data* 11, 935-946. https://doi.org/10.5194/essd-11-935-2019.

Venter, A.D., et al. (2012) An Air Quality Assessment in the Industrialised Western Bushveld Igneous Complex, South Africa. South African Journal of Science, 108, 1-10. https://doi.org/10.4102/sajs.v108i9/10.1059

Wang, X. and Mauzerall, D. L. (2004). "Characterizing Distributions of Surface Ozone and its Impact on Grain Production in China, Japan and South Korea: 1990 and 2020," *Atmospheric Environment,* 38, pp. 4383-4402, 2004. https://doi.org/10.1016/j.atmosenv.2004.03.067

Wang, J., Yue, Y., Wang, Y., Ichoku, C., Ellison, L. and Zeng, J. (2018). Mitigating Satellite-Based Fire Sampling Limitations in Deriving Biomass Burning Emission Rates: Application to WRF-Chem Model Over the Northern sub-Saharan African Region. *Journal of Geophysical Research: Atmospheres* 123(1), 507-528. https://doi.org/10.1002/2017JD026840.

WDI (2021). World Bank's World Development Indicators. https://datatopics.worldbank.org/world-development-indicators/

WDI (2022). World Bank's World Development Indicators. https://datatopics.worldbank.org/world-development-indicators/

WEC (2013). The World Energy Council's Survey of World Energy Resources. https://www.worldenergy.org/publications/entry/world-energy-resources-2013-survey

WEPP (2020). S&P Global Market Intelligence. World Electric Power Plants (WEPP) Database. https://www.spglobal.com/platts/zh/products-services/electric-power/world-electric-power-plants-database.

World Bank (2022a). Getting Down to Earth: Are Satellites Reliable for Measuring Air Pollutants That Cause Mortality in Low- and Middle-Income Countries? International Development in Focus. Washington, DC. https://openknowledge.worldbank.org/handle/10986/36804.

World Bank (2022c). CO2 emissions (kg per PPP $ of GDP) https://data.worldbank.org/indicator/EN.ATM.CO2E.PP.GD

WHO (2019). Cooking and lighting databases: https://www.who.int/data/gho/data/themes/air-pollution/who-household-energy-db

World Health Organization (2021). *WHO global air quality guidelines: particulate matter (PM2.5 and PM10), ozone, nitrogen dioxide, sulfur dioxide and carbon monoxide.* https://apps.who.int/iris/handle/10665/345329.

Wiedinmyer, C., Akagi, S.K., Yokelson, R.J., Emmons, L.K., Al-Saadi, J.A. and Orlando, J.J. (2011). The Fire INventory from NCAR (FINN): a high resolution global model to estimate the emissions from open burning. *Geoscientific Model Development* 4, 625–641, https://doi.org/10.5194/gmd-4-625-2011.

Wiedinmyer, C., Yokelson, R.J. and Gullett, B.K. (2014). Global Emissions of Trace Gases, Particulate Matter, and Hazardous Air Pollutants from Open Burning of Domestic Waste. *Environmental Science & Technology*, 48 (16), 9523-9530. DOI: 10.1021/es502250z

Wiedinmyer, C., Kimura, Y., McDonald-Buller, E., Seto, K., Emmons, L., Tang, W., Buchholz, R., and Orlando, J. (2022). The Fire INventory from NCAR version 2 (FINNv2): updates to a high resolution global fire emissions model, J. Adv. Model. Earth Syst., in preparation, 2022.

WRI GPPDB (2020). World Resources Institute Global Power Plants Database. https://datasets.wri.org/dataset/globalpowerplantdatabase

Young, P. J., Archibald, A. T., Bowman, K. W., Lamarque, J.-F., Naik, V., Stevenson, D. S., Tilmes, S., Voulgarakis, A., Wild, O., Bergmann, D., Cameron-Smith, P., Cionni, I., Collins, W. J., Dalsøren, S. B., Doherty, R. M., Eyring, V., Faluvegi, G., Horowitz, L. W., Josse, B., Lee, Y. H., MacKenzie, I. A., Nagashima, T., Plummer, D. A., Righi, M., Rumbold, S. T., Skeie, R. B., Shindell, D. T., Strode, S. A., Sudo, K., Szopa, S., and Zeng, G. (2013). Pre-industrial to end 21st century projections of tropospheric ozone from the Atmospheric Chemistry and Climate Model Intercomparison Project (ACCMIP), Atmos. Chem. Phys., 13, 2063–2090, https://doi.org/10.5194/acp-13-2063-2013.

Young, P. J., Naik, V., Fiore, A. M., Gaudel, A., Guo, J., Lin, M. Y., Neu, J. L., Parrish, D. D., Rieder, H. E., Schnell, J. L., and Tilmes, S. (2018). Tropospheric Ozone Assessment Report: Assessment of global-scale model performance for global and regional ozone distributions, variability, and trends, Elementa, 6, 10, https://doi.org/10.1525/elementa.265.

Zhang J, Wei Y and Fang Z (2019). Ozone Pollution: A Major Health Hazard Worldwide. Front. Immunol. 10:2518. doi: 10.3389/fimmu.2019.02518

Zhao, C., Liu, X., Leung, L. R., Johnson, B., McFarlane, S. A., Gustafson, W. I. J., *et al.* (2010). The spatial distribution of mineral dust and its shortwave radiative forcing over North Africa: modeling sensitivities to dust emissions and aerosol size treatments. *Atmospheric Chemistry and Physics* 10(18), 8821-8838. https://doi.org/10.5194/acp-10-8821-2010.

Zhao, C., B. Liu, S. Piao, X. Wang, D.B. Lobell, Y. Huang, M. Huang, Y. Yao, S. Bassu, P. Ciais, J.-L. Durand, J. Elliott, F. Ewert, I.A. Janssens, T. Li, E. Lin, Q. Liu, P. Martre, C. Müller, S. Peng, J. Peñuelas, A.C. Ruane, D. Wallach, T. Wang, D. Wu, Z. Liu, Y. Zhu, Z. Zhu, and S. Asseng, (2017). Temperature increase reduces global yields of major crops in four independent estimates. Proc. Natl. Acad. Sci., 114, no. 35, 9326-9331, doi:10.1073/pnas.1701762114.

ABBREVIATIONS AND ACRONYMS

AC	air conditioner
ACCP	African Clean Cities Platform
ADHD	attention deficit/hyperactivity disorder
AEC	African Economic Community
AERONET	Aerosol Robotic Network
AfDB	African Development Bank
AfCFTA	African Continental Free Trade Area
AFOLU	agriculture, forestry and other land use
AFR100	African Forest Landscape Restoration Initiative
AGNES	African Group of Negotiators Expert Support
AMCEN	African Ministerial Conference on the Environment
AMCOMET	African Ministerial Conference on Meteorology
AMCOW	African Ministers' Council on Water
AMMA	African Monsoon Multidisciplinary Analysis
APINA	Air Pollution Information Network for Africa
AOD	aerosol optical depth
ARBE	Department of Agriculture, Rural Development, Blue Economy, and Sustainable Environment (of the African Union)
ARSO	African Regional Organization for Standardisation
ART	acute respiratory-tract infection
ASAP	A Systems Approach to Air Pollution
ASD	autism spectrum disorder
AU	African Union
AUC	African Union Commission
AUDA-NEPAD	African Union Development Agency
AWD	alternate wetting and drying
BC	black carbon
BSC	Barcelona Supercomputing Center
BSFL	black soldier fly larvae
C	carbon
°C	degrees Celsius
CAADP	Comprehensive Africa Agricultural Development Programme
CAMRE	Council of Arab Ministers Responsible for the Environment
CAMS	Copernicus Atmosphere Monitoring Service
CAN	Climat Action Network
CAR	Central African Republic
CArE-Cities	Clean Air Engineering projects – Clean Air Engineering for Cities
CArE-Homes	Clean Air Engineering projects – Clean Air Engineering for Homes
CCAC	Climate and Clean Air Coalition
CCAK	Clean Cooking Association of Kenya
CCS	carbon capture and storage
CEDS	Community Emissions Data System
CIESIN	Center for International Earth Science Information Network
CH_4	methane

CI	confidence interval
CMIP	Coupled Model Intercomparison Project
CMIP6	Sixth Coupled Model Intercomparison Project
CO	carbon monoxide
CO_2	carbon dioxide
CO_2-eq	carbon dioxide equivalent
COMESA	Common Market for Eastern and Southern Africa
COP	Conference of the Parties
COPD	chronic obstructive pulmonary disease
CRS	Common Reporting Standard
CSIR	Council for Scientific and Industrial Research
CSO	civil society organization
CSP	concentrated solar power
3D	three dimensional
DALY	disability-adjusted life years
DCHS	Drakenstein Child Health Study, Western Cape, South Africa
DICCIWA	Dynamics-aerosol-chemistry-cloud interactions in West Africa
DPSIR	drivers, pressures, state, impacts and responses
DRC	Democratic Republic of the Congo
EAC	East African Community
EASFCOM	Eastern Africa Standby Force Coordination Mechanism
ECCAS	Economic Community of Central African States
ECMWF	European Centre for Medium Range Weather Forecasting
ECOWAS	Economic Community for West African States
EDGAR	Emissions Database for Global Atmospheric Research
EEA	European Environment Agency
e.g.	exempli gratia (for example)
EIP	Eco-Industrial Park
EMEP	European Monitoring and Evaluation Programme
ERGP	Economic Recovery and Growth Plan
ETSAP	Energy Technology Systems Analysis Program
EV	electric vehicle
FAO	Food and Agricultural Organization of the United Nations
FDI	Foreign Direct Investment
FEER	Fire Energetics and Emissions Research
F-gas	fluorinated gas
FINN	Fire INventory from NCAR
FRM	Federal Reference Method
GBD	global burden and disease
GCF	Green Climate Fund
GCM	global circulation model
GDL	Global Data Labs
GDP	gross domestic product
GEDAP	Ghana Energy Development and Access Project
GEF	Global Environmental Facility
GEO	geostationary Earth orbit

GEOS	Goddard Earth Observing System
GFED	Global Fire Emissions Database
GFAS	Global Fire Assimilation System
GHAir	Ghana Urban Air Quality Project
GHG	greenhouse gas
GISS	Goddard Institute for Space Studies
GMAO	Global Modeling and Assimilation Office
GMP	Global Methane Pledge
GPI	genuine progress indicators
GPPDB	Global Power Plants Database
GPW	Gridded Population of the World
GRAP	Green Recovery Action Plan (of the African Union)
GSAT	global surface air temperature
GW	gigawatt (109 watts)
GWh	gigawatt hours
GWP	Gridded Population of the World
HFC	hydrofluorocarbon
H_2O	water
hPa	hectopascal
IBC	Integrated Benefits Calculator
IBD	inflammatory bowel disease
IBS	irritable bowel syndrome
ICAO	International Civil Aviation Organisation
ICCT	International Council on Clean Transportation
ICE	internal combustion engine
ICLEI	Local Governments for Sustainability
i.e.	id est (that is)
IEA	International Energy Agency
IGAD	Intergovernmental Authority on Development
ICLEI	Local Governments for Sustainability
IGO	intergovernmental organizations
ILO	International Labour Organization
IMF	International Monetary Fund
IMO	International Maritime Organization
INDAAF	International Network to study Deposition and Atmospheric
IP	Industrial Park chemistry in Africa
IPCC	Intergovernmental Panel on Climate Change
IPPU	industrial processes and product use
IQ	intelligence quotient
IRENA	International Renewable Energy Agency
IWRM	integrated watershed resource management
JICA	Japan International Cooperation Agency
kg	kilogram
KJWA	Koronivia Joint Work on Agriculture
km	kilometre

LEAP	Low Emissions Analysis Platform
LEAP-IBC	Low Emission Analysis Platform – Integrated Benefits Calculator
LED	light-emitting diode
LGV	Ligne à Grande Vitesse Maroc
LMIC	lower middle-income country
LPG	liquified petroleum gas
LRTAP	Convention on Long-Range Transboundary Air Pollution
LRTI	lower respiratory-tract infection
LULUCF	land use, land-use change and forestry
µg	microgram
m	metre
m^2	square metre
m^3	cubic metre
mm	millimetre
MAFLD	metabolic dysfunction-associated fatty liver disease
MDB	multilateral development bank
MEA	multilateral environmental agreement
MEPS	minimum energy-performance standards
MODIS	moderate resolution imaging spectroradiometer
MOPITT	Measurement of Pollution in the Troposphere
MSMEs	micro, small and medium-sized enterprises
MVOC	microbial volatile organic compound
MSW	municipal solid waste
MVA	Manufacturing Value Added
MW	megawatt (106 watts)
N	nitrogen
NAIPS	National Agricultural Investment Plans
NARC	North African Regional Capability
NASA	National Aeronautics and Space Administration
NCAR	US National Center for Atmospheric Research
NCD	non-communicable disease
NDC	Nationally Determined Contributions (to the Paris Agreement)
NEPAD	New Partnership for Africa's Development
NGO	non-governmental organization
NH3	ammonia
NH4	ammonium
NIR	New Industrial Revolution
NMT	non-motorised transport
NMVOC	non-methane volatile organic compound
NO	nitric oxide
N_2O	nitrous oxide
NO_2	nitrogen dioxide
NO_x	nitrogen oxides
NREL	National Renewable Energy Laboratory
NSB	national standards body
O_x	containing oxygen

O_3	ozone
OC	organic carbon
ODA	overseas development assistance
OECD	Organisation for Economic Co-operation and Development
OICA	International Organisation of Motor Vehicle Manufacturers (Organisation internationale des constructeurs automobiles)
OMI	ozone (O3) monitoring instrument
PCFV	Partnership for Clean Fuels and Vehicles
PIDA	Programme for Infrastructure Development in Africa
PIQ	performance intelligence quotient
PM	particulate matter
PM_1	very fine particulate matter (with a diameter of less than 1 micron)
$PM_{2.5}$	fine particulate matter (with a diameter of less than 2.5 microns)
PM_{10}	large particulate matter (with a diameter of 10 microns or less)
POLCA	Pollution de Capitales Africaines
ppb	parts per billion
ppbv	parts per billion by volume
ppm	parts per million
PPP	purchasing power parity
PREFIA	Air Quality Prediction and Forecasting Improvement for Africa
PV	photovoltaic
QFED	Quick Fire Emissions Dataset
R-COOL	Rwanda Cooling Initiative
REC	Regional Economic Community
ReCATH	Regional Climate Action Transparency Hub for Central Africa
RFA	regional framework agreements
RLP	Rural LPG Promotion Programme
3Rs	reuse, reduce and recycle
S	sulphur
SAAQIS	South African Air Quality Information System
SADC	Southern African Development Community
SDG	Sustainable Development Goal
SEI	Stockholm Environment Institute
SEZ	Special Economic Zone
SLCF	short-lived climate forcer
SLCP	short-lived climate pollutant
SNAP	Supporting National Action and Planning on Short-Lived Climate Pollutants
SNAQ	Sensor Network for Air Quality
SO_2	sulphur dioxide
SSP	shared socioeconomic pathway
TAREA	Tanzania Renewable Energy Association
TROPOMI	Tropospheric Monitoring Instrument
TSP	total suspended particulates
TW	terawatt (1012 watts)
TWh	terawatt hour
U4E	United for Efficiency

UHI	urban heat island
UIC	International Union of Railways (Union internationale des chemins de fer)
UMA	Arab Maghreb Union (Union du Maghreb Arabe)
UN	United Nations
UNCTAD	United Nations Conference on Trade and Development
UN DESA	United Nations Department of Economic and Social Affairs
UNDP	United Nations Development Programme
UNEA	United Nations Environment Assembly
UNECA	United Nations Economic Commission for Africa
UNECE	United Nations Economic Commission for Europe
UNEP	United Nations Environment Programme
UNEP ROA	United Nations Environment Programme Regional Office for Africa
UNFCCC	United Nations Framework Convention on Climate Change
UN-Habitat	United Nations Human Settlement Programme
UNIDO	United Nations Industrial Development Organization
UN WPP	UN World Population Prospects
US	United States of America
VAT	value-added tax
VNR	Voluntary National Review
VOC	volatile organic compound
W	watt
WAGP	West African Gas Pipeline
WAPP	West African Power Pool
WDI	World Development Indicators
WEC	World Energy Council
WEPP	World Electric Power Plants Database
WEO	World Economic Outlook
WHA	World Health Assembly
WHO	World Health Organization
WMO	World Meteorological Organization
WRF	Weather and Research Forecasting